Finite Element Method on Riemann Surfaces and Applications to the Laplacian Spectrum

THÈSE N^{O} 5337 (2012)

PRÉSENTÉE LE 23 MARS 2012

À LA FACULTÉ DES SCIENCES DE BASE
CHAIRE DE GÉOMÉTRIE
PROGRAMME DOCTORAL EN MATHÉMATIQUES

ÉCOLE POLYTECHNIQUE FÉDÉRALE DE LAUSANNE

POUR L'OBTENTION DU GRADE DE DOCTEUR ÈS SCIENCES

PAR

Marc MAINTROT

acceptée sur proposition du jury:

Prof. T. Mountford, président du jury
Prof. J. Buser, directeur de thèse
Prof. O. Besson, rapporteur
Prof. J. Dodziuk, rapporteur
Prof. J. Rappaz, rapporteur

ÉCOLE POLYTECHNIQUE
FÉDÉRALE DE LAUSANNE

Suisse
2012

Remerciements

Ma première pensée va naturellement au Professeur Peter Buser qui m'a permis de vivre cette expérience, longue et formatrice. Une pensée à Christian et Patricia, mes parents, qui m'ont toujours soutenu et supporté mes états-d'âme. A Luc, mon frère, qui m'a permis de réviser le programme du baccalauréat en physique et mathématiques.

Les mercis professionnels vont à Klaus-Dieter Semmler pour sa gentillesse, sa disponibilité, sa compétence et ses discussions informelles; à Anthony, pour l'ambiance détendue régnant dans notre bureau; à Manuel, à qui je dois quelques lignes de code, aussi courtes qu'efficaces.

Je remercie les Professeurs Olivier Besson, Jozef Dodziuk, Thomas Mountford, Jacques Rappaz, d'avoir accepté le rôle de membre du jury, et la lecture laborieuse que cela représente.

Un grand merci aux "petites mains des dernières heures"; les mains linguistiques, Fiona, Jan; les mains culinaires, Karin; les mains dessinatrices, Jana, Patrick.

Et enfin, il y a tous ceux que je ne devrais pas remercier, Frederic, Mounir, Yannic, Ylva, Cyril, Benoit, Chloe, Patrick, Remy, Stéphan. Tous des "bad boys" avec qui j'ai traîné mes chaussures de marche ou d'escalade, mes skis, mes ongles, mon parapente et tant d'émotion sur tant de sentiers, de voies d'escalade, de sommets. Sans eux et sans tous ces moments passés ensemble, j'aurais pu finir cette thèse bien avant. J'aurais pu... Ou pas...

A Juli
A Luc
A Christelle, Dani, Gwenola, Jan, Manuel, Nicolas, le cercle des âmes physiciennes errantes et géniales!

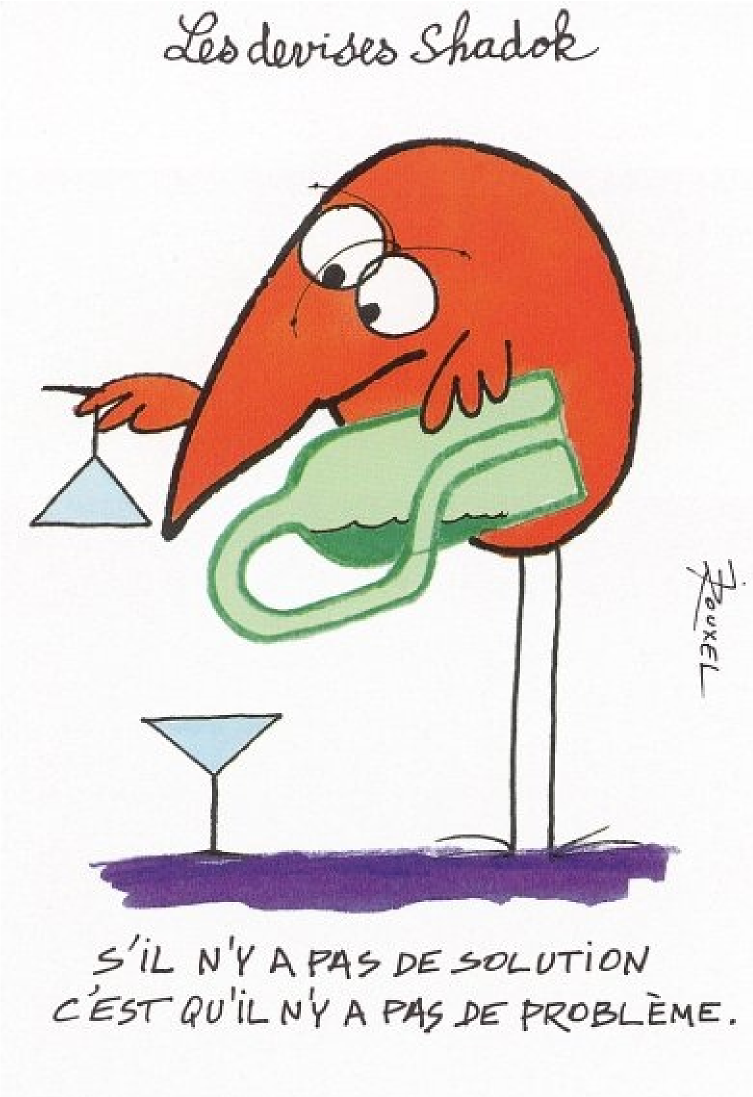
Les devises Shadok
ROUXEL
S'IL N'Y A PAS DE SOLUTION
C'EST QU'IL N'Y A PAS DE PROBLÈME.

Abstract

The objective of this PhD thesis is the approximate computation of the solutions of the Spectral Problem associated with the Laplace operator on a compact Riemann surface without boundaries. A Riemann surface can be seen as a gluing of portions of the Hyperbolic Plane made with suitable conditions to obtain a 2 dimensional manifold. The solutions of the Spectral Problem associated with the Laplace operator are to be understood as the eigenfunctions defined on the surface and their corresponding eigenvalues. This work is separated into two parts: the first part describes the method used to approximate the eigenvalues and eigenfunctions, the second focuses on the design of a program to compute these approximations.

The approximation method is inspired by the Finite Element Method (FEM), in that it relies on the variational expression of the Spectral Problem and the definition of a finite subspace of functions in which the approximated eigenvalues and eigenfunctions are computed. However, it differs from the FEM in that it removes the euclidian basis of the FEM and is invariant under the isometries of the Hyperbolic Plane.

To fulfill this objective, we begin by geodesically triangulating the surface as regularly as possible. This hyperbolic triangulation allows us to define the finite subspace of functions by using the concept of barycentric coordinates associated with each vertex of the triangulation (idea introduced by Whitney and taken up by Dodziuk). We then prove that the approximated solutions convergence to the exact ones when the diameter of the triangulation decreases, as well as the order of convergence.

The program is a practical application of the theoretical work and allows the computation of the approximated eigenfunctions and eigenvalues.

Keywords

Hyperbolic Geometry, Riemann Surfaces, Laplace Operator, Hyperbolic Triangulation, Finite Elements Method, Eigenvalues, Eigenfunctions.

Résumé

L'objectif de ce travail de doctorat est le calcul de solutions approchées du Problème Spectral associé à l'opérateur Laplacien sur une surface de Riemann compacte et sans bord. Une surface de Riemann peut-être vue comme un recollement de portions du Plan Hyperbolique effectué de façon à obtenir une variété de dimension 2. Par solutions du Problème Spectral associé à l'opérateur Laplacien, nous entendons les fonctions propres définies sur la surface et leur valeur propre correspondante. Cette étude est articulée autour de deux axes: d'une part la présentation d'une méthode d'approximation des fonctions et valeurs propres, d'autre part la conception d'un programme permettant leur calcul.

La méthode d'approximation s'inspire très fortement de la Méthode des Eléments Finis, à savoir l'expression variationnelle du Problème Spectral et la définition d'un sous-espace de fonctions de dimension finie dans lequel les fonctions et valeurs propres approchées sont calculées. Elle en diffère cependant en se défaisant du caractère euclidien de la Méthode des Eléments Finis et en étant invariante sous les isométries du Plan Hyperbolique.

Pour ce faire, il est nécessaire d'effectuer une triangulation géodésique sur la surface aussi régulière que possible. Cette triangulation hyperbolique permet alors la définition du sous-espace de fonctions de dimension finie via le concept de coordonnées barycentriques associées à chacun des sommets de la triangulation (idée introduite par Whitney et reprise par Dodziuk). Enfin, nous montrons que les solutions approchées sont proches des solutions exactes lorsque le diamètre de la triangulation est petit; nous mettons aussi en évidence l'ordre de convergence.

Le programme développé en parallèle est une application de cette partie théorique et permet le calcul des fonctions et valeurs propres approchées.

Mots Clés

Géométrie Hyperbolique, Surfaces de Riemann, Laplacien, Problème Spectral, Triangulation Hyperbolique, Méthode des Eléments Finis, Valeur Propre, Fonction Propre.

Introduction

The inspiration for this work lies in the article by Jozef Dodziuk: Finite-Difference Approach to the Hodge Theory of Harmonic Forms (See [Dod76]). Dodziuk shows that with a triangulation of an N-dimensional Riemannian manifold it is possible to define a linear projection application from the q-differential forms ($q = 0 \dots N$) over each triangle to a finite dimensional q-form subspace. Applied to functions in $\mathbb{R}^N$ as the Euclidean space, this projection corresponds to the linear interpolation of the function at the vertices of the triangles.

The central theorem of Dodziuk's work proves that these approximated forms on the manifold uniformly converge to the non-approximated ones when the triangulation becomes finer and finer. It is not possible to directly give a pointwise meaning to convergence as the differential forms on the manifold are smooth, whereas the approximated forms are not, and thus we have to work with Sobolev spaces on the manifolds. Applied to the functions of $\mathbb{R}^N$ as the Euclidean space, the method presented in this article corresponds to the well-known Finite Elements Method.

The work we present here is an implementation of these theoretical results to a particular case: that of the computation of the solutions of the Spectral Problem:

$$\Delta f = \lambda f$$

associated with the Laplace operator Δ on a compact hyperbolic surface without boundaries. The objective is to develop a method which allows the computation of approximated eigenfunctions and eigenvalues of the surface while having control on the convergence speed, as well as the design of a program which concretely computes them. We also want this numerical method to have an intrinsic characteristic, that is, invariance under the isometries of the surface: the Möbius transformations. This explains the title of this work: Finite Element Method on Riemann surfaces.

The surface we study is a Riemann surface of genus g, denoted X, and is issued from the gluing of portions of the Hyperbolic Plane. We assume the reader to be familiar with its two traditional representations: the Poincaré disc $\mathbb{D}$ and the upper half plane $\mathbb{H}$, as well as its representation in $\mathbb{R}^3$ associated with the Minkovski metric (briefly summarized in Paragraph A.5).

The surface is defined by its Fenchel-Nielsen parameters. For the triangulation, we consider it as a set of glued Y-pieces (see Fig. 1). These Y-pieces are split into two hexagons. At this point, it is important to note that we do not cut them in the traditional way, leading to two identical right-angled hexagons, but along geodesics, such that the triangulation is adapted to the twist parameter (a further explanation can be found at the beginning of Paragraph 2.2 and in Figures 2.2 and 2.3).

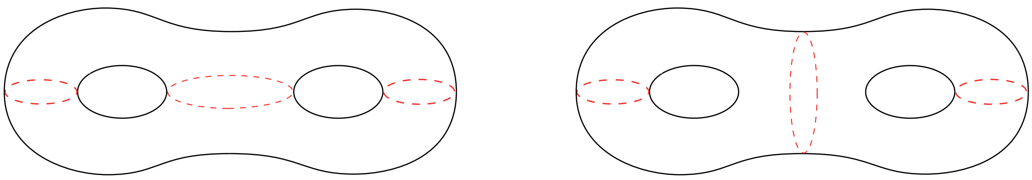

Figure 1: Two different gluing schemes for a surface of genus 2

Chapter 1 is dedicated to the formal statement of the Spectral Problem on a manifold and can be considered as a preliminary. We need to define the Sobolev spaces on a manifold to express the Spectral Problem in its so-called weak form (or variational form). The weak form of the problem not only gives us a proof for the existence of the solutions of the Spectral Problem (even in its strong form or pointwise form), but also an idea of the technique necessary to develop our Finite Element Method.

As mentioned previously, we need to define a projection operator on the triangulation of the surface; hence we need a triangulation. This is the subject of **Chapter 2**. We know from experience that this triangulation has to be as regular as possible, that is, with triangles of more or less the same size and as close as possible to an equilateral triangle. We present an algorithm which produces such a triangulation.

In **Chapter 3**, we define the finite function subspace where we will compute the approximated eigenvalues and eigenfunctions. We define it using barycentric coordinates associated with the vertices of the triangulation of the surface. And finally, we express the Spectral Problem in this finite subspace as an algebraic problem. Finding its solutions then becomes a problem of determining the eigenvalues and eigenvectors of a matrix.

In **Chapter 4**, we show that the eigenvalues and eigenfunctions computed on the finite function subspace are close to the real eigenvalues and eigenfunctions of the surface when the triangulation is sufficiently small. Since we are laying the groundwork for a numerical implementation, we are naturally interested in the "convergence speed" in terms of the power of h, the diameter of the triangulation. The main results of this work lie in Theorems 42 and 46, which we provide here in a simplified version without the formally required hypotheses.

Theorem. *Suppose φ_m is an eigenfunction of the Spectral Problem associated with the eigenvalue λ_m and $\varphi_{m,h}$ an eigenfunction in the finite function space associated with the eigenvalue $\lambda_{m,h}$. Then there exists a constant C such that:*

$$|\lambda_m - \lambda_{m,h}| \leq Ch^2 + O(h^3)$$

Therefore, the convergence speed for the eigenvalues is of order 2 in h.

Theorem. *Suppose $\varphi_m, \dots, \varphi_{m+k-1}$ are eigenfunctions of the Spectral Problem associated with the eigenvalue λ_m of multiplicity $k \geq 1$ and $\varphi_{m+i,h}$ $(0 \leq i \leq k-1)$ is an eigenfunction in the finite function space associated with the eigenvalue $\lambda_{m,h}$. Then there exists $\varphi'_{m,i} \in \mathrm{Span}(\varphi_m, \dots, \varphi_{m+k-1})$ and a constant C such that:*

$$\left\|\varphi'_{m+i} - \varphi_{m+i,h}\right\|_{1,X} \leq Ch + O(h^2)$$

Therefore, the convergence speed for the eigenfunctions is of order 1 in h. The definition of $\| \, . \, \|_{1,X}$ is provided in Chapter 1.

In **Chapter 5**, we present the results obtained from our implemented program for a particular surface, for which some theoretical results are known. This surface, called F_2, has been studied by Jenni in his PhD Thesis: Über das Spektrum des Laplace Operators auf einer Schar Kompakter Riemannscher Flächen [Jen81]. This surface has also been investigated just recently by Strohmaier and Uski in [SU11].

Finally, we mention here that **Appendix A** is dedicated to a matrix representation of the Möbius transformations. This allows us to see points and geodesics on the surface in term of matrices: a point corresponds to a half-turn around itself. Similarly a geodesic corresponds to a symmetry around itself. This type of matrix modeling is of great interest for this work. A reader with no knowledge of this type of modeling may read this appendix prior to the rest of this work.

Since the Laplacian is a fundamental operator in physics, many works have been done studying its eigenfunctions and eigenvalues. We list here a number of contributions that are related to our work.

The first paper in which eigenvalues on Riemann surfaces are approximated numerically seems to be [Jen81]. In [AS89] Aurich and Steiner apply euclidean Finite Elements to symmetric hyperbolic geodesic octagons representing compact Riemann surfaces of genus 2. More accurate results, again for genus 2, were obtained by the same authors in [AS93] using a boundary element method. Surfaces of higher genus do not seem to have been studied in this way.

In [Hej92], [Hej99] and several other works Hejhal uses Maass cusp forms to approach the spectra of certain non compact Riemann surfaces with cusps. Fourier series expansion of the cusp forms allows him to obtain very accurate estimates even for very large eigenvalues. This method was later refined by Booker and Strömbergsson in [BS06] using the Selberg trace formula. In a very recent paper Strohmaier and Uski [SU11] use the method of particular solutions to compact Riemann surfaces by decomposing them into cylinders with piecewise geodesic boundaries and using hypergeometric functions. This article and our method are, as far as we know, the only ones allowing the computation of the eigenvalues and eigenfunctions on arbitrary compact Riemann surfaces.

For the computational approach to Riemann surfaces in general we point out the review article by Mercat [Mer07] and the recent book [BK11] by Bobenko and Klein. In this book we also find a discretisation of the Laplacian based on simplicial approximations of a Riemann surface [BS07a].

For the discretization of the Laplacian in general the literature is quite extended and we mention only the following. [BC07] uses an approach based on barycentric coordinates that is different from the hyperbolic barycentric coordinates we use in this thesis. [Lar00] uses an a posteriori estimate method that is not considered here but might be useful on Riemann surfaces in future work. [AHTK99], [DD07] and also several other papers apply numerical approximations of the Laplace spectrum on surfaces in Euclidean space for image processing. Yet another field of current investigation is the inverse spectral geometry of planar domains where we mention in particular the works of Antunes and Freitas [AF11], [AF08], [AF06] and [AA08]. Finally we mention the overview article by Boffi [Bof10], some part of which is used in Chapter 4.

Notations

Here U represents a relatively compact open set.

General Notations

$\overline{U}$	Closure of U
∂U	Boundary of U
$\\| \, . \, \\|$	Norm in a Hilbert space

Riemann Surfaces

$\mathbb{H}$	Upper half-plane
$\mathbb{D}$	Poincaré's disk
G	Hyperbolic metric tensor
G_{ij}	Components of G
G^{ij}	Components of G^{-1}
dv_G	Volume form associated with G
Γ^i_{jk}	Christoffel symbols associated with G
$\Lambda^q(U)$	Spaces of q-differential forms on U
$\langle . \, , . \rangle$	Inner product associated with G on vector fields, covariant tensor fields or forms
$\| \, . \, \|$	Norm associated to the preceding inner-product
x, y, p	Varying points on X
P_i	Vertex of the triangulation
$\mathrm{dist}(x, y)$	Hyperbolic distance between x and y

Functions

$C^n(U)$	n-times continuously differentiable functions on U
$\mathcal{D}(U)$	Differentiable functions with compact support included in U
$D^n f$	Covariant derivative of order n
$H^n(U)$	Sobolev space of order n on U
$(. \, , .)_{n,U}$	Inner product in $H^n(U)$
$\\| \, . \, \\|_{n,U}$	Norm in $H^n(U)$

Matrices

$M(2,\mathbb{R})$	2×2 matrices with real coefficients
$GL(2,\mathbb{R})$	2×2 invertible matrices with real coefficients
$T0(2,\mathbb{R})$	2×2 real matrices with null trace
det	Determinant of the matrix

Remarks about these notations

When we write $\langle .\, , . \rangle$, it is up to the reader to understand with the context if the inner product is used with vector fields, covariant tensors fields or forms.
In the integration formulae, we sometimes do not write the volume form dv_G associated to the metric tensor G.
Occasionally we use the Einstein notation to make some formulae more readable. For example, a 1-form θ in a coordinate system $\{x^1, \ldots, x^n\}$ is written:

$$\theta = \theta_i dx^i$$

On a triangle
We often have to make calculation on a specific triangle of the triangulation T_j. To avoid the hardly readable notation $T_j = P_{j_0}P_{j_1}P_{j_2}$, we rename the vertices of the triangle:

$$C = P_{j_0}, \quad A = P_{j_1}, \quad B = P_{j_2}$$

We also denote the lengths of the edges as follows:

$$a = \mathrm{dist}(B, C), \quad b = \mathrm{dist}(C, A), \quad c = \mathrm{dist}(A, B)$$

And finally we define the following quantities:

$$\alpha = \cosh a - 1, \quad \beta = \cosh b - 1, \quad \gamma = \cosh c - 1$$

Some formulae recurrently appear in the triangles; we define them from here on:

$$\begin{aligned}
\Gamma &= -\alpha^2 - \beta^2 - \gamma^2 + 2\alpha\beta + 2\alpha\gamma + 2\beta\gamma + 2\alpha\beta\gamma \\
\Lambda &= -\alpha^2 - \beta^2 - \gamma^2 + 2\alpha\beta + 2\alpha\gamma + 2\beta\gamma \\
\Phi &= 1 + 2\beta u(1-u-v) + 2\alpha v(1-u-v) + 2\gamma uv
\end{aligned}$$

where $\Phi(u, v)$ is a function of $u, v \geq 0$ and $u + v \leq 1$.

Contents

Chapter 1

The Spectral Problem on a Manifold

Hodge Theory is a fundamental tool in the Dodziuk's article. In our work, we deal only with functions and one-forms and therefore do not really require this formalism. However, we use it in the first paragraph of this chapter to define the Laplace operator in an intrinsic way (that is, independently of a coordinate chart).

1.1 The Spectral Problem

X is a hyperbolic surface, that is, a 2-dimensional compact and oriented manifold without boundaries provided with the hyperbolic metric tensor G. A large part of this chapter can be generalized to manifolds of higher dimensions, so we denote its dimension as N, and remember that $N = 2$ when it is useful.

In this paragraph, we present a short introduction to Hodge theory of the q-forms on X. Given K, an open subset of X, we denote $\Lambda^q(K), (0 \leq q \leq N)$ the spaces of q-differential forms on K. The hyperbolic metric tensor provides a pointwise inner product for these spaces. In a coordinate chart, at a point p, it is defined by bilinearity on the basis elements of $\Lambda^q(K)$:

$$\langle dx^{i_1} \wedge \cdots \wedge dx^{i_q}, dx^{j_1} \wedge \cdots \wedge dx^{j_q} \rangle(p) = \det \begin{pmatrix} \langle dx^{i_1}, dx^{j_1} \rangle(p) & \ldots & \langle dx^{i_1}, dx^{j_q} \rangle(p) \\ \vdots & & \vdots \\ \langle dx^{i_q}, dx^{j_1} \rangle(p) & \ldots & \langle dx^{i_q}, dx^{j_q} \rangle(p) \end{pmatrix}$$

where $\langle dx^i, dx^j \rangle(p) = G^{ij}(p)$. We remind that $G^{ij}(p)$ are the components of the inverse of the metric tensor: $G^{ij}G_{jk} = \delta^i_k$. Of course, for f and g

functions on K, the inner product is:

$$\langle f, g \rangle = fg$$

This inner product allows us to define the Hodge operator $*$:

$$f \wedge *g = \langle f, g \rangle \sqrt{\det G}\, dx^1 \wedge \cdots \wedge dx^N \quad f, g \in \Lambda^q(K)$$

It is now possible to define a global inner product[1] on Λ^q(K):

$$(f, g)_{0,K} = \int_K f \wedge *g \quad f, g \in \Lambda^q(K)$$

And its associated norm:

$$\|f\|^2_{0,K} = (f, f)_{0,K} = \int_K f \wedge *f$$

Let $d : \Lambda^q(K) \to \Lambda^{q+1}(K)$ be the exterior derivative and $\delta = (-1)^{Nq+N+1} * d*$ its formal adjoint. Indeed:

$$\begin{aligned} d(f \wedge *g) &= df \wedge *g + (-1)^q f \wedge d * g \\ &= df \wedge *g + (-1)^{q+q(n-q)} f \wedge * * d * g \\ &= df \wedge *g - (-1)^{n(q+1)+n+1} f \wedge * * d * g \\ &= df \wedge *g - f \wedge *\delta g \end{aligned}$$

Hence, by Stoke's Theorem:

$$\int_{\partial K} f \wedge *g = (df \wedge g) - (f, \delta g)$$

If $K = X$, as the surfaces we are interested in have no boundaries ($\partial X = \emptyset$), δ is the adjoint of d for this inner product.

Let us define the Laplacian operator on K:

$$\Delta = d\delta + \delta d \tag{1.1}$$

The Spectral Problem associated with the Laplace operator reads : find $f \in \Lambda^q(X)$ and $\lambda \in \mathbb{R}$ such that,

$$\Delta f = \lambda f \tag{1.2}$$

We are interested in finding solutions for this problem when $f \in \Lambda^0(X) = C^\infty(X)$. Unfortunately, it is impossible to find solutions in closed form to this problem when X is any hyperbolic surface. We thus rewrite the problem 1.11 in a variational form on Sobolev function spaces. This variational formulation, also called the weak form, provides proof for the existence of the solutions, as well as a natural way to construct an approximation theory in the Sobolev spaces.

[1] the notation $(.\,,.)_{0,K}$ anticipates the definition of the Sobolev spaces on K

1.2 Sobolev Spaces on an Open Set $K \subset X$

Given an open set $K \subset X$, we need to define the set of the differentiable functions with compact support over K:

$$\mathcal{D}(K) = \{\varphi \in C^{\infty}(K), \operatorname{supp}(\varphi) \subset\subset K\} \tag{1.3}$$

Note that if $K = X$, then $\mathcal{D}(X) = C^{\infty}(X) = \Lambda^0(X)$. From here on we will, however, abandon the 0-form notation.

Definition 1. We define $L^2(K)$ as the completion of $\mathcal{D}(K)$ with respect to the $\|.\|_{0,K}$ norm.

We follow the same logic to define the Sobolev spaces of higher degrees and hence we have to define some global norms with the covariant derivatives of the functions of $\mathcal{D}(K)$. The closure with respect to these norms will define the Sobolev spaces. With this objective in mind, we first have to define a pointwise inner product on the n-covariant tensor fields.

1.2.1 Pointwise Inner Products and Norms on Covariant Tensors

It is important to point out that the following definitions in this paragraph are independent of the coordinate chart.

Definition 2. Given T and S, two n-covariant tensor fields[2], such that $T = T_{i_1 \dots i_n} dx^{i_1} \otimes \dots \otimes dx^{i_n}$ and $S = S_{j_1 \dots j_n} dx^{j_1} \otimes \dots \otimes dx^{j_n}$ on a coordinates chart, we define the following inner product on a point $p \in X$:

$$\langle T, S\rangle(p) = G^{i_1 j_1}(p) \dots G^{i_n j_n}(p) T_{i_1,\dots,i_n}(p) S_{j_1,\dots,j_n}(p)$$

We prefer however to omit the reference to the point p where the inner product is calculated when it does not disturb the comprehension:

$$\langle T, S\rangle = G^{i_1 j_1} \dots G^{i_n j_n} T_{i_1,\dots,i_n} S_{j_1,\dots,j_n}$$

Remark. This definition of inner product differs from the preceding one by a factor $n!$, which means that $\langle dx^{i_1} \wedge \dots \wedge dx^{i_n}, dx^{j_1} \wedge \dots \wedge dx^{j_n}\rangle$ calculated as the inner product of a n-form is equal to $n!\langle dx^{i_1} \wedge \dots \wedge dx^{i_n}, dx^{j_1} \wedge \dots \wedge dx^{j_n}\rangle$ calculated as the inner product of a n-covariant tensor field.

[2] notice the use of the Einstein's summation convention

The covariant derivative of order n of a function is a n-covariant tensor field. In a coordinate system it expands in this form:

$$D^n f = (D^n f)_{i_1 \dots i_n} dx^{i_1} \otimes \dots \otimes dx^{i_n}$$

For $n = 0, 1, 2$, the definition is:

$$\begin{aligned} D^0 f &= f \\ D^1 f &= \partial_i f dx^i \\ D^2 f &= (\partial_{ij} f - \Gamma^k_{ij} \partial_k f) dx^i \otimes dx^j \end{aligned}$$

(where Γ^k_{ij} are the Christoffel symbols). We do not provide the expressions for higher order because we do not need them in this work. For $n = 1$, we will write Df instead of $D^1 f$. From the definition of the inner product, we define the following pointwise norms on the covariant derivative of a function $f \in \mathcal{D}(K)$ in a coordinates system:

$$|D^n f|^2 = G^{i_1 j_1} \dots G^{i_n j_n} (D^n f)_{i_1 \dots i_n} (D^n f)_{j_1 \dots j_n} \tag{1.4}$$

It is also possible to define another norm for a covariant tensor, which is useful for further calculations and equivalent to the preceding one.

Definition 3. Given $f \in \mathcal{D}(X)$. At a point $p \in X$, we define the following "sup-norm" on the covariant derivative of f:

$$|D^n f|_{\text{sup}}(p) = \sup_{\substack{V_1, \dots, V_n \\ |V_i| = 1}} |D^n f(p)(V_1(p), \dots, V_n(p))| \tag{1.5}$$

where the V_i represent some vector fields.

Proposition 4. For $n = 0, 1, 2$, the two norms $|D^n f|$ und $|D^n f|_{\text{sup}}$ are equivalent.

Proof. For $n = 0$, it follows by definition.
For $n = 1$, $|Df| = |\nabla f| = |Df|_{\text{sup}}$.
For $n = 2$, we express the covariant derivative in a Riemannian normal coordinate chart, at the point p where the calculation is made:

$$G^{ij}(p) = \delta^{ij}(p) \quad \text{and} \quad \Gamma^k_{ij}(p) = 0$$

and:

$$\left| D^2 f \right|^2 = \sum_{i,j=1,2} (D^2 f)^2_{ij}$$

From the definition of the sup norm, $\forall (i,j), (D^2 f)^2_{ij} \leq |D^2 f|^2_{\text{sup}}$. Thus:

$$\frac{1}{4}\left|D^2 f\right|^2 \leq \left|D^2 f\right|^2_{\text{sup}}$$

Moreover:

$$D^2 f = M = \begin{pmatrix} a & b \\ c & d \end{pmatrix} = \begin{pmatrix} m_1 \\ m_2 \end{pmatrix}$$

Thus, for $V \in \mathbb{R}^2$:

$$M.V = M \begin{pmatrix} v_1 \\ v_2 \end{pmatrix} = \begin{pmatrix} \langle m_1, V\rangle \\ \langle m_1, V\rangle \end{pmatrix}$$

From the Cauchy-Schwarz inequality, considering a vector V of norm 1:

$$\begin{aligned} \langle m_1, V\rangle &\leq |m_1| \\ \langle m_2, V\rangle &\leq |m_2| \end{aligned}$$

Thus:

$$|M.V|^2 = \langle m_1, V\rangle^2 + \langle m_2, V\rangle^2 \leq |m_1|^2 + |m_2|^2 = (a^2+b^2+c^2+d^2) = |D^2 f|^2$$

Finally, we can conclude that:

$$\frac{1}{4}|D^2 f|^2 \leq \left|D^2 f\right|_{\text{sup}} \leq |D^2 f|^2 \tag{1.6}$$

□

1.2.2 Global Seminorms, Norms and Sobolev Spaces

We define the following global $|\,.\,|_{n,K}$ semi-norm for a function $f \in \mathcal{C}^0(K)$:

$$|f|^2_{n,K} = \int_K |D^n f|^2 \, dv_G \tag{1.7}$$

and the $\|\,.\,\|_{n,K}$ norm:

$$\|f\|^2_{n,K} = \sum_{l=0\ldots n} |f|^2_{l,K} \tag{1.8}$$

where dv_G is the volume form related to G.

Definition 5. We define the Sobolev Space $H^n(K), (n \geq 0)$ as the completion of $\mathcal{D}(K)$ with respect to the $\|\,.\,\|_{n,K}$ norm. (And of course, $H^0(K) = L^2(K)$).

$H^n(K)$ is composed of functions, which are not in $C^\infty(K)$ (sometimes not even continuous). This requires us to give a meaning to the symbol $D^n f$ if $f \in H^n(K)$ and define the concept of weak derivative. Let us suppose that K is included in the coordinate neighborhood, otherwise we cut it in parts adapted to the coordinate charts. Starting from the partial integration formula for differentiable functions with compact support:

$$\int_K \partial_i f g \, dv_G = -\int_K f \partial_i g \, dv_G \quad \forall f, g \in \mathcal{D}(K)$$

If $f, g \in \mathcal{D}(K)$, the boundary term in the last formula cancels and justifies the following definition:

Definition 6. Given a function $f \in H^n(K)$ and α a multi-index. $g \in H^{n-|\alpha|}(X)$ is called the α^{th} weak derivative of f if it satisfies:

$$\int_K g\varphi \, dv_G = (-1)^{|\alpha|} \int_K f \frac{\partial^{|\alpha|}\varphi}{\partial^\alpha x} \, dv_G \quad \forall \varphi \in \mathcal{D}(K) \tag{1.9}$$

and is denoted:

$$g = \frac{\partial^{|\alpha|} f}{\partial^\alpha x}$$

Theorem 7. *$H^n(K)$ associated with the following inner product is a Hilbert space:*

$$(f,g)_{n,K} = \sum_{l=0\ldots n} \int_K \langle D^l f, D^l g \rangle \, dv_G \tag{1.10}$$

Proof. Evident with our definition of $H^n(K)$. □

Theorem 8 (Sobolev embedding Theorem and Rellich-Kondrachov compactity Theorem)**.**
For $n \geq 0$, $H^n(K) \hookrightarrow L^2(K)$ is a compact embedding.
For $n > k+1$, $H^n(K) \hookrightarrow C^k(\overline{K})$ is a compact embedding.

Proof. For an open set of $\mathbb{R}^n$, see Theorem 7.10. in [GT77] page 148 and its Corollary 7.11. page 151 and Theorem 7.22. page 160 (keeping in mind that the dimension of X is 2). For the case of K being a compact manifold, see Paragraphs 3, 7 and 10 in Chapter 2 of [Aub82]. □

The function space $L^2(K)$ is "traditionally" defined as follow: $L^2(K) = \{f, \int_K f^2 < \infty\}$. It is actually the same function space as the space $L^2(K)$ we previously defined. If we indeed admit the "traditional" definition, the density of $\mathcal{D}(K)$ in $L^2(K)$ is a well-known theorem of functional analysis. Reciprocally, any differentiable function has a finite norm $\|.\|_{0,K}$ on K.

The function space $H^1(K)$ is often defined as follows: $H^1(K) = \{f, \int_K f^2 + |\nabla f|^2 < \infty\}$. It is also the same function space as the $H^1(K)$ we previously defined. It is sufficient to remark that $\langle Df, Df\rangle = \langle df, df\rangle = \langle \nabla f, \nabla f\rangle$. And so, we can indifferently define:

$$\begin{aligned} H^1(K) &= \{f \in L^2(K), \int_K f^2 + |\nabla f|^2 < \infty\} \\ &= \{f \in L^2(K), \int_K f^2 + |Df|^2 < \infty\} \end{aligned}$$

1.3 Weak Form of the Spectral Problem

Since we can not find solutions on X to the Spectral Problem 1.11, it is as usual reformulated in a "weak formulation": meaning that the function space where we find the solutions is greater than $C^\infty(X)$ and is actually $H^1(X)$ (we will see afterwards that these two formulations are actually equivalent). Recall that the spectral problem is to find $f \in C^\infty(X)$ and $\lambda \in \mathbb{R}$ such that:

$$\Delta f = \lambda f \tag{1.11}$$

Given a function $g \in C^\infty(X)$, then:

$$\begin{aligned} \Delta f = \lambda f \Rightarrow\ & (\Delta f)g = \lambda fg \\ \Rightarrow & \int_X \langle df, dg\rangle = \lambda \int_X fg \\ \Leftrightarrow & \int_X \langle \nabla f, \nabla g\rangle = \lambda \int_X fg \end{aligned}$$

Expressed in this form, the weakest condition we can expect for f is to be in $H^1(X)$. It is moreover known that the eigenfunction associated with the eigenvalue 0 is the constant function. For a non-zero eigenvalue, it is easy to check that the average of f has to be zero on X (for example, replacing g by $\tilde{g} = g + c$ where $c \in \mathbb{R}$). We can also recall the well-known theorem of linear algebra stating that the eigenfunctions are orthogonal. That is why we have to define the Sobolev Spaces of null-average functions, orthogonal to the subspace spanned by the constant function:

Definition 9. For all $m \in \mathbb{N}, H_0^m(X)$ is the function subspace of $H^m(X)$ with zero average.

The weak formulation of the Spectral Problem reads thus: find $f \in H_0^1(X)$ and $\lambda \in \mathbb{R}$ such that for all $g \in H^1(X)$:

$$\int_X \langle df, dg \rangle dv_G = \lambda \int_X fg dv_G \tag{1.12}$$

This problem has solutions and these solutions satisfy the Spectral Problem in its "strong formulation" (Equation 1.11). We recall hereafter how we obtain them.

1.4 Existence of the Solutions

To show the existence of the solutions we follow the method described in Paragraph 6.2 page 135 of [RT98]. As an introduction, we recall two theorems from linear algebra and functional analysis that are required to fulfill our aim.

With the first theorem, we will prove the existence of solutions to the Spectral Problem in its weak formulation. Given $(V, \langle . , . \rangle)$ a Hilbert space, a linear operator $T : V \to V$ is bounded if:

$$\|T\| = \sup_{v \in V \setminus \{0\}} \frac{\|Tv\|}{\|v\|} < \infty,$$

symmetric if:

$$\forall v, w \in V, \quad \langle Tv, w \rangle = \langle v, Tw \rangle,$$

and compact if: for any bounded sequence in V it possible to extract a convergent subsequence from the image sequence.

Theorem 10 (Spectral Theorem for Operators)**.** *Given $(V, \langle . , . \rangle)$ a Hilbert space of infinite dimension* [3] *and T a linear, compact and symmetric operator such that $\|T\| > 0$, then there exists an orthonormal hilbertian basis $\{e_n\}_{n \in \mathbb{N}}$ of V and a positive decreasing real sequence $\{\mu_n\}_{n \in \mathbb{N}}$ such that:*

i) $\forall n \in \mathbb{N}$, *e_n is an eigenvector of T:* $Te_n = \mu_n e_n$.

ii) $\lim_{n \to \infty} \mu_n = 0$.

iii) Every eigenvalue of T is in the sequence $\{\mu_n\}$.

[3] in the finite case, the modification is obvious

iv) Every eigen subspace has a finite dimension.

The second theorem implies that these solutions also are solutions of the Spectral Problem in its strong formulation. A 2^{nd} order linear differential operator L on a Riemmannian compact manifold M of dimension N is said to be elliptic if in all coordinate charts it is written:

$$L(x) = a^{ij}(x)\frac{\partial^2}{\partial x^i \partial x^j} + b^k(x)\frac{\partial}{\partial x^k} + c(x)$$

with the following properties: all the functions a_{ij}, b^k, c are differentiable functions on M and $\exists H > 0$ such that $\forall x$ and $\forall \xi = (\xi_1, \ldots, \xi_N) \in \mathbb{R}^N$, $\frac{1}{H}\|\xi\|^2 \leq a^{ij}(x)\xi_i\xi_j \leq H\|\xi\|^2$.

Such an operator works naturally on the $C^{n+2}(K)$ function space, $L : C^{n+2}(K) \to C^n(K)$. However, it has a natural extension to the Sobolev Spaces, considering L as a bounded operator, $L : H^{n+2}(K) \to H^n(K)$ and the derivatives in the weak sense.

Theorem 11 (Elliptic Regularity Theorem)**.** *Given L a 2^{nd} order linear differential operator on a compact Riemannian manifold M, then there exists a constant $C_{M,L}$ such that for all $f \in H^{n+2}(M)$:*

$$\|f\|_{n+2,M} \leq C_{M,L}(\|f\|_{0,M} + \|Lf\|_{n,M}) \tag{1.13}$$

Proof. See Theorem 8.8. p. 173 in [GT77] or Paragraph 6 of Chapter 3 in [Aub82]. □

It is easy to use this last theorem to prove the regularity of the solutions of the Spectral Problem since the Laplacian is an elliptic operator. It is, however, not a compact operator, which forbids us to directly use the first theorem to prove the existence of the solutions. We have to make a detour, defining a compact operator from the Spectral Problem, which will finally give us the existence of the solutions.

The two last theorems we need are simply tools to go through this detour.

Theorem 12 (Riez's Representation Theorem)**.** *For every continuous linear functional F on a Hilbert space V, there exists a unique element $f \in V$ such that $\forall x \in V$, $F(x) = \langle f, x\rangle$. Moreover $\|F\| = \|f\|$.*

Proof. See Theorem 5.7. page 77 in [GT77]. □

Theorem 13 (Poincaré Inequality)**.** *Given M, a compact Riemannian manifold, then there exists a constant C_P (See Equation 1.18 for its expression) such that:*

$$\left\|f-\bar{f}\right\|_{0,M} \leq C_p \left\|\nabla f\right\|_{0,M} \tag{1.14}$$

where $\bar{f}=\frac{\int_M f dv_G}{\int_M dv_G}$ is the average of f.

Proof. See page 157 in [GT77]. □

With the Poincaré inequality, $(\nabla f,\nabla g)_{0,X}$ becomes an inner product on $H^1_0(X)$, whose induced norm is equivalent to $\|.\|_{1,X}$:

$$\frac{1}{(1+C_P)^2}\left\|f\right\|^2_{1,X} \leq (\nabla f,\nabla f)_{0,X} = |f|^2_{1,X} \leq \left\|f\right\|^2_{1,X}$$

For a given function $f \in L^2_0(X)$, the linear functional $F_f : g \rightarrow F_f(g) = \int_X fg\, dv_G$ is obviously continuous on $L^2_0(X)$. It suffices to apply the Cauchy-Schwarz inequality to prove it : $(\int_X fg)^2 \leq \int_X f^2 \int_X g^2$. As $H^1(X) \hookrightarrow L^2(X)$ is a compact embedding, F_f is also continuous on $H^1_0(X)$ (we prove it again hereafter when we prove that T is bounded). From the Riez's Representation Theorem 12, there exists a unique function $\tilde{f} \in H^1_0(X)$ such that:

$$(\nabla \tilde{f},\nabla g)_{0,X} = F_f(g) \quad \forall g \in H^1_0(X)$$

It is then possible to define the linear operator T:

$$\begin{array}{rccc} T: & L^2_0(X) & \rightarrow & H^1_0(X) \\ & f & \mapsto & Tf=\tilde{f} \end{array}$$

T is characterized by the equation:

$$(\nabla Tf,\nabla g)_{0,X} = \int_X fg\, dv_G \quad \forall g \in H^1(X) \tag{1.15}$$

Finally, the Spectral Problem then becomes:

$$f=\lambda Tf$$

To show the existence of the solutions, one only needs to prove that T is a positive, symmetric and compact operator and then to apply the Spectral Theorem 10 to T.

Lemma 14. On $H^1_0(X)$ provided with the inner product $(\nabla.\,,\nabla.)_{0,X}$, T is positive, symmetric, bounded and compact operator.

Proof. We prove successively the different properties:
T is positive: given $f \in H_0^1(X)$, by the Cauchy-Schwarz inequality,

$$\begin{array}{rrcl} & (\nabla Tf, \nabla f)_{0,X} & \leq & |Tf|_{1,X} \, |f|_{1,X} \\ \Leftrightarrow & \|f\|_{0,X}^2 & \leq & |Tf|_{1,X} \, |f|_{1,X} \\ \Rightarrow & 0 & < & |Tf|_{1,X} \end{array}$$

T is symmetric: given $f, g \in H_0^1(X)$,

$$(\nabla Tf, \nabla g)_{0,X} = \int_X fg = \int_X gf = (\nabla Tg, \nabla f)_{0,X} = (\nabla f, \nabla Tg)_{0,X}$$

T is bounded: given $f \in L^2(X)$,

$$\begin{aligned} \|F_f\| &= \sup_{g \in H^1(X),\, g \neq 0} \frac{\left| \int_X fg \right|}{|g|_{1,X}} \\ &\leq \sup_{g \in H^1(X),\, g \neq 0} \|f\|_{0,X} \frac{\|g\|_{0,X}}{|g|_{1,X}} \\ &\leq C_P \|f\|_{0,X} \end{aligned}$$

(where C_P is again the Poincaré's constant). In the next equation, we use the characterization 1.15 of T:

$$|Tf|_{1,X}^2 = (\nabla Tf, \nabla Tf)_{0,X} = \int_X f\, Tf \leq \|F_f\| \, |Tf|_{1,X}$$

because, from the definition of $\|F_f\|$:

$$\|F_f\| \geq \frac{\left| \int_X f\, Tf \right|}{|Tf|_{1,X}}$$

Thus:

$$|Tf|_{1,X} \leq \|F_f\| \leq C_P \|f\|_{0,X} \leq C_P^2 \, |f|_{1,X}$$

T is compact: Given $\{f_n\}_{n\in\mathbb{N}}$ a bounded sequence in $H_0^1(X)$. As $H^1(X) \hookrightarrow L^2(X)$ is a compact embedding, it is possible to extract from this sequence a subsequence, which converges in $L^2(X)$. As T is a bounded linear operator, it is also continuous and the image of this convergent subsequence is also convergent. T is thus compact. □

Theorem 15 (Spectral Theorem for the Laplacian)**.** *There exists an orthonormal Hilbert basis $\{\varphi_n\}_{n\in\mathbb{N}}$ of $L_0^2(X)$ and a sequence $\{\lambda_n\}_{n\in\mathbb{N}}$ of elements of $\mathbb{R}$, such that:*

i) $\varphi_n \in C^\infty(X)$.

ii) $(\varphi_n, \varphi_m)_{0,X} = \int_X \varphi_n \varphi_m = \delta_{nm}$.

iii) $\Delta \varphi_n = \lambda_n \varphi_n$.

iv) $E_n = \{f \in L_0^2(X), \Delta f = \lambda_n f\}$ *has a finite dimension.*

v) $\{\lambda_n\}_{n\in\mathbb{N}}$ *is a increasing positive sequence and* $\lambda_n \underset{n\to\infty}{\longrightarrow} \infty$.

Proof. From Lemma 14, it is possible to apply the Spectral Theorem for Operators 10 to the operator T, when it is defined on $H_0^1(X)$ provided with the $(\nabla. , \nabla.)_{0,X}$ inner product. Its eigenvalues $\{\mu_n\}_{n\in N}$ form a decreasing sequence of positive elements converging to 0 and there exists a Hilbert basis $\{\psi_n\}_{n\in\mathbb{N}}$ of $H_0^1(X)$, orthonormal for the $(\nabla. , \nabla.)_{0,X}$ inner product such that:

$$T\psi_n = \mu_n \psi_n$$

Let us define:

$$\lambda_n = \frac{1}{\mu_n}$$
$$\varphi_n = \sqrt{\lambda_n}\psi_n$$

Then $\forall g \in H^1(X)$:

$$\begin{array}{rrcl} & (\nabla T\varphi_n, \nabla g)_{0,X} & = & \int_X \varphi_n g \\ \Leftrightarrow & (\sqrt{\lambda_n}\nabla T\psi_n, \nabla g)_{0,X} & = & \int_X \varphi_n g \\ \Leftrightarrow & (\sqrt{\lambda_n}\mu_n \nabla \psi_n, \nabla g)_{0,X} & = & \int_X \varphi_n g \\ \Leftrightarrow & (\nabla \varphi_n, \nabla g)_{0,X} & = & \lambda_n \int_X \varphi_n g \end{array}$$

φ_n is thus a weak solution of the Spectral Problem. From the Elliptic Regularity Theorem 11, we deduce that φ_n is a differentiable function of X. And finally:

$$\begin{aligned} (\varphi_n, \varphi_m)_{0,X} &= (\nabla T\varphi_n, \nabla \varphi_m)_{0,X} \\ &= (\sqrt{\lambda_n}\nabla T\psi_n, \sqrt{\lambda_m}\nabla \psi_m)_{0,X} \\ &= \sqrt{\lambda_n}\sqrt{\lambda_m}\,\mu_n(\nabla \psi_n, \nabla \psi_m)_{0,X} \\ &= \delta_{nm} \end{aligned}$$

□

Proposition 16 (Eigenvalues Characterization)**.** The eigenvalues are moreover characterized by:

$$\lambda_m = \min_{E_m \in \mathcal{V}_m} \max_{\substack{f \in E_m \\ f \neq 0}} \frac{|f|_{1,X}^2}{\|f\|_{0,X}^2} \tag{1.16}$$

where $\mathcal{V}_m$ is the set of the m-dimensional subspaces E_m of $H_0^1(X)$.

Proof. See page 139 in [RT98]. □

The quotient:

$$\mathcal{R}(f) = \frac{|f|_{1,X}^2}{\|f\|_{0,X}^2} \tag{1.17}$$

is named the Rayleigh Quotient.

Remark. From this characterization, it is possible to express the constant of the Poincaré's Inequality Theorem 13 on X with the first eigenvalue. If $m = 1$ in the preceding theorem, then $\mathcal{V}_1$ is the set of all 1-dimensional of $H_0^1(X)$ and for a non-zero function in any E_1:

$$\begin{aligned}\frac{|f|_{1,X}^2}{\|f\|_{0,X}^2} &= \frac{(\nabla f, \nabla f)_{0,X}}{\|f\|_{0,X}^2} \\ &= \frac{(\nabla \alpha f, \nabla \alpha f)_{0,X}}{\|\alpha f\|_{0,X}^2}\end{aligned}$$

where $\alpha \in \mathbb{R}$ (and of course non-zero). Thus, $\mathcal{V}_1$ is $H_0^1(X)$ itself and:

$$\lambda_1 = \min_{\substack{f \in H_0^1(X) \\ f \neq 0}} \frac{|f|_{1,X}^2}{\|f\|_{0,X}^2} \tag{1.18}$$

Hence, $\forall f \in H_0^1(X)$:

$$\|f\|_{0,X} \leq \frac{1}{\lambda_1} \|\nabla f\|_{0,X}$$

The rest of this work develops a method to construct approximation functions of the eigenfunctions φ_n. We follow the idea of the Finite Elements Method meaning that we solve the Spectral Problem on a function space of finite dimension. This finite function space is defined in a sufficiently "smart" way, such that we are able to show that the approximate solutions converge to the real solutions of the Spectral Problem. In this regard, we need to triangulate the surface, then construct the finite function space with these triangles by defining its basis elements.

Chapter 2

Triangulation of the surface

2.1 Triangulation on a Surface

The concept of triangulation on a surface is quite intuitive but we need to give it a formal definition. The idea is to build a simplicial complex such that each simplex is included in a coordinate chart of the surface and the set of all the simplexes and their associated coordinate chart in the complex represent an atlas of the surface.

Let us define S the standard simplex of $\mathbb{R}^2$, that is the filled euclidean triangle with vertices $\{a_0 = (0,0), a_1 = (1,0), a_2 = (0,1)\}$. The simplicial abstract complex representing the triangulation is a set $\{S_1 \dots, S_N\}$, composed of identical copies of S, given with the relation between the edges and vertices of each simplex. As X is a compact surface without boundaries, each edge or vertex of each simplex must be shared with another simplex.

Definition 17. A triangulation on X is a simplicial complex and a family of diffeomorphisms π_j with the following properties:

i) $\forall j = 1 \dots N$, $\pi_j : \mathcal{U}_j \to \Omega_j$, where $\mathcal{U}_j$ is an open subset of $\mathbb{R}^2$ containing S and Ω_j is an open subset of X. (In other words, (Ω_j, π_j^{-1}) is a coordinate chart of X).

ii) $\{(\Omega_j, \pi_j^{-1})\}_{j=1\dots N}$ is an atlas of X.

iii) $\forall j = 1 \dots N$, $\pi_j(S) = T_j$ is a triangle on the surface.

iv) $\forall i \neq j$, $T_i \cap T_j$ is either empty, or a common vertex, or a common edge.

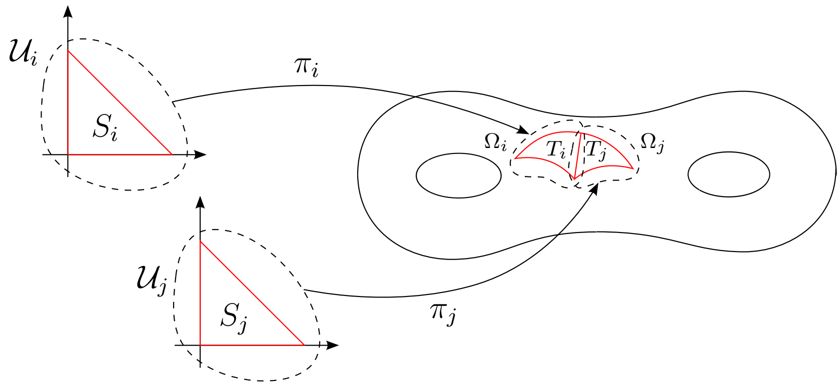

Figure 2.1: Triangulation of the Surface

2.2 Triangulation Algorithm

We take the "opposite way" as in the preceding definition. As discussed in the Introduction, the surface X is defined by its Fenchel-Nielsen parameters and thus seen as a collection of Y-pieces. Each of these Y-pieces is cut into two hexagons. As we have tools to create triangles in $\mathbb{H}$ (See the presentation of the Matrix Model in Appendix A), we will create a geodesic triangulation of these hexagons (triangulation being yet understood in its common sense: a set of triangles). The triangulation of X is then obtained by gluing together all the hexagons.

We point out that the triangles with an edge on two glued sides of two hexagons have to be compatible: they share only a common vertex or a common edge (or nothing). If the twist parameters of a Y-piece are all zero, then we cut it into two identical right-angled hexagons. If not, the decomposition of the Y-pieces is not done as usual along the shortest geodesics, but along geodesics, such that the triangles with an edge on the boundary of the hexagon are compatible with the twist parameter. In the two Figures bellow, we have triangulated the surface described in Chapter 5.2.1 to illustrate the preceding explanation. This surface is given by identical length Fenchel-Nielsen parameters $l_i = 2\text{arccosh}(\sqrt{2}+1)$ and identical twist parameters $t_i = 0.321281$. In Figure 2.2, each Y-pieces is cut in the usual way leading to two identical right-angled hexagons, whereas in Figure 2.3, it is cut a way such that the triangulations of each hexagon are compatible.

The algorithm we present here aims to triangulate a convex compact geodesic polygon domain Ω with all interior angles greater than $\pi/3$, creating triangles as less flat as possible. The isomorphisms of Definition 17 will be defined afterwards in Paragraph 3.2 in Chapter 3. The triangles on the

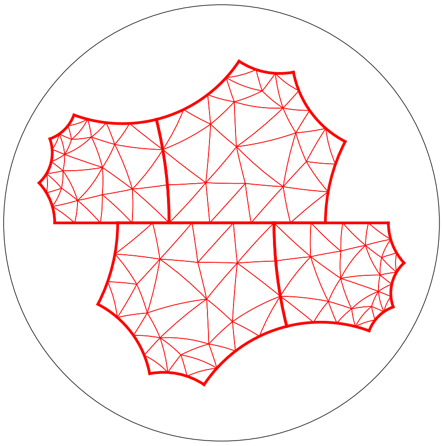

Figure 2.2: Triangulation with right-angled hexagons

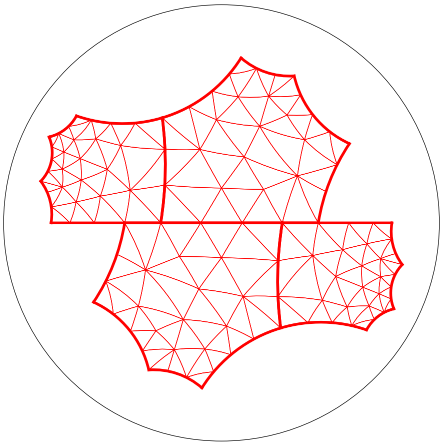

Figure 2.3: Triangulation with deformed hexagons

surface are built by creating a set of vertices in Ω, which satisfy the properies of the ε-net:

Definition 18. Given $\varepsilon \in \mathbb{R}, \varepsilon > 0$, an ε-*net* on a metric space X is a set of points such that:

i) The open balls of radius ε centered on these points cover X.

ii) The open balls of radius $\varepsilon/2$ are pairwise disjoint.

From this definition we can conclude that two points of an ε-net are at a distance greater or equal to ε.

Theorem 19. *Given $\varepsilon > 0$ and any metric space X, then there exists an ε-net on X.*

Proof. Let us define a pre-ε-net: a set of points satisfying condition ii) of the preceding definition. A chain of pre-ε-nets is an ordered set of pre-ε-nets for the inclusion. The union of the pre-ε-nets of a chain is obviously an upper bound for this chain. From the Zorn's Lemma, there exists a maximal pre-ε-net, which actually satisfies the condition i) as well. Supposing it does not, there would exist a non-covered point of X at a distance greater than ε from the other, which could be added to the maximal pre-ε-net. $\square$

Proposition 20. If the metric space X is compact, then the ε-net is finite.

Proof. From Definition 18 an ε-net is a covering. Since X is compact there exists a finite under-covering composed of balls around vertices. If we add a point to the set of vertices of this under-covering, it will be in an open ball of radius ε around another point, and the new set of points will not satisfy ii), thus, the ε-net and the finite under-covering are the same. □

Let us now define the following notations we will use for the algorithm:

- $\mathcal{B}_P^\varepsilon$: open disc of radius ε around P.
- $\mathcal{D}_{P_iP_jP_k}$: open disc defined by the circumcircle of $P_iP_jP_k$.
- P_iP_j : geodesic segment between P_i and P_j (this notation holds only for this chapter).

Remark. In the figures of this chapter, the dotted circles represent the $\mathcal{B}_P^\varepsilon$ whereas the continued line circles represent the $\partial\mathcal{D}_{P_iP_jP_k}$ or circles defined by their diameter

Let us also define the following quantities:

- $s(\Omega)$ the length of the shortest side of Ω. We point out that $s(\Omega) \leq \operatorname{arccosh} 2$, which corresponds to the symmetric hexagon.
- $a(\Omega)$ the shortest distance between two non-intersecting sides of the polygon (If it is an hexagon, then it corresponds to the length of the shortest altitude of Ω).
- ε_0 by the rule :

$$\varepsilon_0 = \min\left\{\frac{1}{3}s(\Omega), a(\Omega)\right\} \tag{2.1}$$

For the triangulation ε is assumed to satisfy:

$$0 < \varepsilon < \varepsilon_0$$

We initiate the triangulation of Ω by the subdivision of the boundary $\partial\Omega$, which provides a set of vertices on $\partial\Omega$, denoted $\mathcal{V}_0$. Each side of Ω is regularly subdivided such that two adjacent points P_i, P_j satisfy:

$$\varepsilon \leq \operatorname{dist}(P_i, P_j) < d_\varepsilon$$

where d_ε is defined by the rule[1]:

$$\cosh(d_\varepsilon) = 2\cosh\varepsilon - 1$$

[1]this condition appears later on in Lemma 23

From this initial situation (the 0-th iteration), we run the algorithm, creating a triangle at each iteration, which satisfies condition ii) of the ε-net. After n iterations, we define:

- $\mathcal{V}_n = \{P_i\}$: set of the vertices of the triangulation.
- $\mathcal{T}_n$: set of the n triangles (at each iteration, a triangle is created).
- $\mathcal{S}_n$: set of the geodesic segments: either the edges of the triangles, or the geodesic arc between two adjacent points of $\mathcal{V}_n$ on $\partial\Omega$.
- $E_n \subset \Omega$: the closed part of Ω already triangulated together with $\partial\Omega$.
- $I_n = \Omega \backslash E_n$: the open part of Ω still to be triangulated.
- The front: the boundary of I_n.

We will show that after each iteration of the algorithm, $\mathcal{V}_n$, $\mathcal{S}_n$ and $\mathcal{T}_n$ satisfy the followings properties:

H1) $\mathcal{V}_n \subset \Omega$.

H2) $\forall P_i, P_j \in \mathcal{V}_n, i \neq j$, $\text{dist}(P_i, P_j) \geq \varepsilon$.

H3) $\forall P_iP_jP_k \in \mathcal{T}_n$, $\mathcal{D}_{P_iP_jP_k} \cap \mathcal{V}_n = \emptyset$.

H4) $\forall P_iP_jP_k \in \mathcal{T}_n$, $\mathcal{D}_{P_iP_jP_k}$ is covered by $\bigcup_{P_i \in \mathcal{V}_n} \mathcal{B}^{\varepsilon}_{P_i}$.

H5) $\forall P_iP_jP_k$ and $P_rP_sP_t \in \mathcal{T}_n$, if $\mathcal{D}_{P_iP_jP_k} = \mathcal{D}_{P_rP_sP_t}$, then $P_iP_jP_k \cap P_rP_sP_t$ is either empty or a vertex of $\mathcal{V}_n$ or a segment of $\mathcal{S}_n$.

We point out that even if the hexagons are not right-angled, their deformation compared to the right-angled hexagon is not large, it is at most a half of a subdivision of the twisted edge, and thus their interior angles are greater than $\pi/3$. Through the hypotheses required for Ω, ε and d_ε and the remark of the last sentence, the initial set of vertices $\mathcal{V}_0$ satisfies all the properties H1 to H5. We point out that H1 to H5 can also be made true for $\mathcal{V}_0$ under less restrictive assumptions.

Proposition 21. If $\mathcal{T}_n$ satisfies H1 to H5, then for two triangles $P_iP_jP_k$ and $P_rP_sP_t$, $P_iP_jP_k \cap P_rP_sP_t$ is either empty or a common vertex or a common edge.

Proof. Consider the circumcircle of these triangles and their intersection.
If $\mathcal{D}_{P_iP_jP_k} \cap \mathcal{D}_{P_rP_sP_t} = \emptyset$ or P (a single point), then $P_iP_jP_k \cap P_rP_sP_t$ is either empty or P.
If $\mathcal{D}_{P_iP_jP_k} \cap \mathcal{D}_{P_rP_sP_t} = \{P, Q\}$ (two points), then by applying the Lemma 22 ii), no edge of $P_iP_jP_k$ intersects an edge of $P_rP_sP_t$. In the limit case of this Lemma, either P or Q is a common vertex or even PQ is a common edge of the two triangles.
If $\mathcal{D}_{P_iP_jP_k} = \mathcal{D}_{P_rP_sP_t}$, then by H5, $P_iP_jP_k \cap P_rP_sP_t$ consists only in an edge or a vertex. □

Observe also that H2 implies that $\mathcal{V}_n$ satisfies the condition ii) in the ε-net definition 18 and that H4 implies that a triangle of $\mathcal{T}_n$ has a circumcircle of radius smaller than ε.

Before presenting the algorithm which works by inductions, we want to state three useful Lemmas. The first two hold in general but we put them here because they will not be used elsewhere. For the first one, the configuration is as follows: Given two open discs $\mathcal{D}_1$ and $\mathcal{D}_2$ in the unit disc $\mathbb{D}$, such that $\partial\mathcal{D}_1$ and $\partial\mathcal{D}_2$ intersect in exactly two points P and Q. Each circle $\partial\mathcal{D}_1$ and $\partial\mathcal{D}_2$ is divided into two arcs: an interior contained in the other disc and an exterior. The geodesic through P and Q divides the unit disc into two parts, U containing the exterior arc of $\partial\mathcal{D}_1$ and L containing the exterior arc of $\partial\mathcal{D}_2$ (See Fig 2.4).

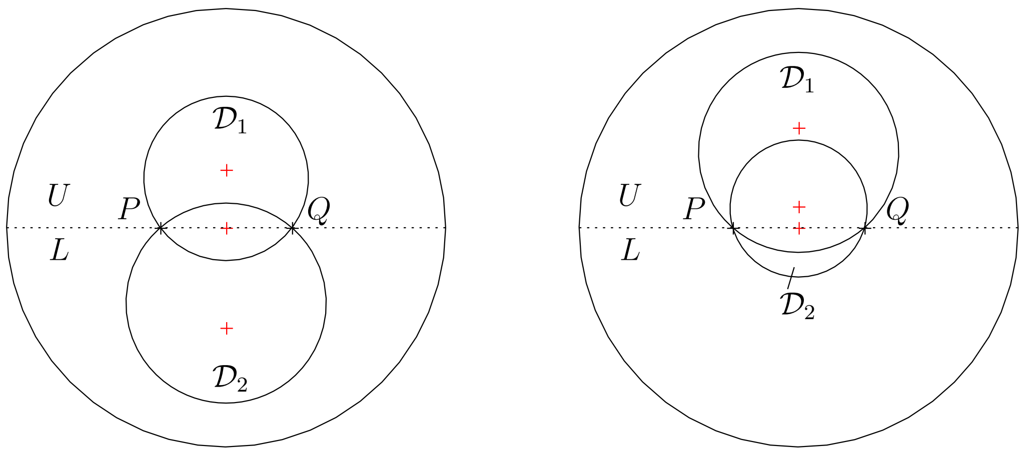

Figure 2.4: Circles inclusions

Lemma 22. With the preceding configuration:

i) $\mathcal{D}_2 \cap U \subset \mathcal{D}_1$ and $\mathcal{D}_1 \cap L \subset \mathcal{D}_2$.

ii) If $A_1, B_1 \in \partial\mathcal{D}_1 \backslash \overline{\mathcal{D}_2}$ and $A_2, B_2 \in \partial\mathcal{D}_2 \backslash \overline{\mathcal{D}_1}$, then the cords A_1B_1 and A_2B_2 do not intersect each other.

Proof. We move the two circles isometrically such that P, Q lie on a straight line in $\mathbb{D}$. The property i) then becomes a well-know property of the Euclidean circles, and ii) comes from the fact that U and L are geodesically convex. □

Lemma 23. Given a triangle PQR such that $\operatorname{dist}(P, R) = \operatorname{dist}(Q, R) = \varepsilon$, and $\operatorname{dist}(P, Q) \leq d_\varepsilon$ (See Fig. 2.5), then:

$$\mathcal{D}_{PQR} \subset \mathcal{B}_P^\varepsilon \cup \mathcal{B}_Q^\varepsilon.$$

Proof. In the limit case the point R has to be the symmetric point around PQ of the second intersection between $\mathcal{B}_P^\varepsilon$ and $\mathcal{B}_Q^\varepsilon$. Applying Lemma 22 i) to $\mathcal{D}_{PQR}$ and $\mathcal{B}_P^\varepsilon$ then to $\mathcal{D}_{PQR}$ and $\mathcal{B}_Q^\varepsilon$, we can conclude that $\mathcal{D}_{PQR}$ is covered as required. Denoting $d_\varepsilon = \operatorname{dist}(P, Q)$ and applying the trigonometry rules to the triangle PQR lead to:

$$\begin{aligned} & \cosh^2 \frac{d_\varepsilon}{2} = \cosh \varepsilon \\ \Leftrightarrow \quad & \cosh d_\varepsilon = 2\cosh \varepsilon - 1 \end{aligned}$$

□

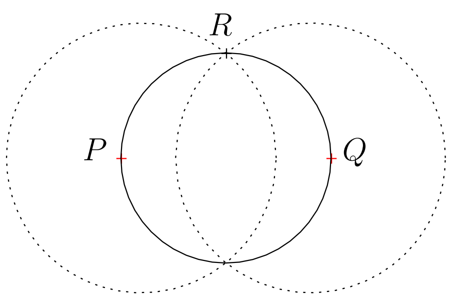

Figure 2.5: Limit case for $\mathcal{D}_{PQR}$ to be covered by $\mathcal{B}_P^\varepsilon \cup \mathcal{B}_Q^\varepsilon$

Lemma 24. Given two points P_i, P_j such that $P_iP_j \in \mathcal{S}_n$ and a third point P such that $\mathcal{D}_{P_iP_jP}$ does not contain any point of $\mathcal{V}_n$. If $P_iP_j \in \partial\Omega$, we then also include the hypothesis that at least one of the geodesic segments P_iP, P_jP enters into Ω. Then :

$$P \in \Omega \cup \big(\bigcup_{P_k \in \mathcal{V}_n} \mathcal{B}^{\varepsilon}_{P_k} \big)$$

Proof. Suppose P is outside of Ω. Then $\mathcal{D}_{P_iP_jP}$ intersects $\partial\Omega$. Moving along $\partial\mathcal{D}_{P_iP_jP}$ from P in either direction, we reach two intersections of $\partial\mathcal{D}_{P_iP_jP}$ and $\partial\Omega$, such that the segment between these two intersections is a part $\partial\Omega$. As $\mathcal{D}_{P_iP_jP}$ does not contain any point of $\mathcal{V}_n$, these two intersections lie on a segment of $\mathcal{S}_n$, say P_rP_s (Maybe P_i or P_j is P_r or P_s, but $\{P_i, P_j\} \neq \{P_r, P_s\}$ because of the additional hypothesis if $P_iP_j \in \partial\Omega$). From H2 and Lemma 23, P_i and P_j have to be outside the disc of diameter P_rP_s. By Lemma 22 i), P lies in the disc of diameter P_rP_s and by Lemma 23, $P \in \bigcup_{P_k \in \mathcal{V}_n} \mathcal{B}^{\varepsilon}_{P_k}$. $\square$

Let us now begin with the algorithm. Given two adjacent points of the front P_1 and P_2, that is $P_1P_2 \in \mathcal{S}_n$ (we use the notation P_1, P_2 here even if they are not the two first points of $\mathcal{V}_n$, since it will simplify the reading of the following proofs). If they are both on $\partial\Omega$, we call U the part of the unit disc containing Ω around P_1P_2. If they are both not on the front, then there exists a point P_k such that $P_1P_2P_k \in \mathcal{T}_n$, and we call L the part of the unit containing $P_1P_2P_k$ (See Fig. 2.6).

2.2.1 Step One

From P_1 and P_2 , we construct P_{test} in U at distance ε from P_1 and P_2. (See Fig. 2.6).

Question : Is there a point of $\mathcal{V}_n$ in $B^{\varepsilon}_{P_{test}}$?

Case 1 : No. Then we set $\mathcal{V}_{n+1} = \mathcal{V}_n \cup P_{test}$, $\mathcal{S}_{n+1} = \mathcal{S}_n \cup P_1P_{test} \cup P_2P_{test}$ and $\mathcal{T}_{n+1} = \mathcal{T}_n \cup P_1P_2P_{test}$. And go to the beginning of the algorithm.

Proposition 25. $\mathcal{V}_{n+1}$ and $\mathcal{T}_{n+1}$ satisfy H1, H2, H3, H4, H5.

Proof. We first state $H3$ because we need this hypothesis to apply the Lemma 24 for the proof of $H1$.

H3 : $\mathcal{D}_{P_1P_2P_{test}} \cap U \subset \mathcal{B}_{P^{\varepsilon}_{test}}$ and $\mathcal{B}^{\varepsilon}_{P_{test}} \cap \mathcal{V}_n = \emptyset$ by the hypothesis we made on $\mathcal{B}^{\varepsilon}_{P_{test}}$. If $P_1, P_2 \in \partial\Omega$, then $(\mathcal{D}_{P_1P_2P_{test}} \cap L) \cap \Omega = \emptyset$, hence can not contain

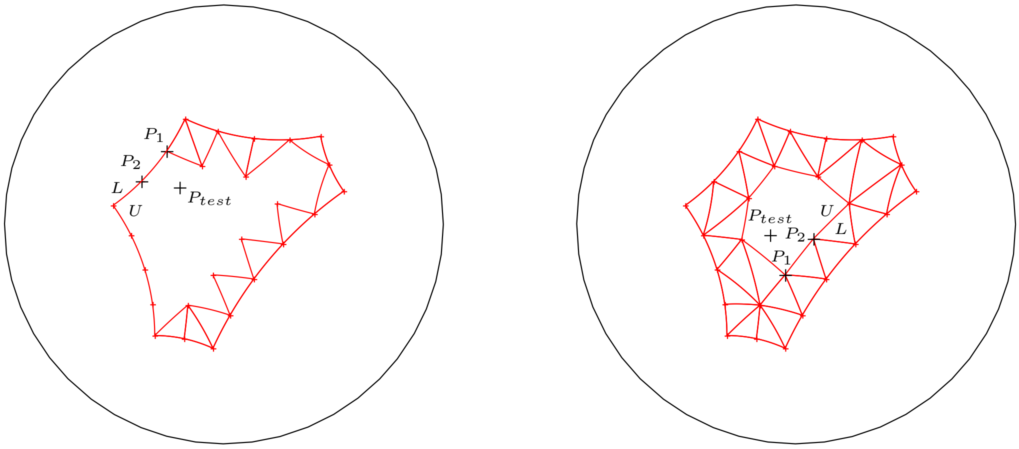

Figure 2.6: P_{test} at distance ε from P_1 and P_2

any point of $\mathcal{V}_n$. If P_1, P_2 are not both on the boundary, then there exists $P_k \in L$ such that $P_1P_2P_k \in \mathcal{T}_n$ and $\mathcal{D}_{P_1P_2P_{test}} \cap L \subset \mathcal{D}_{P_1P_2P_k}$ by Lemma 22 i). Finally $\mathcal{D}_{P_1P_2P_k} \cap \mathcal{V}_n = \emptyset$ by H3 for $P_1P_2P_k$, therefore $(\mathcal{D}_{P_1P_2P_{test}} \cap L) \cap \mathcal{V}_n = \emptyset$.

We now have to prove that P_{test} is not in any circumdisc of a triangle of $\mathcal{T}_n$. Suppose $\mathcal{D}_{P_rP_sP_t}$ contains P_{test} where $P_rP_sP_t \in \mathcal{T}_n$. As $\mathcal{B}^{\varepsilon}_{P_{test}}$ is empty, then P_{test} (now as a point of $\mathcal{D}_{P_rP_sP_t}$) would not be covered, which contradicts H4 for $\mathcal{D}_{P_rP_sP_t}$.

H1 : We know from Lemma 24 that $P_{test} \in \Omega \cup (\bigcup_{P_j \in \mathcal{V}_n} \mathcal{B}^{\varepsilon}_{P_j})$. If it is not in Ω then it is in a particular $\mathcal{B}^{\varepsilon}_{P_r}$ and thus is at a distance smaller than ε from P_r and this contradicts the hypothesis we made on P_{test}.

H2 : By construction.

H4 : If $P_1, P_2 \in \partial\Omega$, then the proof comes from Lemma 23. If P_1, P_2 are not both on the boundary, then $\mathcal{D}_{P_1P_2P_{test}} \cap U \subset \mathcal{B}^{\varepsilon}_{P_{test}}$. Moreover, $\mathcal{D}_{P_1P_2P_{test}} \cap L \subset \mathcal{D}_{P_1P_2P_k}$ and $\mathcal{D}_{P_1P_2P_k} \subset \cup_{P_i \in \mathcal{V}_N} \mathcal{B}^{\varepsilon}_{P_i}$ by hypothesis H4 on $\mathcal{D}_{P_1P_2P_k}$.

H5 : If $\mathcal{D}_{P_1P_2P_{test}} = \mathcal{D}_{P_iP_jP_k}$, then $P_i, P_j, P_k \in L$ because $\mathcal{D}_{P_1P_2P_{test}} \cap U \subset \mathcal{B}^{\varepsilon}_{P_{test}}$. □

Case 2 : Yes. There exists at least one vertex of $\mathcal{V}_n$ in $\mathcal{B}^{\varepsilon}_{P_{test}}$. We go to step 2.

2.2.2 Step Two

We search, among the points of $\mathcal{V}_n$ in $\mathcal{B}^{\varepsilon}_{P_{test}}$, the point, denoted P_i, such that the oriented distance between the centre of $\mathcal{D}_{P_1P_2P_i}$ and the geodesic through P_1 and P_2 is minimal (distances are positive in U, negative in L).

If there are several of these points, at least one is in U (see the proof of the Proposition 26), and we choose one, also denoted P_i, such that P_1P_i and P_2P_i do not intersect any edge of a triangle (from this set of candidates, P_i is actually one of the two nearest points to P_1P_2). We point out that, from a programming point of view, this last hypothesis is quite easy to test applying Proposition 53 iii and iv in Appendix A.

Question: Is $\mathcal{D}_{P_iP_1P_2}$ covered by $\bigcup_{P_j \in \mathcal{V}_n} \mathcal{B}^{\varepsilon}_{P_j}$?

Case 1 : Yes. (See Fig. 2.7) Then we set $\mathcal{V}_{n+1} = \mathcal{V}_n$, $\mathcal{S}_{n+1} = \mathcal{S}_n \cup P_1P_i \cup P_2P_i$ (one of P_1P_i, P_2P_i is eventually already in $\mathcal{S}_n$) and $\mathcal{T}_{n+1} = \mathcal{T}_n \cup P_1P_2P_i$. And go to the beginning of the algorithm.

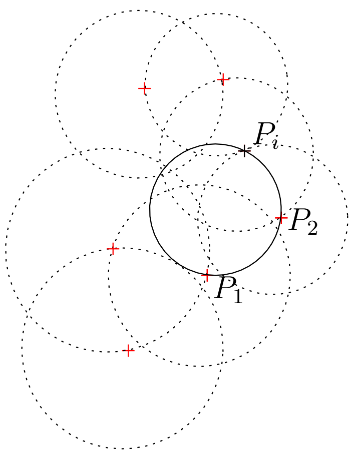

Figure 2.7: $\mathcal{D}_{P_1P_2P_i}$ is covered by $\bigcup_{P_j \in \mathcal{V}_n} \mathcal{B}^{\varepsilon}_{P_j}$

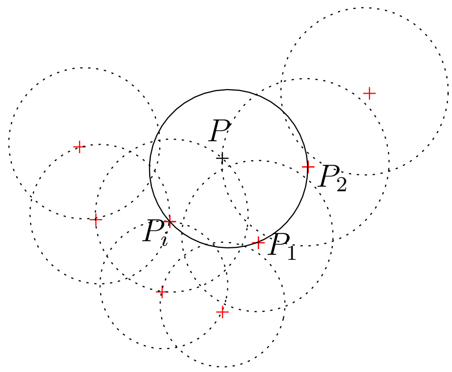

Figure 2.8: $\mathcal{D}_{P_1P_2P_i}$ is not covered by $\bigcup_{P_j \in \mathcal{V}_n} \mathcal{B}^{\varepsilon}_{P_j}$

Proposition 26. $\mathcal{V}_{n+1}$ and $\mathcal{T}_{n+1}$ satisfy H1, H2, H3, H4, H5.

Proof. H1 and H2 : We do not change $\mathcal{V}_n$, the hypothesis hold.

H3 : We prove first that $P_i \in U$. If there are several points on $\partial\mathcal{D}_{P_1P_2P_i}$ and if we suppose that they all lie in L, at least one, say P_k is such that $P_1P_2P_k \in \mathcal{T}_n$ (maybe $P_k = P_i$). Then $\mathcal{D}_{P_1P_2P_k}$ would contain P_{test}, which would not be covered and this contradicts H4 for $\mathcal{D}_{P_1P_2P_k}$.

By construction $\mathcal{D}_{P_1P_2P_i} \cap U$ does not contain any point of $\mathcal{V}_n$. If $P_1, P_2 \in \partial\Omega$ $(\mathcal{D}_{P_1P_2P_i} \cap L) \cap \Omega = \emptyset$. If $P_1P_2 \notin \partial\Omega$ there exists $P_k \in L$ such that

$P_1P_2P_k \in \mathcal{T}_n$ and $\mathcal{D}_{P_1P_2P_i} \cap L \subset \mathcal{D}_{P_1P_2P_k}$, therefore $\mathcal{D}_{P_1P_2P_i} \cap L$ can not contain any vertex of $\mathcal{V}_n$ by H3 on $P_1P_2P_k$.

H4 : By hypothesis we made on $\mathcal{D}_{P_1P_2P_i}$.

H5 : By the choice of P_i we have done. □

Case 2 : No. (See Fig. 2.8) We go to step 3.

2.2.3 Step Three

We find the point P in the uncovered part $\mathcal{P}$ of $\mathcal{D}_{P_iP_1P_2}$, such that the oriented distance between the centre of $\mathcal{D}_{P_1P_2P}$ and the geodesic through P_1 and P_2 is minimal. If there are many, choose one of them.

Then we set $\mathcal{V}_{n+1} = \mathcal{V}_n \cup P$, $\mathcal{S}_{n+1} = \mathcal{S}_n \cup P_1P \cup P_2P$ and $\mathcal{T}_{n+1} = \mathcal{T}_n \cup P_1P_2P$.

Proposition 27. $\mathcal{V}_{n+1}$ and $\mathcal{T}_{n+1}$ satisfy H1, H2, H3, H4,H5.

Proof. As for Proposition 25, we first state $H3$.

H3 : $P \in U$ because $\mathcal{D}_{P_1P_2P_i} \cap L$ is covered, either by $\mathcal{D}_{P_1P_2P_{test}}$ if $P_1, P_2 \in \partial\Omega$ (this last disc being covered by definition of ε and Lemma 23), or by $\mathcal{D}_{P_1P_2P_k}$ otherwise (where P_k is still the "famous" vertex in L such that $P_1P_2P_k \in \mathcal{T}_n$). $\mathcal{D}_{P_1P_2P} \cap U \subset \mathcal{D}_{P_1P_2P_i}$ and $\mathcal{D}_{P_1P_2P_i} \cap \mathcal{V}_n = \emptyset$. $(\mathcal{D}_{P_1P_2P_i} \cap L) \cap \Omega = \emptyset$ if $P_1, P_2 \in \partial\Omega$ and $\mathcal{D}_{P_iP_1P_2} \cap L \subset \mathcal{D}_{P_1P_2P_k}$ otherwise, therefore $\mathcal{D}_{P_iP_1P_2} \cap L$ can not contain any vertex of $\mathcal{V}_n$.

For the same reasons as in Proposition 25, P is not in a circumdisc of an existing triangle.

H1 : For the same reasons as in Proposition 25.

H2 : By construction.

H4 : $\mathcal{D}_{P_1P_2P} \cap U$ is covered by construction. $\mathcal{D}_{P_1P_2P} \cap L$ is covered, as we explained in H3.

H5 : For the same reasons as in Proposition 25. □

From a computational point of view, finding the point P in the uncovered part $\mathcal{P}$ (that is finding one point in an infinite set of points) is an extremely difficult task. Fortunately, it is possible to prove that P is actually an intersection of the type $\partial\mathcal{B}^{\varepsilon}_{P_r} \cap \partial\mathcal{B}^{\varepsilon}_{P_s}$, which transforms the preceding problem into a discrete and finite problem.

$\mathcal{P}$ is composed of one or more connected components whose boundaries are made up of the $\partial\mathcal{B}^{\varepsilon}_{P_j}$. Let us consider the disc $\mathcal{D}$ of diameter P_1P_2. If $P \notin \mathcal{D}$ (see Fig 2.9), increase the radius of $\mathcal{D}$ moving its centre along the perpendicular bisector of P_1P_2 toward U until $\partial\mathcal{D}$ reaches the boundary of

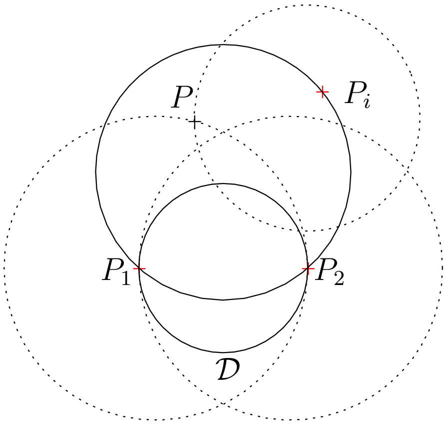

Figure 2.9: P is outside $\mathcal{D}$

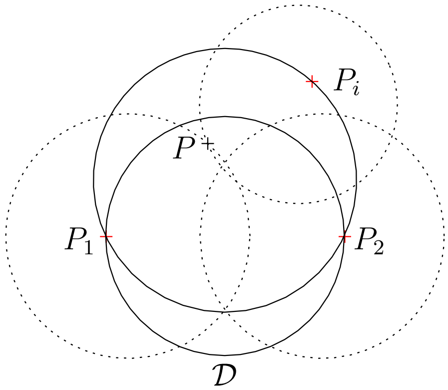

Figure 2.10: P is inside $\mathcal{D}$

uncovered part $\mathcal{P}$ of $\mathcal{D}_{P_1P_2P_i}$. Let us suppose that the contact point P (if there are more than one, it does not change the following argumentation) between $\partial\mathcal{D}$ (or now $\mathcal{D}_{P_1P_2P}$) and $\mathcal{P}$ is not an intersection of the type $\partial\mathcal{B}^{\varepsilon}_{P_r} \cap \partial\mathcal{B}^{\varepsilon}_{P_s}$. In this case, $\mathcal{D}_{P_1P_2P}$ is tangent to an edge of $\mathcal{P}$, given by, say $\partial\mathcal{B}^{\varepsilon}_{P_n}$. Hence, $\mathcal{D}_{P_1P_2P}$ and $\mathcal{B}^{\varepsilon}_{P_n}$ are two tangent discs. If $\mathcal{D}_{P_1P_2P} \cap \mathcal{B}^{\varepsilon}_{P_n} = \emptyset$, their would be a part of $\mathcal{P}$ in the interior of $\mathcal{D}_{P_1P_2P}$, which contradicts the definition of $\mathcal{D}_{P_1P_2P}$. If $\mathcal{D}_{P_1P_2P} \cap \mathcal{B}^{\varepsilon}_{P_n} \neq \emptyset$, then either $P, P_1, P_2 \in \mathcal{B}^{\varepsilon}_{P_n}$ if $\mathcal{D}_{P_1P_2P} \subset \mathcal{B}^{\varepsilon}_{P_n}$, which is excluded by hypothesis H2, or $P_n \in \mathcal{D}_{P_1P_2P}$ is not covered if $\mathcal{B}^{\varepsilon}_{P_n} \subset \mathcal{D}_{P_1P_2P}$.

If $P \in \mathcal{D}$ (See Fig 2.10), increase the radius of $\mathcal{D}$ moving its centre along the perpendicular bisector of P_1P_2 toward L until the boundary of $\mathcal{D}$ reaches the boundary of the uncovered part $\mathcal{P}$ of $\mathcal{D}_{P_1P_2P_i}$. Use the same argument as before.

2.3 Properties of the Triangulation

If the algorithm does not move forward, Ω is triangulated. We denote N the number of triangles obtained at the end of the algorithm and $\mathcal{T}_N$ the associated set of triangles. We also denote I the number of vertices in $\mathcal{V}_N$. The way the algorithm works gives the triangles some geometrical properties. Let us denote ρ the radius of the inscribed circle of a triangle, R the radius of its circumcircle and h the diameter of the triangulation, that is the length of the longest edge in $\mathcal{S}_n$.

Theorem 28. *The triangles in $\mathcal{T}_N$ satisfy the following properties:*

i) The length of their edges is between ε and 2ε.

ii) The circumcircle of each triangle has a radius smaller than ε.

iii) The quotient between the radii of the circumcircle and the inscribed circle satisfies:

$$2 \leq \frac{\sinh R}{\sinh \rho} \leq \frac{2}{2\sqrt{3}-3}(1+O(h^2))$$

Proof. i) From the properties H2 and H4. If an edge of a triangle would indeed be longer than 2ε, then the centre of the circumcircle would not be covered.

ii) From H4 (and for the same reason as in i)).

iii) See Appendix A, paragraph A.6. We prove there that if $h < \frac{2}{3}\text{arccosh}2$ (which is from Equation 2.1 the upper bound for h), the largest value for the quotient is obtained with a triangle with edges of length ε, ε and $2\,\text{arccosh}\frac{\cosh\varepsilon}{\cosh\varepsilon/2}$ and the smallest for an equilateral triangle of length ε. That is:

$$4 \leq \frac{\sinh^2 R}{\sinh^2 \rho} \leq \frac{4}{3(\sqrt{3}-2)^2} + \frac{h^2}{4}$$

We remark that the term $O(h)$ is also and stays small, even if h is not small. Notice also that the values 2 and $\frac{2}{2\sqrt{3}-3^2}$ correspond to the euclidean case.

□

2.4 Triangulation Refinement

Common sense tells us that the smaller the triangulation is, the better the approximation of the eigenvalues and eigenfunctions. In Chapter 4 we will prove that this assumption is true. It would thus be useful to have a generic method to refine the triangulation we obtain with the algorithm. The simplest but smartest method to do so, is to make four triangles from each triangle in the triangulation, dividing each edge into two equal parts (see Fig. 5.3, 5.4, 5.5 and 5.6 in Chapter 5). Doing this, we divide ε and h by 2 and then reduce the quotient $\frac{\sinh R}{\sinh \rho}$, which tends toward its euclidean limit.

Chapter 3

Algebraic Problem

This chapter is perhaps the kernel of this thesis. From the triangulation obtained in the previous chapter, we want to fulfill the requirements of the definition of the triangulation (see the Definition 17), giving a concrete example of the diffeormophisms π_j between each standard simplex of $\mathbb{R}^2$ in the complex and the triangles on the surface.

With the Matrix Model originally discussed by Fenchel in [Fen89] and further developed by Semmler in [ADBS11] associating 2×2 real matrices with null trace to the points and the geodesics of the upper half plane $\mathbb{H}$, the definition of barycentric coordinates on the triangles of the surface will turn out to be straight-forward. The diffeomorphisms then will be the identity diffeomorphism between these barycentric coordinates on the triangles and the usual euclidean barycentric coordinates in the standard simplex of $\mathbb{R}^2$.

We provide a short summary of the basic definitions and properties of the Matrix Model in the first paragraph of this chapter, for further details we refer to Appendix A. The barycentric coordinates on the triangles on the surface not only allow us to define the diffeomorphims π_j of the triangulation definition, but also provide a natural definition for the finite function space where we calculate the approximated eigenvalues and eigenfunctions.

3.1 Matrix Model

Here we recall the principal ideas of the Matrix Model. The isometries of the upper half plane $\mathbb{H}$ are given by the Moebius transformations of the followings types:

$$
\begin{aligned}
z \in \mathbb{H} \mapsto \frac{az+b}{cz+d} \quad \text{if } \det\begin{pmatrix} a & b \\ c & d \end{pmatrix} > 0 \\
z \in \mathbb{H} \mapsto \frac{a\bar{z}+b}{c\bar{z}+d} \quad \text{if } \det\begin{pmatrix} a & b \\ c & d \end{pmatrix} < 0
\end{aligned}
$$

3.1.1 Points and Geodesics

We associate the corresponding matrix $M \in \mathrm{GL}(2,\mathbb{R})$ to a Möbius transformation. We identify a point of $\mathbb{H}$ with the half-turn around this point and the corresponding matrix in $\mathrm{GL}(2,\mathbb{R})$. For a point $p = r + is \in \mathbb{H}$, the corresponding normalized matrix is:

$$
\frac{1}{s}\begin{pmatrix} -r & r^2+s^2 \\ -1 & r \end{pmatrix}
$$

From here on, the letter p will denote either the geometric point in $\mathbb{H}$ or the Möbius transformation corresponding to the half-turn around it, or the corresponding matrix (usually normalized like the preceding one, but not always).

As for the points, we identify a geodesic in $\mathbb{H}$ with the symmetry around it and the corresponding matrix in $\mathrm{GL}(2,\mathbb{R})$. For a geodesic γ defined by the Euclidean circle with center $\rho \in \mathbb{R}$ and radius σ, the corresponding normalized matrix is:

$$
\pm\frac{1}{\sigma}\begin{pmatrix} \rho & -\rho^2+\sigma^2 \\ 1 & \rho \end{pmatrix}
$$

The notation γ will denote either the geometric geodesic in $\mathbb{H}$ or the Möbius transformation corresponding to the symmetry around it, or the corresponding matrix (usually normalized like the preceding one, but not always).

Remark. We point out that we choose the sign of the point matrices such that the bottom-left component is negative whereas the sign of the geodesic matrices is left free, allowing the definition of an orientation of them (See Paragraphs A.1.2 and A.2 for the explanation).

3.2 Barycentric Coordinates

3.2.1 On a Triangle of the Triangulation

Theorem 29. *If we consider three points $p_0, p_1, p_2 \in \mathbb{H}$ and the linear combination $(1 - x^1 - x^2)p_0 + x^1 p_1 + x^2 p_2$, where $x^1, x^2 \in [0, 1]$ and $x^1 + x^2 \leq 1$, then the normalized matrix :*

$$p = \frac{(1 - x^1 - x^2)p_0 + x^1 p_1 + x^2 p_2}{\sqrt{\det\big((1 - x^1 - x^2)p_0 + x^1 p_1 + x^2 p_2\big)}} \tag{3.1}$$

is a point lying in the geodesic triangle $p_0p_1p_2$ and this decomposition is unique.

Proof. See Theorem 56 in Appendix A □

With this property, we are now able to provide an explicit definition of the diffeomorphisms π_j we introduced in the Triangulation Definition 17. We denote P_i the vertices of the triangulation on X. Given a point x in an open set $\mathcal{U}_j \subset \mathbb{R}^2$ containing the standard simplex $S = a_0a_1a_2$ (See Paragraph 2.1 for the definition of S) and such that $x = (1 - x^1 - x^2)a_0 + x^1 a_1 + x^2 a_2$, then we define the diffeormorphism between $\mathcal{U}_j$ and an open set Ω_j containing the j-th triangle $T_j = P_{j,0}P_{j,1}P_{j,2}$ as:

$$\begin{array}{rccl} \pi_j : & \mathcal{U}_j & \to & \Omega_j \\ & x & \mapsto & p = \dfrac{\big((1 - x^1 - x^2)P_{j,0} + x^1 P_{j,1} + x^2 P_{j,2}\big)}{\sqrt{\det\big((1 - x^1 - x^2)P_{j,0} + x^1 P_{j,1} + x^2 P_{j,2}\big)}} \end{array}$$

Let us define u^0, u^1, u^2 the barycentric coordinates in $\mathcal{U}_j$ respectively associated to each summit a_0, a_1, a_2 of S. For a point $x = (x^1, x^2) \in \mathbb{R}^2$:

$$\begin{aligned} u^0(x) &= 1 - x^1 - x^2 \\ u^1(x) &= x^1 \\ u^2(x) &= x^2 \end{aligned}$$

On $\mathcal{U}_j$, u^i is possibly negative or greater than one, but $u^i\big|_S \in [0, 1]$ and $u^0 + u^1 + u^2 = 1$. On Ω_j and for $l = 0, 1, 2$, we define the functions:

$$\begin{array}{rccl} \tilde{\mu}^{j,l} : & \Omega_j & \to & \mathbb{R} \\ & p & \mapsto & u^l \circ \pi_j^{-1}(p) \end{array}$$

For a point p in the triangle $T_j = P_{j,0}P_{j,1}P_{j,2}$ such that $P_{j,l} = \pi_j(a_l)$, we define the barycentric coordinate of p associated to the vertex $P_{j,l}$:

$$\mu^{j,l} = \tilde{\mu}^{j,l}\big|_{T_j}$$

Proposition 30. Given p in $T_j = P_{j,0}P_{j,1}P_{j,2}$ such that:

$$p = \frac{\big((1-x^1-x^2)P_{j,0} + x^1P_{j,1} + x^2P_{j,2}\big)}{\sqrt{\det\big((1-x^1-x^2)P_{j,0} + x^1P_{j,1} + x^2P_{j,2}\big)}}$$

Then:

$$\begin{aligned}\mu^{j,0}(p) &= 1 - x^1 - x^2\\ \mu^{j,1}(p) &= x^1\\ \mu^{j,2}(p) &= x^2\end{aligned}$$

And:

$$\forall l = 0,1,2, \quad \mu^{j,l}(p) \in [0,1] \quad \text{and} \quad \mu^{j,0}(p) + \mu^{j,1}(p) + \mu^{j,2}(p) = 1$$

Proof. From Theorem 29, we know that the decomposition $p = \frac{((1-x^1-x^2)P_{j,0}+x^1P_{j,1}+x^2P_{j,2})}{\sqrt{\det((1-x^1-x^2)P_{j,0}+x^1P_{j,1}+x^2P_{j,2})}}$ is unique and that $x^1, x^2 \in [0,1]$ with $x^1 + x^2 \leq 1$. $\square$

3.2.2 Induced Metric Tensor

For a triangle $T_j = P_{j,0}P_{j,1}P_{j,2}$, we use the notations defined on a triangle (see Notations): a, b, c are the lengths of the respective geodesics arcs $P_{j,2}P_{j,0}, P_{j,0}P_{j,1}, P_{j,1}P_{j,2}$ and α, β, γ are:

$$\begin{aligned}\alpha &= \cosh a - 1\\ \beta &= \cosh b - 1\\ \gamma &= \cosh c - 1\end{aligned}$$

We recall that:

$$\begin{aligned}\Gamma &= -\alpha^2 - \beta^2 - \gamma^2 + 2\alpha\beta + 2\alpha\gamma + 2\beta\gamma + 2\alpha\beta\gamma\\ \Lambda &= -\alpha^2 - \beta^2 - \gamma^2 + 2\alpha\beta + 2\alpha\gamma + 2\beta\gamma\\ \Phi &= 1 + 2\beta u(1-u-v) + 2\alpha v(1-u-v) + 2\gamma uv\end{aligned}$$

In the barycentric coordinates the metric tensor[1] $G(u,v)$ is given by the following components:

$$G_{11}(u,v) = \frac{1}{\Phi^2}\Big[\beta(\beta+2) - 2v\beta(-\alpha+\beta-\gamma) - v^2\Lambda\Big]$$
$$G_{12}(u,v) = \frac{1}{\Phi^2}\Big[\alpha+\beta-\gamma+\alpha\beta+u\beta(-\alpha+\beta-\gamma)+v\alpha(\alpha-\beta-\gamma)+uv\Lambda\Big]$$
$$G_{21}(u,v) = \frac{1}{\Phi^2}\Big[\alpha+\beta-\gamma+\alpha\beta+u\beta(-\alpha+\beta-\gamma)+v\alpha(\alpha-\beta-\gamma)+uv\Lambda\Big]$$
$$G_{22}(u,v) = \frac{1}{\Phi^2}\Big[\alpha(\alpha+2) - 2u\alpha(\alpha-\beta-\gamma) - u^2\Lambda\Big]$$

The volume form $dv_G = \sqrt{\det G}$ in this coordnate system also has a nice formulation:

$$\begin{aligned} dv_G &= \frac{\big(-\alpha^2-\beta^2-\gamma^2+2\alpha\beta+2\alpha\gamma+2\beta\gamma+2\alpha\beta\gamma\big)^{1/2}}{\big(1+2\beta u(1-u-v)+2\alpha v(1-u-v)+2\gamma uv\big)^{3/2}} \\ &= \frac{\Gamma^{1/2}}{\Phi^{3/2}} \end{aligned} \tag{3.2}$$

Remark. The calculations to establish the formulae of the metric tensor are quite long but when given it is quite easy to verify them with symbolic mathematical software. An idea to simplify the calculations is to isometrically move $P_{j,0}$ onto i in $\mathbb{H}$ and $P_{j,2}$ onto the vertical axis.

For the inner product of covariant tensors, the inverse of the metric tensor is used, that is why we provide its expression as well:

$$G^{11}(u,v) = \frac{\Phi}{\Gamma}\Big[\alpha(\alpha+2) - 2u\alpha(\alpha-\beta-\gamma) - u^2\Lambda\Big]$$
$$G^{12}(u,v) = \frac{\Phi}{\Gamma}\Big[-\alpha-\beta+\gamma-\alpha\beta-u\beta(-\alpha+\beta-\gamma)-v\alpha(\alpha-\beta-\gamma)-uv\Lambda\Big]$$
$$G^{21}(u,v) = \frac{\Phi}{\Gamma}\Big[-\alpha-\beta+\gamma-\alpha\beta-u\beta(-\alpha+\beta-\gamma)-v\alpha(\alpha-\beta-\gamma)-uv\Lambda\Big]$$
$$G^{22}(u,v) = \frac{\Phi}{\Gamma}\Big[\beta(\beta+2) - 2v\beta(-\alpha+\beta-\gamma) - v^2\Lambda\Big]$$

3.3 Finite Functions Space V_h

We can now define the finite function space in which we will calculate the eigenvalues and eigenfunctions of the Spectral Problem. These solutions give us an approximation of the Spectral Problem eigenvalues and eigenfunctions on X.

[1] here we use u, v as coordinate to avoid the clumsy $(x^1)^2$ or $(x^2)^2$ notation

3.3.1 Finite Element

Definition 31. A triangle from the triangulation $T_j = P_{j,0}P_{j,1}P_{j,2}$ with a set of three functions (called basis functions) defined on this triangle is called a Finite Element, denoted $(T_j, \{\nu^{j,0}, \nu^{j,1}, \nu^{j,2}\})$, if the functions satisfy:

$$\nu^{j,k}(P_{j,l}) = \delta_l^k$$

A definition for the functions $\nu^{j,l}$ comes naturally when using the barycentric coordinates. For a point $p \in T_j$, $\nu^{j,i}(p)$ is the barycentric coordinate of p associated with the point $P_{j,l}$:

$$\nu^{j,i}(p) = \mu^{j,i}(p)$$

This explains why appropriate barycentric coordinates (from which the metric tensor is computable as previously shown) are one of the keys of this work.

3.3.2 Basis functions of V_h

The idea is to define a finite function space V_h on the surface X through its basis functions and such that the restriction of a function $f_h \in V_h$ to a triangle is a linear combination of these basis functions. We expand the definition of the barycentric coordinates on a triangle as discussed in paragraph 3.2.1 to the entire surface and will use them as basis functions for V_h. For a vertex P_k of the triangulation and a point $p \in X$, we define the barycentric coordinate of p associated with P_k:

$$\mu^k(p) = \begin{cases} \mu^{j,k}(p) & \text{if } p \in T_j \text{ and } P_k \text{ is a summit of } T_j \\ \\ 0 & \text{otherwise} \end{cases}$$

μ^k is thus a sort of pyramidal function, and its restriction to a triangle is:

$$\mu^k\big|_{T_j} = \mu^{j,k}$$

The preceding definition could seem ambiguous if p lies on a edge of the triangulation. However, because the barycentric coordinates of a point lying on the common edge of two triangles are the same, it is not and μ^k is thus a continuous function on X. We can, moreover, remark that if T_i and T_j are two adjacent triangles sharing the edge P_kP_m, the tangential part of $d\mu^{i,k}$ and $d\mu^{j,k}$ on P_kP_m is continuous (in other words, the pullbacks of $d\mu^{i,k}$ and $d\mu^{j,k}$ on P_kP_m are the same).

We then define the finite function space V_h as the linear combinations of the functions μ^k:

$$V_h = \mathrm{Span}(\{\mu^k\}_{k=1\ldots I}) \tag{3.3}$$

Recall that we denoted I the number of vertices of the triangulation.

As mentioned at the beginning of this chapter, we want to compute the approximated eigenvalues and eigenfunctions in the function space V_h. To compare these values and functions to the real solutions, V_h has to be a subspace of the function space, where we searched for the solutions of the Spectral Problem, that is, we have to be sure that V_h is a subspace of $H^1(X)$.

Theorem 32. *V_h is subspace of $H^1(X)$.*

Proof. It is well-known that these pyramidal functions are in $H^1(\mathbb{R}^2)$. In [Heb99] page 22 Proposition 2.2, it is shown that the Sobolev spaces do not depend on the metric when the manifold is compact. □

As we look for the solutions of the Spectral Problem in the subspace $H_0^1(X)$ of the functions with a null-average, we have to define $V_{h,0}$, the subspace of V_h such that:

$$V_{h,0} = \left\{ f_h \in V_h, \int_X f_h = 0 \right\} \tag{3.4}$$

3.4 Algebraic Problem

In this paragraph we want to solve the Spectral Problem in its weak formulation on the finite function space $V_{h,0}$ we have just defined. That is, finding $f_h \in V_{h,0}$ and λ_h such that for all $g_h \in V_h$:

$$\int_X \langle df_h, dg_h \rangle \, dv_G = \lambda_h \int_X f_h g_h \, dv_G \tag{3.5}$$

3.4.1 Solutions of the Spectral Problem in V_h

Theorem 33. *There exists a basis* $\{\varphi_{n,h}\}_{n=1\dots I}$ *of* $V_{h,0}$ *and a sequence* $\{\lambda_{n,h}\}_{n=1\dots I}$ *of elements of* $\mathbb{R}$ *such that:*

i) $\varphi_{n,h} \in V_{h,0}$

ii) $(\varphi_{n,h}, \varphi_{m,h})_{0,X} = \int_X \varphi_{n,h}\varphi_{m,h}\, dv_G = \delta_{nm}$

iii) $\int_X \langle d\varphi_{n,h}, dg_h\rangle\, dv_G = \lambda_{n,h} \int_X \varphi_{n,h}\, g_h\, dv_G, \quad \forall g_h \in V_h$

iv) $0 < \lambda_{1,h} \le \lambda_{2,h} \le \cdots \le \lambda_{I,h}$

Proof. Apply the Spectral Theorem 15 to $V_{h,0}$. □

Proposition 34. The eigenvalues are characterized by the Rayleigh quotient:

$$\lambda_{m,h} = \min_{E_m \in \mathcal{V}_{m,h}} \max_{\substack{f_h \in E_m \\ f_h \neq 0}} \frac{|f_h|^2_{1,X}}{\|f_h\|^2_{0,X}} \tag{3.6}$$

where $\mathcal{V}_{m,h}$ is the set of all the m-dimensional subspaces $E_m \subset V_{h,0}$.

Proof. Apply the Eigenvalues Characterization Proposition 16 to $V_{h,0}$. □

3.4.2 Finite Spectral Problem as an Algebraic Problem

Theorem 33 is actually not so much interesting in the sense that it proves the existence of solutions, but it does not build them. This is what we want to do now (it could be considered as a constructive proof of Theorem 33). Given a function $f_h \in V_{h,0}$, as $\{\mu^j\}_{j=1\dots I}$ is a basis of V_h, we can write:

$$f_h = f_{h,j}\, \mu^j$$

The Spectral Problem then becomes: find a function $f_h = f_{h,j}\, \mu^j \in V_{h,0}$ such that for all $i = 1 \dots I$:

$$\begin{aligned}
\int_X \langle d(f_{h,j}\, \mu^j), d\mu^i\rangle\, dv_G &= \lambda_h \int_X f_{h,j}\mu^j \mu^i\, dv_G \\
\Leftrightarrow \quad f_{h,j} \int_X \langle d\mu^j, d\mu^i\rangle\, dv_G &= \lambda_h\, f_{h,j} \int_X \mu^j \mu^i\, dv_G \\
\Leftrightarrow \quad MU_h &= \lambda_h\, NU_h
\end{aligned}$$

where M and N are square real matrices of dimension I and U is a vector of dimension I such that:

$$M^{ij} = \int_X \langle d\mu^j, d\mu^i \rangle \, dv_G \tag{3.7}$$

$$N^{ij} = \int_X \mu^j \mu^i \, dv_G \tag{3.8}$$

$$U_{h,j} = f_{h,j} \tag{3.9}$$

As every function μ^j is non-zero only on the star around the vertex P_j (the union of all adjacent triangles, denoted $\mathrm{St}(P_j)$), it is possible to define the domain of integration of the components of the matrices M and N.

$$M^{ij} = \int_{\mathrm{St}(P_j)\cap\mathrm{St}(P_i)} \langle d\mu^j, d\mu^i \rangle \, dv_G$$

$$N^{ij} = \int_{\mathrm{St}(P_j)\cap\mathrm{St}(P_i)} \mu^j \mu^i \, dv_G$$

With these formulae, we observe that these matrices are symmetric and we can explicitly write each integral. There are two cases to distinguish.

3.4.3 Diagonal Elements M_{ii} and N_{ii}

If $i = j$ and $\mathrm{St}(P_i) = \{T_1, \ldots, T_m\}$, then :

$$M^{ii} = \int_{T_1} \langle d\mu^i, d\mu^i \rangle + \cdots + \int_{T_m} \langle d\mu^i, d\mu^i \rangle$$

$$N^{ii} = \int_{T_1} \mu^i \mu^i + \cdots + \int_{T_m} \mu^i \mu^i$$

We denote a triangle $T_k \in \mathrm{St}(P_i)$ as $P_{k,0}P_{k,1}P_{k,2}$ and suppose that P_i corresponds to the vertex $P_{k,0}$, then for the elements of the matrix M:

$$\begin{aligned}
&\int_{T_k} \langle d\mu^i, d\mu^i \rangle \\
=&\int_{T_k} G^{11} + 2G^{12} + G^{22} \\
=&\frac{1}{\Gamma^{1/2}} \int_0^1 \int_0^{1-u} \frac{\gamma(\gamma+2) - 2(1-u-v)\gamma(-\alpha-\beta+\gamma) - (1-u-v)^2\Lambda}{\big(1 + 2\beta u(1-u-v) + 2\alpha v(1-u-v) + 2\gamma uv\big)^{1/2}} dv du
\end{aligned} \tag{3.10}$$

For the elements of the matrix N:

$$\int_{T_1} \mu^i \mu^i = \int_0^1 \int_0^{1-u} \frac{\Gamma^{1/2}(1-u-v)^2}{\big(1+2\beta u(1-u-v)+2\alpha v(1-u-v)+2\gamma uv\big)^{3/2}} dvdu \tag{3.11}$$

3.4.4 Non Diagonal Elements M_{ij} and N_{ij}

If $i \neq j$ and $\mathrm{St}(P_i) \cap \mathrm{St}(P_j) = \{T_1, T_2\}$, then :

$$M^{ij} = \int_{T_1} \langle d\mu^j, d\mu^i \rangle + \int_{T_2} \langle d\mu^j, d\mu^i \rangle$$
$$N^{ij} = \int_{T_1} \mu^j \mu^i + \int_{T_2} \mu^j \mu^i$$

We denote a triangle $T_k \in \mathrm{St}(P_i) \cap \mathrm{St}(P_j)$ as $P_{k,0}P_{k,1}P_{k,2}$ and suppose that P_j and P_i correspond respectively to the vertices $P_{k,0}$ and $P_{k,1}$ (these assumptions are allowed by the symmetry of M and N and a cyclic permutations of the vertices $P_{k,0}$, $P_{k,1}$, $P_{k,2}$), then for the elements of the matrix M:

$$\begin{aligned}
&\int_{T_k} \langle d\mu^j, d\mu^i \rangle \\
=&\int_{T_k} -G^{11} - G^{12} \\
=&\frac{-1}{\Gamma^{1/2}}. \\
&\int_0^1 \int_0^{1-u} \frac{\alpha-\beta+\gamma+\alpha\gamma+u\gamma(-\alpha-\beta+\gamma)+(1-u-v)\alpha(\alpha-\beta-\gamma)+(1-u-v)u\Lambda}{\big(1+2\beta u(1-u-v)+2\alpha v(1-u-v)+2\gamma uv\big)^{1/2}} dvdu
\end{aligned} \tag{3.12}$$

For the elements of the matrix N:

$$\int_{T_k} \mu^j \mu^i = \int_0^1 \int_0^{1-u} \frac{\Gamma^{1/2}u(1-u-v)}{\big(1+2\beta u(1-u-v)+2\alpha v(1-u-v)+2\gamma uv\big)^{3/2}} dvdu \tag{3.13}$$

With these "quadrature formulae" 3.10, 3.11, 3.12 and 3.13 (using the same terminology as in the Finite Element Method), we can fill the matrices M and N and solve the algebraic problem as the matrix N is positive and symmetric, and hence invertible:

$$\begin{aligned}
MU_h &= \lambda N U_h \\
\Leftrightarrow \quad N^{-1} M U_h &= \lambda U_h
\end{aligned}$$

This problem is a very well-knowm matrix eigenvalue problem, for which robust algorithms exist and have been implemented for a long time. We point out that even if we could not calculate the integrals of the quadrature formulae, it is possible to approximate them with an arbitrary precision using a Taylor expansion of the function to integrate.

Chapter 4

Convergence of the Numerical Method

The eigenvalues and eigenfunctions of the Spectral Problem in the finite subspace V_h we have found would be useless if we can not prove that they converge to the eigevalues and eigenfunctions in $H_0^1(X)$. In this chapter, we define the notion of convergence and find a way to estimate the error. In this regard, we have to go through a little detour by the Taylor expansion and the Lagrange interpolation of a function. This provides the formulae we need to estimate the error.

4.1 Taylor Expansion of a Function

Given an open set $K \subset X$ and a differentiable function $f \in C^\infty(K)$, we want to write down the Integral Taylor Formula between two points p and x lying on a geodesic of the surface as well as an estimate of the $\|.\|_{0,K}$ norm of the rest.

4.1.1 Taylor Formula

Proposition 35. Given $\gamma : [0,1] \to K$ a geodesic such that $\gamma(0) = x$ and $\gamma(1) = p$. The order two Integral Taylor Formula for the function f reads[1]:

$$f(p) = f(x) + Df(x)[\gamma'(0)] + \int_0^1 (1-s)D^2 f(\gamma(s))[\gamma'(s), \gamma'(s)]\, ds \tag{4.1}$$

[1] recall that Df represents the covariant derivative of f

Proof. We give the proof for a more general case, that is, for a differentiable curve $c : [0,1] \to K$, with $c(0) = x$ and $c(1) = p$. We also define the function $F : \mathbb{R} \to \mathbb{R}$ such that $F(s) = f \circ \gamma(s)$. It is a real function, whose Taylor expansion reads:

$$F(1) = F(0) + F'(0) + \int_0^1 (1-s)F''(s)\,ds$$

Let us develop each term. For the first order term at $x = c(s)$:

$$F'(s) = df(x)[c'(s)] = Df(x)[c'(s)]$$

For the second order term, we use the musical isomorphism $\sharp$ between the vector fields and the 1-forms on K, whose definition is: given a 1-form α on K, ${}^\sharp\alpha$ is the vector field such that for any vector field w, $\langle {}^\sharp\alpha, w\rangle = \alpha(w)$. In this proof we use the fact that $\sharp$ and the covariant derivative commute. We postpone the proof of this commutativity to Appendix B since it is rather technical and does not add anything to the comprehension of the following equations.

$$\begin{aligned}
F''(s) &= \frac{dF'}{ds}(s) \\
&= \frac{d}{ds} df(c(s))[c'(s)] \\
&= \frac{d}{ds} \langle {}^\sharp df(c(s)), c'(s)\rangle \\
&= \langle D_{c'(s)}{}^\sharp df(c(s)), c'(s)\rangle + \langle {}^\sharp df(c(s)), D_{c'(s)}c'(s)\rangle \\
&= \langle {}^\sharp D_{c'(s)} df(c(s)), c'(s)\rangle + \langle {}^\sharp df(c(s)), D_{c'(s)}c'(s)\rangle \\
&= D_{c'(s)} df(c(s))[c'(s)] + df(c(s))[D_{c'(s)}c'(s)] \\
&= D^2 f(c(s))[c'(s), c'(s)] + df(c(s))[D_{c'(s)}c'(s)]
\end{aligned}$$

If c is a geodesic γ, then $D_{\gamma'(s)}\gamma'(s) = 0$ and we obtain the formula. □

Remark. We now suppose that p and x are aligned on the first coordinate. We also define $c(s) = x + s(p-x)$. If we apply the formula of the proof, keeping in mind the fact that $c'(s) = (p^1 - x^1)\frac{\partial}{\partial x^1}$:

$$\begin{aligned}
F'(0) &= (p^1 - x^1)\frac{\partial f}{\partial x^1}(x) \\
F''(s) &= D^2 f(c(s))[c'(s), c'(s)] + df(c(s))[D_{c'(s)}c'(s)] \\
&= \Big(\frac{\partial^2 f}{\partial (x^1)^2} - \Gamma^k_{11}\frac{\partial f}{\partial x^k}\Big)(p^1 - x^1)^2 + (p^1 - x^1)^2 \Gamma^k_{11}\frac{\partial f}{\partial x^k} \\
&= (p^1 - x^1)^2 \frac{\partial^2 f}{\partial (x^1)^2}
\end{aligned}$$

We denote u instead of x^1 for convenience and then find the well-known Taylor Formula:

$$f(p) = f(x) + (p^1 - x^1)\frac{\partial f}{\partial u}(x) + (p^1 - x^1)^2 \int_0^1 (1-s)\frac{\partial^2 f}{\partial u^2}(x + s(p-x))\,ds$$

4.1.2 Estimate of the Remaining

This paragraph was inspired by the article by Ciarlet and Raviart [CR72] . Given an open set $K \subset X$, $f \in \mathcal{C}^\infty(K)$ and γ a geodesic between p and x as defined in the last proposition ($\gamma(0) = x$ and $\gamma(1) = p$), we denote $J(f,p)(x)$ the remaining term in the Taylor Formula 4.1:

$$J(f,p)(x) = \int_0^1 (1-s) D^2 f(\gamma(s))[\gamma'(s), \gamma'(s)]\,ds$$

From here on, we assume that K is bounded and that any two points in K are joined, inside K, by a unique geodesic arc.

Proposition 36. Under the above hypothesis, denoting h the diameter of K, we have:

$$\|J(f,p)\|_{0,K} \leq h^2 \sqrt{\frac{\sinh h}{h}} |f|_{2,K} \tag{4.2}$$

Proof. By definition of the $|.|_{\text{sup}}$ norm:

$$\left|D^2 f(\gamma(s))[\gamma'(s), \gamma'(s)]\right| \leq \left|D^2 f\right|_{\text{sup}}(\gamma(s))\, |\gamma'(s)|^2 \leq \left|D^2 f\right|_{\text{sup}}(\gamma(s))\, h^2$$

because γ is a geodesic parametrized over $[0,1]$ and $|\gamma'(s)| = \text{dist}(p,x) \leq h$. Thus, using the Cauchy-Schwarz inequality to state the second inequality:

$$\begin{aligned}
|J(f,p)(x)| &\leq h^2 \int_0^1 (1-s) \left|D^2 f\right|_{\text{sup}}(\gamma(s))\,ds \\
&\leq h^2 \Big(\int_0^1 (1-s)^2 \left|D^2 f\right|^2_{\text{sup}}(\gamma(s))\,ds \Big)^{1/2} \\
\Rightarrow \quad \|J(f,p)\|^2_{0,K} &= \int_K (J(f,p)(x))^2\, dv_G(x) \\
&\leq h^4 \int_{K\times[0,1]} (1-s)^2 \left|D^2 f\right|^2_{\text{sup}}(\gamma(s))\, ds dv_G(x)
\end{aligned}$$

Observe in this last formula that γ depends on x. We then need to make a variable substitution. Let us move p to the centre of a polar coordinates chart (ρ, θ). K thus becomes $\left\{(\rho, \theta) \in \mathbb{R}^2, \rho \in [0, r(\theta)], \theta \in [0, 2\pi]\right\}$ and γ is such that $\gamma(0) = x = (\rho, \theta)$ and $\gamma(1) = p = (0, 0)$. For a given s, $\gamma(s)$ is thus the point $((1-s)\rho, \theta)$. Hence, the domain of integration may be viewed as a cone with basis K and height 1. The following inequalities end the proof of the proposition. The hint to go from line 3 to 4 is given just afterwards.

$$
\begin{aligned}
&\int_0^1 \int_K (1-s)^2 \left|D^2 f\right|^2_{\text{sup}}(\gamma(s))\, ds dv_G \\
&= \int_0^1 \int_0^{2\pi} \int_0^{r(\theta)} (1-s)^2 \left|D^2 f\right|^2_{\text{sup}}((1-s)\rho, \theta)\, \sinh(\rho)\, d\rho d\theta ds \\
&= \int_0^1 \int_0^{2\pi} \int_0^{(1-s)r(\theta)} \left|D^2 f\right|^2_{\text{sup}}(\rho', \theta)\, \sinh(\frac{\rho'}{1-s})(1-s)\, d\rho' d\theta ds \\
&\leq \int_0^1 \int_0^{2\pi} \int_0^{(1-s)r(\theta)} \left|D^2 f\right|^2_{\text{sup}}(\rho', \theta)\, \sinh(\rho') \frac{\sinh h}{h}\, d\rho' d\theta ds \\
&\leq \frac{\sinh h}{h} \int_0^1 \int_0^{2\pi} \int_0^{(1-s)r(\theta)} \left|D^2 f\right|^2(\rho', \theta)\, \sinh(\rho')\, d\rho' d\theta ds \\
&\leq \frac{\sinh h}{h} \int_0^1 ds \int_0^{2\pi} \int_0^{r(\theta)} \left|D^2 f\right|^2(\rho', \theta)\, \sinh(\rho')\, d\rho' d\theta \\
&\leq \frac{\sinh h}{h} \left|f\right|^2_{2,K}
\end{aligned}
$$

For $\rho' \in [0, (1-s)r(\theta)]$ and $s \in [0, 1]$we have indeed by convexity of sinh:

$$
\rho' \leq \sinh \rho' \leq (1-s) \sinh\left(\frac{\rho'}{1-s}\right)
$$

Moreover, as $r(\theta) \leq h$:

$$
\sinh\left(\frac{\rho'}{1-s}\right) \leq \frac{\rho'}{(1-s)h} \sinh h
$$

Which implies that:

$$
(1-s) \sinh\left(\frac{\rho'}{1-s}\right) \leq \sinh \rho' \frac{\sinh h}{h}
$$

□

4.2 Lagrange Interpolation of a Function

This paragraph also was inspired by the article [CR72]. Given a triangulation of a closed subset of $\mathbb{R}^2$, the Lagrange linear interpolation of a differentiable function f can be defined as the piecewise linear function which interpolates f at the vertices of the triangulation. We will follow the same idea for our method, except that the concept of linearity has no sense in non-euclidean geometry.

4.2.1 Definition of the Lagrange Interpolation

From the triangulation of the surface we obtained we were able to define the finite space of functions V_h. We define the Lagrange interpolation of a differentiable function in a triangle T_j on the triangulation in the same way as it is done on $\mathbb{R}^2$ except that the projection is done on the basis functions $\mu^{j,i}$.

Definition 37. Given $(T_j, \{\mu^{j,0}, \mu^{j,1}, \mu^{j,2}\})$ a finite element from the triangulation of X whose vertices are $\{P_{j,i}\}_{i=0,1,2}$ and $\{\mu^{j,i}\}_{i=0,1,2}$ their associated barycentric coordinates (See Definition 31). For f a differentiable function on T_j the Lagrange interpolation projection operator is defined as:

$$L : f \mapsto Lf = \sum_{i=0,1,2} f(P_{j,i})\mu^{j,i} \tag{4.3}$$

This definition could seem useless because we stated the Spectral Problem in its weak formulation for functions in $H_0^1(X)$, whose elements are not always continuous. Recall however that our aim is to find approximations of the Spectral Problem solutions, which we have already proved are differentiable functions.

Remark. From here on, if we do not specify the index over which the sum is done, it is to be understood as $i = 0, 1, 2$. Furthermore, for $P_{j,i}$ on T_j, we frequently write P_i.

4.2.2 Interpolation Error Estimate

After having given the definition of the Lagrange interpolation operator, we then attempt to estimate the error we make by interpolating a function onto a single triangle $T_j = P_{j,0}P_{j,1}P_{j,2}$.

Lemma 38. Given a function $f \in C^\infty(T_j)$. In a point $x_0 \in T_j$, $Df(x_0) = B_1\, dx^1 + B_2\, dx^2$, where $B_1, B_2 \in \mathbb{R}$. For a point $x = (x^1, x^2) \in T_j$ we define $\tilde{f}_{x_0}(x) = f(x_0) + B_1(x^1 - x_0^1) + B_2(x^2 - x_0^2)$. Then we have for all $m = 0, 1$:

$$D^m Lf(x) - D^m f(x) = \sum \Big[J(f, P_i)(x) - J(\tilde{f}_x, P_i)(x) \Big] D^m \mu^{j,i}(x) \tag{4.4}$$

Proof. From the Lagrange projection operator:

$$\begin{aligned} Lf(x) &= \sum f(P_i)\mu^{j,i}(x) \\ \Rightarrow \quad DLf(x) &= \sum f(P_i) D\mu^{j,i}(x) \end{aligned}$$

Moreover, from the Taylor expansion formula 4.1, assuming γ_i is a geodesic from x to P_i such that $\gamma_i(0) = x$ and $\gamma_i(1) = P_i$:

$$f(P_i) = f(x) + Df(x)[\gamma_i'(0)] + \int_0^1 (1-s) D^2 f(\gamma_i(s))[\gamma_i'(s), \gamma_i'(s)]\, ds$$

Thus:

$$\begin{aligned} D^m Lf(x) = &\sum \Big(f(x) + Df(x)[\gamma_i'(0)] \Big) D^m \mu^{j,i}(x) \\ &+ \sum \Big(\int_0^1 (1-s) D^2 f(\gamma_i(s))[\gamma_i'(s), \gamma_i'(s)]\, ds \Big) D^m \mu^{j,i}(x) \end{aligned} \tag{4.5}$$

We now want to prove that:

$$\sum \Big(f(x) + Df(x)[\gamma_i'(0)] \Big) D^m \mu^{j,i}(x) = D^m f(x) + \text{a remainder}$$

For m=0

$$\sum f(x) \mu^{j,i}(x) = f(x) \tag{4.6}$$

because $\sum \mu^{j,i}(x) = 1$.
From the definition of $\tilde{f}_{x_0}$, $L\tilde{f}_{x_0}(x) = \tilde{f}_{x_0}(x)$. If we write the equation 4.5 with $\tilde{f}_{x_0}$ and combined with 4.6, we obtain:

$$\begin{aligned} L\tilde{f}_{x_0}(x) = \tilde{f}_{x_0}(x) + &\sum D\tilde{f}_{x_0}(x)[\gamma_i'(0)] \mu^{j,i}(x) \\ &+ \sum \Big(\int_0^1 (1-s) D^2 \tilde{f}_{x_0}(\gamma_i(s))[\gamma_i'(s), \gamma_i'(s)]\, ds \Big) \mu^{j,i}(x) \\ = &\tilde{f}_{x_0}(x) \end{aligned}$$

Moreover, $\forall x, D\tilde{f}_{x_0}(x) = Df(x_0)$, thus:

$$\sum Df(x_0)[\gamma_i'(0)]\mu^{j,i}(x) = -\sum \Big(\int_0^1 (1-s)D^2\tilde{f}_{x_0}(\gamma_i(s))[\gamma_i'(s), \gamma_i'(s)]\, ds\Big)\mu^{j,i}(x)$$

As we have not made any hypothesis regarding the x_0 we chose, this last equation is true in any point, in particular in x:

$$\sum Df(x)[\gamma_i'(0)]\mu^{j,i}(x) = -\sum \Big(\int_0^1 (1-s)D^2\tilde{f}_{x}(\gamma_i(s))[\gamma_i'(s), \gamma_i'(s)]\, ds\Big)\mu^{j,i}(x)$$

And thus, for $m = 0$, Equation 4.5 becomes:

$$\begin{aligned} Lf(x) = f(x) &+ \sum \Big(\int_0^1 (1-s)D^2 f(\gamma_i(s))[\gamma_i'(s), \gamma_i'(s)]\, ds\Big)\mu^{j,i}(x) \\ &- \sum \Big(\int_0^1 (1-s)D^2\tilde{f}_{x}(\gamma_i(s))[\gamma_i'(s), \gamma_i'(s)]\, ds\Big)\mu^{j,i}(x) \end{aligned}$$

This proves the Lemma for $m = 0$.

For m=1:

$$\sum f(x)D\mu^{j,i}(x) = 0 \tag{4.7}$$

because $\sum \mu^{j,i}(x) = 1 \Rightarrow \sum D\mu^{j,i}(x) = 0$.

We write the equation 4.5 for $\tilde{f}_{x_0}$ again, this time combined with 4.7:

$$\begin{aligned} DL\tilde{f}_{x_0}(x) =& \sum D\tilde{f}_{x_0}(x)[\gamma_i'(0)]D\mu^{j,i}(x) \\ &+ \sum \Big(\int_0^1 (1-s)D^2\tilde{f}_{x_0}(\gamma_i(s))[\gamma_i'(s), \gamma_i'(s)]\, ds\Big)D\mu^{j,i}(x) \\ =& D\tilde{f}_{x_0}(x) \end{aligned}$$

Again, $D\tilde{f}_{x_0}(x) = Df(x_0)$, this implies:

$$\begin{aligned} Df(x_0) =& \sum Df(x_0)[\gamma_i'(0)]D\mu^{j,i}(x) \\ &+ \sum \Big(\int_0^1 (1-s)D^2\tilde{f}_{x_0}(\gamma_i(s))[\gamma_i'(s), \gamma_i'(s)]\, ds\Big)D\mu^{j,i}(x) \end{aligned}$$

And thus, for $m = 1$, Equation 4.5 becomes:

$$\begin{aligned} DLf(x) = Df(x) &+ \sum \Big(\int_0^1 (1-s)D^2 f(\gamma_i(s))[\gamma_i'(s), \gamma_i'(s)]\, ds\Big)D\mu^{j,i}(x) \\ &- \sum \Big(\int_0^1 (1-s)D^2\tilde{f}_{x}(\gamma_i(s))[\gamma_i'(s), \gamma_i'(s)]\, ds\Big)D\mu^{j,i}(x) \end{aligned}$$

It proves the Lemma for $m = 1$.

$\square$

With the preceding Lemma, it is clear that we will estimate the error of the interpolation by calculating the $\|.\|_{0,T_j}$ norm of Equation 4.4 over a triangle T_j of the triangulation and finding an upper bound for the terms of the right-hand side. We have already found an estimate for the term $\|J(f, P_i)\|_{0,T_j}$ (see Equation 4.2 in Proposition 36), however, it still misses an upper bound for $\|J(\tilde{f}_x, P_i)\|_{0,T_j}$ and (we will see that it appears so) $\sum \sup_{x\in T_j} |D^m \mu^{j,i}|$. To estimate these two terms, we have to study the functions $G^{ij}(x)$ and the Christoffel symbols $\Gamma^k_{ij}(x)$ associated with the barycentric coordinates and for $x \in T_j$. $|D\mu^{j,i}|$ is indeed a linear combination of the components G^{ij} and we will see that an expansion of the functions $G^{ij}(x)$ and $\Gamma^k_{ij}(x)$ according to h allows us to find an upper-bound for $\|J(\tilde{f}_x, P_i)\|_{0,T_j}$.

The entire study of these functions can be found in Appendix C and we recall just the results. For a point $x \in T_j$, we denote (u, v) its barycentric coordinates and use the notations defined on a triangle (see Chapter Notations at the beginning of this thesis), then for the components of the inverse of the metric tensor:

$$\begin{array}{rcccl}
\dfrac{2\alpha}{\Gamma} & \leq & G^{11}(u,v) & \leq & \dfrac{2\alpha}{\Gamma}\big(1+O(h^2)\big) \\
\dfrac{2\beta}{\Gamma} & \leq & G^{22}(u,v) & \leq & \dfrac{2\beta}{\Gamma}\big(1+O(h^2)\big) \\
\dfrac{k(-\alpha-\beta+\gamma)}{\Gamma} - O(1) & \leq & G^{12}(u,v) & \leq & \dfrac{k'(-\alpha-\beta+\gamma)}{\Gamma} + O(1)
\end{array}$$

where k, k' are 1 or -4. In these formulae, we point out that the Appendix C gives us an estimate for all $O()$-terms. For the Christoffel symbols, we do not have these estimates but we know that:

$$\Gamma^i_{jk} = O(h^2)$$

Theorem 39 (Lagrange Interpolation Estimate)**.** *Let L be the Lagrange interpolation operator on a finite element $(T_j, \{\mu^{j,0}, \mu^{j,1}, \mu^{j,2}\})$. Given a function $f \in C^\infty(T_j)$, then for all $m = 0, 1$:*

$$|f - Lf|_{m,T_j} \leq \sqrt{\frac{\sinh h}{h}}\, \frac{3h^2}{\sinh^m \rho}\, |f|_{2,T_j} + O(h^3) \tag{4.8}$$

Proof. From the preceding Lemma:

$$D^m Lf(x) - D^m f(x) = \sum J(f, P_i)(x) D^m \mu^{j,i}(x) - \sum J(\tilde{f}_x, P_i)(x) D^m \mu^{j,i}(x)$$

Let us integrate this equation on T_j:

$$\begin{aligned}
|f - Lf|_{m,T_j} &= \Big(\int_{T_j} \big| D^m f(x) - D^m Lf(x) \big|^2 \Big)^{1/2} \\
&\leq \Big(\int_{T_j} \big| \sum J(f, P_i)(x) D^m \mu^{j,i}(x) \big|^2 \Big)^{1/2} \\
&\quad + \Big(\int_{T_j} \big| \sum J(\tilde{f}_x, P_i)(x) D^m \mu^{j,i}(x) \big|^2 \Big)^{1/2} \\
&\leq \sum \Big(\int_{T_j} J(f, P_i)^2(x) \big| D^m \mu^{j,i} \big|^2(x) \Big)^{1/2} \\
&\quad + \sum \Big(\int_{T_j} J(\tilde{f}_x, P_i)^2(x) \big| D^m \mu^{j,i} \big|^2(x) \Big)^{1/2} \\
&\leq \sum \sup_{x \in T_j} |D^m \mu^{j,i}|(x) \bigg(\Big(\int_{T_j} J(f, P_i)^2(x) \Big)^{1/2} + \Big(\int_{T_j} J(\tilde{f}_x, P_i)^2(x) \Big)^{1/2} \bigg)
\end{aligned}$$

Using Equation 4.2 in Proposition 36, we have an upper bound for the first term in the parenthesis:

$$\Big(\int_{T_j} (J(f, P_i)(x))^2 \, dx \Big)^{1/2} \leq h^2 \sqrt{\frac{\sinh h}{h}} |f|_{2,T_j}$$

It remains to find an upper bound for the second term (we follow the idea of the inequalities in the proof of the proposition 36 again):

$$\begin{aligned}
\int_{T_j} J(\tilde{f}_x, P_i)^2(x) \, dx &= \int_{T_j} \Big(\int_0^1 (1-s) D^2 \tilde{f}_x(\gamma_i(s))[\gamma_i'(s), \gamma_i'(s)] \, ds \Big)^2 dv_G(x) \\
&\leq h^4 \int_{T_j} \int_0^1 (1-s)^2 \left| D^2 \tilde{f}_x \right|_{\sup}^2 (\gamma_i(s)) \, ds dv_G(x) \\
&\leq h^4 \int_{T_j} \int_0^1 \left| D^2 \tilde{f}_x \right|_{\sup}^2 (\gamma_i(s)) \, ds dv_G(x)
\end{aligned}$$

From the definition of $\tilde{f}_x$:

$$\begin{aligned}
\big(D^2 \tilde{f}_x(\gamma_i(s)) \big)_{jk} &= \frac{\partial^2 \tilde{f}_x}{\partial x^j \partial x^k} - \Gamma^n_{jk}(\gamma_i(s)) \frac{\partial \tilde{f}_x}{\partial x^n}(\gamma_i(s)) \\
&= -\Gamma^n_{jk}(\gamma_i(s)) \frac{\partial f}{\partial x^n}(x)
\end{aligned}$$

We can now explain the function to integrate (Recall that by formula 1.6, we have $|\,.\,|_{\text{sup}} \leq |\,.\,|$):

$$\begin{aligned}\left|D^2\tilde{f}_x\right|^2(\gamma_i(s)) &= G^{jl}(\gamma_i(s))G^{km}(\gamma_i(s))(D^2\tilde{f}_x(\gamma_i(s)))_{jk}(D^2\tilde{f}_x(\gamma_i(s)))_{lm}\\ &= G^{jl}(\gamma_i(s))G^{km}(\gamma_i(s))\Gamma^n_{jk}(\gamma_i(s))\Gamma^p_{lm}(\gamma_i(s))\frac{\partial f}{\partial x^n}(x)\frac{\partial f}{\partial x^p}(x)\end{aligned}$$

Using the results we have recalled before the preceding theorem about the approximation of the components G^{ij} and Γ^i_{jk}, we can conclude that:

$$\left|D^2\tilde{f}_x\right|^2(\gamma_i(s)) = O(h^2)|Df|^2(x)$$

Integrating over the triangle:

$$\int_{T_j} J(\tilde{f}_x, P_i)^2(x)\,dx = O(h^6)\,|f|^2_{1,T_j}$$

Finally:

$$|f - Lf|_{m,T_j} \leq \sum \sup_{x\in T_j} |D^m\mu^{j,i}|(x)\Big(\sqrt{\frac{\sinh h}{h}}h^2\,|f|_{2,T_j} + O(h^3)\,|f|_{1,T_j}\Big)$$

To achieve the proof it remains to prove that $\sum \sup_{x\in T_j}\left|D^m\mu^{j,i}\right|(x) \leq \frac{3}{\sinh^m\rho}$, where ρ is the radius of the inscribed circle of the triangle.
For $m = 0$:

$$\sum \sup_{x\in T_j}\left|\mu^{j,i}\right|(x) = 3$$

For $m = 1$:
The situation is a bit more complicated. We use the lower and upper bounds for G^{11}, G^{22} and G^{12} we have found in the Appendix C and which we have recalled before the theorem. We explicitly make the calculation for $\sup_{x\in T_j}\left|D\mu^{j,1}\right|(x)$. We denote (u, v) the coordinate system, l_A is the length of the altitude from $A = P_{j,1}$ and one can refer to Paragraph A.6.4 for the explanation of the identity $\Gamma = (\sinh a\sinh b\sin\phi)^2$:

$$\begin{aligned}\left|D\mu^{j,1}\right|^2(u,v) &= G^{11}(u,v)\\ &\leq \frac{2\alpha}{\Gamma}(1+O(h^2))\\ &\leq \frac{2(\cosh a - 1)}{(\sinh a\sinh b\sin\phi)^2}(1+O(h^2))\\ &\leq \frac{2(\cosh a - 1)}{\sinh^2 a\sinh^2 l_A}(1+O(h^2))\\ &\leq \frac{1}{\sinh^2\rho}(1+O(h^2))\end{aligned}$$

We directly have the same result for $|D\mu^{j,2}|^2$. For $|D\mu^{j,0}|^2$, it can seem to be a bit more complicated, but actually not:

$$\begin{aligned}\left|D\mu^{j,0}\right|^2(u,v) &= G^{11}(u,v) + 2G^{12}(u,v) + G^{22}(uv)\\ &= \frac{\Phi(u,v)}{\Gamma}\big(\gamma(\gamma+2)-2(1-u-v)\gamma(-\alpha-\beta+\gamma)-(1-u-v)^2\Lambda\big)\end{aligned}$$

We notice that $\left|D\mu^{j,0}\right|^2(u,v)$ is similar to $G^{11}(u,v)$. Following exactly the same method as for G^{11} in Appendix C, we have also the same upper bound for $\left|D\mu^{j,0}\right|^2(u,v) \leq \frac{1}{\sinh^2\rho}(1+O(h^2))$. And finally:

$$\sum \sup_{x\in K}\left|D\mu^{j,i}\right|(x) \leq \frac{3}{\sinh\rho}(1+O(h^2))$$

□

In the two next Paragraphs, we want to show that the solutions (eigenvalues and eigenfunctions) of the Spectral Problem computer on $V_{h,0}$ are good approximation of the ones computed on $H^1_0(X)$. A very powerful method for this has been developed by Babuška and Osborn in [BO91]. Our approach is more simple and basically follows the method described in [RT98].

4.3 Convergence of the Eigenvalues

The objective of this paragraph is to show that the eigenvalues of the Laplacian computed on $V_{h,0}$ are close to the ones computed on $H^1_0(X)$ when h is small[2]. We follow the method of [RT98] in Paragraphs 6.4 and 6.5. We recall that $\forall i \in \mathbb{N}, \varphi_i$ is a solution of the Spectral Problem on $H^1_0(X)$ associated to the eigenvalue λ_i. I is the dimension of the finite function space V_h and $\forall i \in [1,I]$, $\varphi_{i,h}$ is a solution of the Spectral Problem on $V_{h,0}$ associated to eigenvalue $\lambda_{i,h}$. That is, $\forall g \in H^1(X)$ and $\forall g_h \in V_h$:

$$(\nabla\varphi_i, \nabla g)_{0,X} = \lambda_i(\varphi_i, g)_{0,X} \tag{4.9}$$

$$(\nabla\varphi_{i,h}, \nabla g_h)_{0,X} = \lambda_{i,h}(\varphi_{i,h}, g_h)_{0,X} \tag{4.10}$$

As mentioned in Paragraph 1.3, for a non-zero eigenvalue, the average of $\varphi_{i,h}$ as to be zero on X. For the eigenvalue 0, the eigenfunction is the constant function, that is why we consider $V_{h,0}$ for the function space where we find the eigenfunctions.

[2] $V_{h,0}$ and $H^1_0(X)$ are the functions in V_h and $H^1(X)$ respectively with a zero average on X.

We next recall that $\forall m \leq I$, $\mathcal{V}_{m,h}$ and $\mathcal{V}_m$ are the sets of all m-dimensional subspaces of $V_{h,0}$ and $H_0^1(X)$ respectively. $V_{h,0} \subset H_0^1(X)$, and thus $\mathcal{V}_{m,h} \subset \mathcal{V}_m$. With the characterization of the eigenvalues given in Equations 1.16 and 3.6, the following inequality is straight-forward:

$$\lambda_{m,h} = \min_{E_m \in \mathcal{V}_{m,h}} \max_{\substack{f_h \in E_m \\ f_h \neq 0}} \mathcal{R}(f_h) \geq \min_{E_m \in \mathcal{V}_m} \max_{\substack{f \in E_m \\ f \neq 0}} \mathcal{R}(f) = \lambda_m$$

To obtain an inequality in the other direction, we define the elliptic projection operator Π_h from $H_0^1(X)$ to $V_{h,0}$ with respect to the same inner product as the one defined in paragraph 1.4 $(\nabla . , \nabla .)_{0,X}$. For a function $f \in H_0^1(X)$:

$$(\nabla(f - \Pi_h f), \nabla g_h)_{0,X} = 0 \quad \forall g_h \in V_h \tag{4.11}$$

We now denote V_m the subspace of $H_0^1(X)$ spanned by the m first eigenvectors:

$$V_m = \operatorname{Span}(\varphi_1, \ldots, \varphi_m)$$

Lemma 40. For $m \in \mathbb{N}$ such that $1 \leq m \leq I$, let us define:

$$\sigma_{m,h} = \inf_{\substack{f \in V_m \\ \|f\|_{0,X} = 1}} \|\Pi_h f\|_{0,X}$$

Then, if $\sigma_{m,h} > 0$:

$$\lambda_{m,h} \leq \sigma_{m,h}^{-2} \lambda_m$$

Proof. We may assume that $\sigma_{m,h} > 0$. Then, $\dim(\Pi_h V_m) = m$ (If this was not the case, a function $f_0 \neq 0 \in V_m$ would exist such that $\Pi_h f_0 = 0$, which contradicts the hypothesis $\sigma_{m,h} > 0$). Thus:

$$\lambda_{m,h} = \min_{E_m \in \mathcal{V}_{m,h}} \max_{\substack{f_h \in E_m \\ f_h \neq 0}} \mathcal{R}(f_h) \leq \max_{\substack{f_h \in \Pi_h V_m \\ f_h \neq 0}} \frac{|f_h|_{1,X}^2}{\|f_h\|_{0,X}^2} = \max_{\substack{f \in V_m \\ \|f\|_{0,X} = 1}} \frac{|\Pi_h f|_{1,X}^2}{\|\Pi_h f\|_{0,X}^2}$$

As Π_h is the orthogonal projection for the inner product $(\nabla . , \nabla .)_{0,X}$:

$$|\Pi_h f|_{1,X}^2 = |f|_{1,X}^2 - |f - \Pi_h f|_{1,X}^2 \leq |f|_{1,X}^2$$

Moreover, we know that $\lambda_m = \max_{\substack{f \in V_m \\ f \neq 0}} \mathcal{R}(f)$ (See Proposition 16), hence:

$$\lambda_{m,h} \leq \sup_{\substack{f \in V_m \\ \|f\|_{0,X} = 1}} \frac{|f|_{1,X}^2}{\|\Pi_h f\|_{0,X}^2} \leq \lambda_m \sup_{\substack{f \in V_m \\ \|f\|_{0,X} = 1}} \frac{1}{\|\Pi_h f\|_{0,X}^2}$$

$\square$

We now have to find a lower bound for the term $\sigma_{m,h}$.

Lemma 41. For $m \in \mathbb{N}$ such that $1 \leq m \leq I$, the following inequality holds:

$$\sigma_{m,h} \geq 1 - \frac{2\sqrt{m}}{\lambda_1} \sup_{\substack{f \in V_m \\ \|f\|_{0,X}=1}} |f - \Pi_h f|^2_{1,X}$$

Proof. Let $f \in V_m$ such that $\|f\|_{0,X} = 1$. Then, $f = \sum_{i=1}^m f_i \varphi_i$ with $\sum_{i=1}^m f_i^2 = 1$ because the φ_i are orthogonal with norm 1. It holds hence:

$$\begin{aligned}
1 - \|\Pi_h f\|^2_{0,X} &= (f - \Pi_h f, f + \Pi_h f)_{0,X} \\
&= (f - \Pi_h f, -f + \Pi_h f + 2f)_{0,X} \\
&= -\|f - \Pi_h f\|^2_{0,X} + 2(f - \Pi_h f, f)_{0,X} \\
\Rightarrow \qquad \|\Pi_h f\|^2_{0,X} &\geq 1 - 2(f - \Pi_h f, f)_{0,X}
\end{aligned}$$

Let us find an upper bound for the term $(f - \Pi_h f, f)_{0,X}$. As we know that every φ_i is a solution of the Spectral Problem:

$$(f - \Pi_h f, f)_{0,X} = \sum_{i=1}^m f_i (f - \Pi_h f, \varphi_i)_{0,X} = \sum_{i=1}^m \frac{f_i}{\lambda_i} (\nabla(f - \Pi_h f), \nabla \varphi_i)_{0,X}$$

Morevover, $f - \Pi_h f$ is orthogonal to $V_{h,0}$ for the inner product $(\nabla . , \nabla .)_{0,X}$, and thus:

$$(f - \Pi_h f, f)_{0,X} = \sum_{i=1}^m \frac{f_i}{\lambda_i} (\nabla(f - \Pi_h f), \nabla(\varphi_i - \Pi_h \varphi_i))_{0,X}$$

From the Cauchy-Schwarz inequalities, we can deduce:

$$\begin{aligned}
(f - \Pi_h f, f)_{0,X} &\leq |f - \Pi_h f|_{1,X} \sum_{i=1}^m \left| \frac{f_i}{\lambda_i} \right| |\varphi_i - \Pi_h \varphi_i|_{1,X} \\
&\leq |f - \Pi_h f|_{1,X} \left(\sum_{i=1}^m \left| \frac{f_i}{\lambda_i} \right|^2 \right)^{1/2} \left(\sum_{i=1}^m |\varphi_i - \Pi_h \varphi_i|^2_{1,X} \right)^{1/2} \\
&\leq |f - \Pi_h f|_{1,X} \frac{1}{\lambda_1} \left(\sum_{i=1}^m \sup_{\substack{g \in V_m \\ \|g\|_{0,X}=1}} |g - \Pi_h g|^2_{1,X} \right)^{1/2} \\
&\leq \frac{\sqrt{m}}{\lambda_1} \sup_{\substack{f \in V_m \\ \|f\|_{0,X}=1}} |f - \Pi_h f|^2_{1,X}
\end{aligned}$$

□

We are now able to prove the following theorem for the approximation of the eigenvalues of the surface. We suppose that φ_m is a solution of the Spectral Problem 4.9 associated with the eigenvalue λ_m and that for all $m \in \mathbb{N}$ such that $1 \leq m \leq I$, $\varphi_{m,h}$ a solution of 4.10 associated with the eigenvalue $\lambda_{m,h}$. We recall also for the proof that the eigenfunctions φ_i are $C^\infty(X)$.

Theorem 42 (Approximation of the Eigenvalues)**.** *Under the preceding asumptions, there exists a constant $C = C(m, X)$ (whose expression is given in the proof), such that:*

$$|\lambda_m - \lambda_{m,h}| \leq Ch^2 + O(h^3) \tag{4.12}$$

Proof. From the preceding Lemmas and anticipating that for sufficiently small h, the sup occuring in the next inequality is also small, we have:

$$\begin{aligned}\lambda_{m,h} &\leq \lambda_m \Big(1 - \frac{2\sqrt{m}}{\lambda_1} \sup_{\substack{f \in V_m \\ \|f\|_{0,X}=1}} |f - \Pi_h f|^2_{1,X}\Big)^{-1} \\ &\leq \lambda_m \Big(1 + \frac{2\sqrt{m}}{\lambda_1} \sup_{\substack{f \in V_m \\ \|f\|_{0,X}=1}} |f - \Pi_h f|^2_{1,X} + O\big(\sup_{\substack{f \in V_m \\ \|f\|_{0,X}=1}} |f - \Pi_h f|^4_{1,X}\big)\Big)\end{aligned}$$

Now, we will show that the sup is indeed small. For a function $f = \sum_{i=1}^m f_i \varphi_i$ in the subspace V_m with $\|f\|_{0,X} = 1$, the following inequality holds (it comes from the Cauchy-Schwarz inequality):

$$|f - \Pi_h f|_{1,X} = \Big|\sum_{i=1}^m f_i(\varphi_i - \Pi_h \varphi_i)\Big|_{1,X} \leq \Big(\sum_{i=1}^m |\varphi_i - \Pi_h \varphi_i|^2_{1,X}\Big)^{1/2}$$

Thus:

$$\sup_{\substack{f \in V_m \\ \|f\|_{0,X}=1}} |f - \Pi_h f|^2_{1,X} \leq \sum_{i=1}^m |\varphi_i - \Pi_h \varphi_i|^2_{1,X}$$

For any function $f \in V_m$, as $\Pi_h f$ is the orthogonal projection of f on $V_{h,0}$ with respect to the $(\nabla . , \nabla .)_{0,X}$ inner product:

$$|f - \Pi_h f|_{1,X} = \inf_{f_h \in V_{h,0}} |f - f_h|_{1,X} = \inf_{f_h \in V_h} |f - f_h|_{1,X} \leq |f - Lf|_{1,X}$$

And finally, from Equation 4.8 obtained in the Lagrange Interpolation Estimation Theorem 39, for any function $f \in C^\infty(X)$:

$$\begin{aligned}
|f - Lf|_{1,X}^2 &= \sum_{T \in \mathcal{T}_h} |f - Lf|_{1,T}^2 \\
&\leq \sum_{T \in \mathcal{T}_h} \frac{\sinh h}{h} \frac{9h^4}{\sinh^2 \rho} |f|_{2,T}^2 \big(1 + O(h)\big) \\
&\leq 9h^2 \frac{\sinh^2 h}{\sinh^2 \rho} |f|_{2,X}^2 \big(1 + O(h)\big)
\end{aligned}$$

We know moreover from paragraph A.6.3 that:

$$\frac{\sinh h}{\sinh \rho} \leq \frac{\sinh R}{\sinh \rho} \leq \sigma + O(h^2)$$

where $\sigma = \frac{4}{3(\sqrt{3}-2)^2}$ and $O(h^2) = 1.94h^2$. Thus:

$$\begin{aligned}
\lambda_{m,h} - \lambda_m &\leq \frac{2\lambda_m\sqrt{m}}{\lambda_1} \sum_{i=1}^{m} |\varphi_i - \Pi_h\varphi_i|_{1,X}^2 + O(\sup_{i=1\ldots m} |\varphi_i - \Pi_h\varphi_i|_{1,X}^4) \\
&\leq \frac{18\lambda_m\sqrt{m}}{\lambda_1} h^2\sigma^2 \sum_{i=1}^{m} |\varphi_i|_{2,X}^2 + O(h^3) \\
&\leq \frac{18\lambda_m\sqrt{m}}{\lambda_1} h^2\sigma^2 \sum_{i=1}^{m} C_X^2(1 + \lambda_i)^2 + O(h^3)
\end{aligned}$$

We have used the Elliptic Regularity Theorem 11 to state the last line. C_X is the constant appearing in this theorem. □

4.4 Convergence of the Eigenfunctions

As for the eigenvalues, we want to prove that the eigenfunctions of the Laplacian computed in $V_{h,0}$ are a good approximation of the eigenfunctions of the Laplacian computed in H_0^1X, when h tends to zero. Again, we follow the method described in [RT98] paragraphs 6.4 and 6.5 and completed in [Bof10] pages 53 to 58. We will prove it in two steps: first for the eigenvalues of multiplicity 1 (or simple eigenvalue) and then for eigenvalues of higher multiplicity (or a multiple eigenvalue).

Given $m \leq I$ and an eigenvalue λ_m of multiplicity 1, $\varphi_{m,h}$ will not necessarily be close to φ_m, because the span of φ_m or $-\varphi_m$ is the same eigensubspace. We therefore have to define the following vector $\varphi'_m = \pm\varphi_m$ such that φ'_m and $\varphi_{m,h}$ point "in the same direction":

$$(\varphi_m, \varphi_{m,h})_{0,X} \geq 0$$

Remark. Anticipating that $\varphi_{m,h}$ and φ_m are close to each other, and then not orthogonal with respect to the $(.\,,.)_{0,X}$ inner product, φ'_m is given by:

$$\varphi'_m = \frac{(\varphi_m, \varphi_{m,h})_{0,X}}{\left|(\varphi_m, \varphi_{m,h})_{0,X}\right|}\varphi_m$$

We also introduce the following quantity:

$$\tau_m = \max_{\substack{1 \leq i \leq I \\ i \neq m}} \frac{\lambda_m}{|\lambda_m - \lambda_{i,h}|}$$

This quantity makes sense since we know that for a sufficiently small h, $\lambda_{i,h}$ tends to $\lambda_i \neq \lambda_m$.

Lemma 43. If λ_m is a simple eigenvalue, then for a sufficiently small h and with the preceding definitions:

$$\|\varphi'_m - \varphi_{m,h}\|_{0,X} \leq 2(1 + \tau_m)\, \|\varphi'_m - \Pi_h \varphi'_m\|_{0,X} \tag{4.13}$$

Proof. Let $\eta_{m,h}$ be the orthogonal projection in $L^2(X)$ of $\Pi_h \varphi'_m$ on $\varphi_{m,h}$:

$$\eta_{m,h} = (\Pi_h \varphi'_m, \varphi_{m,h})_{0,X}\, \varphi_{m,h}$$

We will prove the Lemma by finding an upper bound of each term of the following inequality:

$$\|\varphi'_m - \varphi_{m,h}\|_{0,X} \leq \|\varphi'_m - \Pi_h \varphi'_m\|_{0,X} + \|\Pi_h \varphi'_m - \eta_{m,h}\|_{0,X} + \|\eta_{m,h} - \varphi_{m,h}\|_{0,X} \tag{4.14}$$

We start with the second term. As $\Pi_h \varphi'_m - \eta_{m,h} \in V_h$ and $\{\varphi_{i,h}\}$ is an orthonormal basis of V_h:

$$\Pi_h \varphi'_m - \eta_{m,h} = \sum_{\substack{i=1 \ldots I \\ i \neq m}} (\Pi_h \varphi'_m, \varphi_{i,h})_{0,X}\, \varphi_{i,h} \tag{4.15}$$

Recall that $\varphi_{i,h}$ is a solution of the Spectral Problem in $V_{h,0}$ (see Equation 4.10), Π_h is the orthogonal projection associated with the $(\nabla.\,, \nabla.)_{0,X}$ inner product (See Equation 4.11) and φ_i is a solution of the Spectral Problem in $H_0^1(X)$ (See Equation 4.9), thus:

$$\begin{aligned}(\Pi_h\varphi'_m, \varphi_{i,h})_{0,X} &= \frac{1}{\lambda_{i,h}}(\nabla\Pi_h\varphi'_m, \nabla\varphi_{i,h})_{0,X} \\ &= \frac{1}{\lambda_{i,h}}(\nabla\varphi'_m, \nabla\varphi_{i,h})_{0,X} \\ &= \frac{\lambda_m}{\lambda_{i,h}}(\varphi'_m, \varphi_{i,h})_{0,X}\end{aligned}$$

Thus:

$$(\lambda_{i,h} - \lambda_m)(\Pi_h\varphi'_m, \varphi_{i,h})_{0,X} = \lambda_m(\varphi'_m - \Pi_h\varphi'_m, \varphi_{i,h})_{0,X}$$

which leads to the following inequality if h is sufficiently small and $i = 1, \ldots, I, i \neq m$:

$$\left|(\Pi_h\varphi'_m, \varphi_{i,h})_{0,X}\right| \leq \tau_m \left|(\varphi'_m - \Pi_h\varphi'_m, \varphi_{i,h})_{0,X}\right|$$

Using now Equation 4.15:

$$\begin{aligned}\|\Pi_h\varphi'_m - \eta_{m,h}\|_{0,X}^2 &\leq \tau_m^2 \sum_{\substack{i=1\ldots I\\ i\neq m}} (\varphi'_m - \Pi_h\varphi'_m, \varphi_{i,h})_{0,X}^2 \\ &\leq \tau_m^2 \sum_{i=1\ldots I} (\varphi'_m - \Pi_h\varphi'_m, \varphi_{i,h})_{0,X}^2\end{aligned}$$

As $\{\varphi_{i,h}\}_{i=1\ldots I}$ is an orthonormal basis of V_h, this last sum represents the square of the norm of $\varphi'_m - \Pi_h\varphi'_m$, so that:

$$\|\Pi_h\varphi'_m - \eta_{m,h}\|_{0,X} \leq \tau_m \|\varphi'_m - \Pi_h\varphi'_m\|_{0,X} \tag{4.16}$$

Let us find an upper bound for the third term of the inequality. As $\eta_{m,h}$ is the orthogonal projection of $\Pi_h\varphi'_m$ on $\varphi_{m,h}$:

$$\eta_{m,h} - \varphi_{m,h} = \big((\Pi_h\varphi'_m, \varphi_{m,h})_{0,X} - 1\big)\varphi_{m,h}$$

Moreover, with the normalization of φ'_m and $\varphi_{m,h}$:

$$\begin{aligned}& \|\varphi'_m\|_{0,X} - \|\varphi'_m - \eta_{m,h}\|_{0,X} \leq \|\eta_{m,h}\|_{0,X} \leq \|\varphi'_m\|_{0,X} + \|\varphi'_m - \eta_{m,h}\|_{0,X} \\ \Leftrightarrow\quad & 1 - \|\varphi'_m - \eta_{m,h}\|_{0,X} \leq \left|(\Pi_h\varphi'_m, \varphi_{m,h})_{0,X}\right| \leq 1 + \|\varphi'_m - \eta_{m,h}\|_{0,X} \\ \Leftrightarrow\quad & \left|\left|(\Pi_h\varphi'_m, \varphi_{m,h})_{0,X}\right| - 1\right| \leq \|\varphi'_m - \eta_{m,h}\|_{0,X}\end{aligned}$$

Here is the point where the definition of φ'_m is important. Since $(\varphi'_m, \varphi_{m,h})_{0,X} \geq 0$, then $(\Pi_h\varphi'_m, \varphi_{m,h})_{0,X} \geq 0$, and we have:

$$\begin{aligned} \|\eta_{m,h} - \varphi_{m,h}\|_{0,X} &\leq \|\eta_{m,h} - \varphi'_m\|_{0,X} \\ &\leq \|\eta_{m,h} - \Pi_h\varphi'_m\|_{0,X} + \|\Pi_h\varphi'_m - \varphi'_m\|_{0,X} \end{aligned} \quad (4.17)$$

We have already found an upper bound for the first term of this last inequality. Combining Equations 4.14 with 4.16 and 4.17, the proof of the Lemma is achieved. □

We now want to state the corresponding lemma if the eigenvalue is multiple. We provide the proof for the multiplicity 2 but the method can be generalized to any other multiplicity. Let λ_m be an eigenvalue of multiplicity 2, that is $\lambda_m = \lambda_{m+1}$. As we pointed out before the preceding lemma with the choice of $\pm\varphi_m$, the problem is more complicated here and $\varphi_{m,h}$ is not close to φ_m or φ_{m+1}, but to a linear combination of them. The idea is to chose a normalized vector φ'_m such that its orthogonal projection in $L^2(X)$ on $\varphi_{m+1,h}$ is null:

$$\begin{aligned} (\varphi'_m, \varphi_{m,h})_{0,X} &\geq 0 \\ (\varphi'_m, \varphi_{m+1,h})_{0,X} &= 0 \end{aligned}$$

Remark. With the preceding assumptions, the linear combination to consider for the eigenfunction φ'_m is thus:

$$\varphi'_m = \epsilon \frac{(\varphi_{m+1}, \varphi_{m+1,h})_{0,X}\varphi_m - (\varphi_m, \varphi_{m+1,h})_{0,X}\varphi_{m+1}}{\sqrt{(\varphi_m, \varphi_{m+1,h})^2_{0,X} + (\varphi_{m+1}, \varphi_{m+1,h})^2_{0,X}}}$$

where:

$$\epsilon = \operatorname{sign}\left[(\varphi_m, \varphi_{m,h})_{0,X}(\varphi_{m+1}, \varphi_{m+1,h})_{0,X} - (\varphi_m, \varphi_{m+1,h})_{0,X}(\varphi_{m+1}, \varphi_{m,h})_{0,X}\right]$$

ϵ actually corresponds to the coherence of the orientations of the basis $\{\varphi_m, \varphi_{m+1}\}$ and $\{\varphi_{m,h}, \varphi_{m+1,h}\}$ in the respective eigen-subspaces.

We also define:

$$\tau_m = \max_{\substack{1\leq i\leq I \\ i\neq m,m+1}} \frac{\lambda_m}{|\lambda_m - \lambda_{i,h}|}$$

Lemma 44. If λ_m is a double eigenvalue, then for a sufficiently small h and with the preceding definitions:

$$\|\varphi'_m - \varphi_{m,h}\|_{0,X} \leq 2(1+\tau_m)\,\|\varphi'_m - \Pi_h\varphi'_m\|_{0,X} \quad (4.18)$$

Proof. We follow exactly the same argumentation as in Lemma 43. Let $\eta_{m,h}$ be the orthogonal projection in $L^2(X)$ of $\Pi_h\varphi'_m$ on $\varphi_{m,h}$:

$$\eta_{m,h} = (\Pi_h\varphi'_m, \varphi_{m,h})_{0,X}\, \varphi_{m,h}$$

Again, we prove the lemma by finding an upper bound of each term of the following inequality:

$$\|\varphi'_m - \varphi_{m,h}\|_{0,X} \le \|\varphi'_m - \Pi_h\varphi'_m\|_{0,X} + \|\Pi_h\varphi'_m - \eta_{m,h}\|_{0,X} + \|\eta_{m,h} - \varphi_{m,h}\|_{0,X} \tag{4.19}$$

Only the estimate of the second term differs from Lemma 43. Here again is the point where the definition of φ'_m comes in. As we know that $(\Pi_h\varphi'_m, \varphi_{m+1,h})_{0,X} = 0$, we have:

$$\Pi_h\varphi'_m - \eta_{m,h} = \sum_{\substack{i=1\ldots I\\ i\neq m,m+1}} (\Pi_h\varphi'_m, \varphi_{i,h})_{0,X}\, \varphi_{i,h} \tag{4.20}$$

We still have the other inequalities if h is sufficiently small, but this time for $\forall i = 1\ldots I, i \neq m, m+1$:

$$\left|(\Pi_h\varphi'_m, \varphi_{i,h})_{0,X}\right| \le \tau_m \left|(\varphi'_m - \Pi_h\varphi'_m, \varphi_{i,h})_{0,X}\right| \tag{4.21}$$

It is important that the term $i = m+1$ in the sum vanishes, otherwise, we could not state the following inequalities. Using Equation 4.20:

$$\begin{aligned}
\|\Pi_h\varphi'_m - \eta_{m,h}\|^2_{0,X} &\le \tau_m^2 \sum_{\substack{i=1\ldots I\\ i\neq m,m+1}} (\varphi'_m - \Pi_h\varphi'_m, \varphi_{i,h})^2_{0,X} \qquad (4.22)\\
&\le \tau_m^2 \sum_{i=1\ldots I} (\varphi'_m - \Pi_h\varphi'_m, \varphi_{i,h})^2_{0,X}
\end{aligned}$$

And finally:

$$\|\Pi_h\varphi'_m - \eta_{m,h}\|_{0,X} \le \tau_m \|\varphi'_m - \Pi_h\varphi'_m\|_{0,X}$$

We do not include the rest of the proof because it is exactly the same as in Lemma 43, we remark only that:

$$\operatorname{sign}\Big[(\Pi_h\varphi'_m, \varphi_{m,h})_{0,X}\Big] = \operatorname{sign}\Big[\frac{\lambda_m}{\lambda_{m,h}}(\varphi'_m, \varphi_{m,h})_{0,X}\Big] = \epsilon^2 \ge 0$$

□

For eigenvalues of higher multiplicity, the method stays exactly the same. As we want to estimate the error of the approximation in the $\|.\|_{1,X}$ norm, we have to state the following lemma:

Lemma 45. For $\varphi_{m,h}$ and φ'_m as previously defined, we have the following identity between the $|\,.\,|_{1,X}$ seminorm and the $\|\,.\,\|_{0,X}$ norm:

$$|\varphi'_m - \varphi_{m,h}|^2_{1,X} = \lambda_m \|\varphi'_m - \varphi_{m,h}\|^2_{0,X} + \lambda_{m,h} - \lambda_m \tag{4.23}$$

Proof. The proof is immediate:

$$\begin{aligned}
|\varphi'_m - \varphi_{m,h}|^2_{1,X} &= |\varphi'_m|^2_{1,X} + |\varphi_{m,h}|^2_{1,X} - 2(\nabla\varphi'_m, \nabla\varphi_{m,h})_{0,X} \\
&= \lambda_m + \lambda_{m,h} - 2\lambda_m(\varphi'_m, \varphi_{m,h})_{0,X} \\
&= -\lambda_m + \lambda_{m,h} - \lambda_m\big(2(\varphi'_m, \varphi_{m,h})_{0,X} - 2\big) \\
&= -\lambda_m + \lambda_{m,h} - \lambda_m\big(2(\varphi'_m, \varphi_{m,h})_{0,X} - \|\varphi'_m\|^2_{0,X} - \|\varphi_{m,h}\|^2_{0,X}\big) \\
&= -\lambda_m + \lambda_{m,h} + \lambda_m \|\varphi'_m - \varphi_{m,h}\|^2_{0,X}
\end{aligned}$$

□

We summarize all these results in the following theorem:

Theorem 46 (Approximation for the Eigenfunctions)**.** *Suppose that $\varphi_m, \ldots, \varphi_{m+k-1}$ are solutions of the Spectral Problem* 4.9 *associated with the eigenvalue λ_m of multiplicity $k \geq 1$. Suppose also that $\varphi_{m,h}, \ldots, \varphi_{m+k-1,h}$ are solutions of* 4.10 *associated with the eigenvalues $\lambda_{m,h}, \ldots \lambda_{m+k-1,h}$. Then for $0 \leq i \leq k-1$, there exists $\varphi'_{m+i} \in \mathrm{Span}(\varphi_m, \ldots, \varphi_{m+k-1})$ and a constant $C = C(m+i, X)$ (whose expression is given in the proof), such that:*

$$\left\|\varphi'_{m+i} - \varphi_{m+i,h}\right\|_{1,X} \leq Ch + O(h^2) \tag{4.24}$$

Proof. We first recall the result we obtained in the proof of the Eigenvalue Approximation Theorem 42. For any function $f \in C^\infty(X)$ with $\int_X f = 0$:

$$|f - \Pi_h f|^2_{1,X} \leq |f - Lf|^2_{1,X} \leq 9h^2\sigma^2 \, |f|^2_{2,X} \, 1 + O(h^3)$$

From preceding Lemmas 44 and 45 and using that $\varphi'_m \in C^\infty(X)$, we have:

$$\begin{aligned}
\left\|\varphi'_{m+i} - \varphi_{m+i,h}\right\|^2_{1,X} &= \left\|\varphi'_{m+i} - \varphi_{m+i,h}\right\|^2_{0,X} + \left|\varphi'_{m+i} - \varphi_{m+i,h}\right|^2_{1,X} \\
&\leq (\lambda_m + 1) \left\|\varphi'_{m+i} - \varphi_{m+i,h}\right\|^2_{0,X} + \lambda_{m+i,h} - \lambda_m \\
&\leq 2(\lambda_m + 1)(1 + \tau_m) \left\|\varphi'_{m+i} - \Pi_h \varphi'_{m+i}\right\|^2_{0,X} + \lambda_{m+i,h} - \lambda_m \\
&\leq \frac{2(\lambda_m + 1)(1 + \tau_m)}{\lambda_1} \left|\varphi'_{m+i} - \Pi_h \varphi'_{m+i}\right|^2_{1,X} + \lambda_{m+i,h} - \lambda_m \\
&\leq \frac{18(\lambda_m + 1)(1 + \tau_m)}{\lambda_1} h^2 \sigma^2 \left|\varphi'_{m+i}\right|^2_{2,X} + \lambda_{m+i,h} - \lambda_m \\
&\leq \frac{18(\lambda_m + 1)(1 + \tau_m)}{\lambda_1} h^2 \sigma^2 C_X^2 (1 + \lambda_m)^2 \\
&\quad + \frac{18\lambda_m \sqrt{m+i}}{\lambda_1} h^2 \sigma^2 \sum_{j=1}^{m+i} C_X^2 (1 + \lambda_j)^2 + O(h^3)
\end{aligned}$$

where C_X is the constant appearing in the Elliptic Regularity Theorem 11.

□

Chapter 5

Numerical Results

5.1 Presentation of the Program

In its final version, the program will be able to compute the eigenfunctions and eigenvalues of any Riemann surface. However, our "beta-version" is limited to surfaces of genus 2 in a "mw" gluing scheme (see Fig. 5.1). It triangulates the surface by successively triangulating the hexagons issued from the Y-pieces constituting the surface. The triangulation algorithm, presented in Chapter 2, has been implemented in c++ whereas the algebraic problem has been solved with Mathematica.

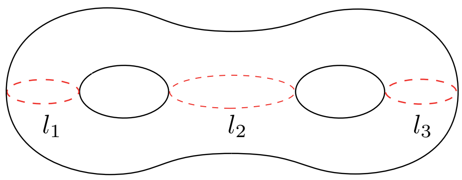

Figure 5.1: "mw" gluing scheme

We have seen in Paragraph 3.4 how we find the quadrature formulae for the matrices M and N of the Algebraic Problem. However, as mentioned at the end of Paragraph 3.4.4, we could not find a closed form for the integrals allowing the computation of the components of the matrices M and N. We have thus used a taylor expansion of the function to integrate, and computed the integral of this expansion. This leads to the following results.

5.1.1 Computation of the Diagonal Components of the Matrices M and N

As seen in Paragraph 3.4.3:

$$M^{ii} = \int_{T_1} \langle d\mu^i, d\mu^i \rangle + \cdots + \int_{T_m} \langle d\mu^i, d\mu^i \rangle$$
$$N^{ii} = \int_{T_1} \mu^i \mu^i + \cdots + \int_{T_m} \mu^i \mu^i$$

For the components of the matrix M:

$$\int_{T_k} \langle d\mu^i, d\mu^i \rangle = \frac{1}{\Gamma^{1/2}} \int_0^1 \int_0^{1-u} \frac{\gamma(\gamma+2) - 2(1-u-v)\gamma(-\alpha-\beta+\gamma) - (1-u-v)^2 \Lambda}{\big(1+2\beta u(1-u-v)+2\alpha v(1-u-v)+2\gamma uv\big)^{1/2}} dv du$$

Using now a taylor expansion in α, β and γ of the order 6 of the function to integrate (that is, order 8 in h)[1], we obtain:

$$\begin{aligned}
\int_{T_k} \langle d\mu^i, d\mu^i \rangle \approx \frac{1}{\Gamma^{1/2}} \Big(& \gamma + \frac{\alpha^2}{12} + \frac{\beta^2}{12} + \frac{\gamma^2}{6} - \frac{\alpha\beta}{6} + \frac{\beta\gamma}{12} + \frac{\gamma\alpha}{12} - \frac{\alpha^3}{120} - \frac{\beta^3}{120} - \frac{\gamma^3}{90} \\
& + \frac{\alpha^2\beta}{120} + \frac{\alpha\beta^2}{120} - \frac{\alpha^2\gamma}{360} - \frac{\alpha\gamma^2}{90} - \frac{\beta^2\gamma}{360} - \frac{\beta\gamma^2}{90} - \frac{\alpha\beta\gamma}{90} + \frac{\alpha^4}{560} + \frac{\beta^4}{560} \\
& + \frac{\gamma^4}{560} - \frac{\alpha^3\beta}{560} - \frac{\alpha\beta^3}{560} + \frac{\beta^2\gamma^2}{560} + \frac{\beta\gamma^3}{560} + \frac{\alpha^2\gamma^2}{560} + \frac{\alpha\gamma^3}{560} + \frac{\alpha^2\beta\gamma}{560} \\
& + \frac{\alpha\beta^2\gamma}{560} + \frac{\alpha\beta\gamma^2}{420} - \frac{\alpha^5}{2016} - \frac{\beta^5}{2016} - \frac{\gamma^5}{2520} + \frac{\alpha^4\beta}{2016} + \frac{\alpha\beta^4}{2016} + \frac{\beta^4\gamma}{10080} \\
& - \frac{\beta^3\gamma^2}{2520} - \frac{\beta^2\gamma^3}{2520} - \frac{\beta\gamma^4}{2520} + \frac{\alpha^4\gamma}{10080} - \frac{\alpha^3\gamma^2}{2520} - \frac{\alpha^2\gamma^3}{2520} - \frac{\alpha\gamma^4}{2520} - \frac{\alpha^3\beta\gamma}{2520} \\
& - \frac{\alpha^2\beta^2\gamma}{2520} - \frac{\alpha\beta^3\gamma}{2520} - \frac{\alpha\beta^2\gamma^2}{1680} - \frac{\alpha\beta\gamma^3}{1680} - \frac{\alpha^2\beta\gamma^2}{1680} + \frac{\alpha^6}{6336} + \frac{\beta^6}{6336} \\
& + \frac{\gamma^6}{1728} - \frac{\alpha^5\beta}{6336} - \frac{\alpha\beta^5}{6336} + \frac{\beta^5\gamma}{2376} + \frac{\beta^4\gamma^2}{1728} + \frac{\beta^3\gamma^3}{1728} + \frac{\beta^2\gamma^4}{1728} + \frac{\beta\gamma^5}{1728} \\
& + \frac{\alpha^5\gamma}{2376} + \frac{\alpha^4\gamma^2}{1728} + \frac{\alpha^3\gamma^3}{1728} + \frac{\alpha^2\gamma^4}{1728} + \frac{\alpha\gamma^5}{1728} + \frac{\alpha^4\beta\gamma}{1728} + \frac{\alpha^3\beta^2\gamma}{1728} + \frac{\alpha^2\beta^3\gamma}{1728} \\
& + \frac{\alpha\beta^4\gamma}{1728} + \frac{\alpha\beta^3\gamma^2}{1080} + \frac{\alpha\beta^2\gamma^3}{960} + \frac{\alpha\beta\gamma^4}{1080} + \frac{\alpha^2\beta\gamma^3}{960} + \frac{\alpha^3\beta\gamma^2}{1080} + \frac{\alpha^2\beta^2\gamma^2}{960} \Big)
\end{aligned}$$

For the components of the matrix N:

$$\int_{T_1} \mu^i \mu^i = \Gamma^{1/2} \int_0^1 \int_0^{1-u} \frac{(1-u-v)^2}{\big(1 + 2\beta u(1-u-v) + 2\alpha v(1-u-v) + 2\gamma uv\big)^{3/2}} dv du$$

[1] the number of terms in this expansion is probably too large, but we did not want the error coming from this expansion to interfere with the intrinsic error of the approximation method

Using a taylor expansion in α, β and γ of the order 4 (in the other integration, we divided by $\Gamma^{1/2}$, whereas we here multiply by $\Gamma^{1/2}$), we obtain:

$$\begin{aligned}\int_{T_k}\mu^i\mu^i \approx \Gamma^{1/2}\Big(&\frac{1}{12}-\frac{\alpha}{40}-\frac{\beta}{40}-\frac{\gamma}{120}+\frac{\alpha^2}{112}+\frac{\beta^2}{112}+\frac{\gamma^2}{672}+\frac{\alpha\beta}{112}+\frac{\beta\gamma}{224}+\frac{\gamma\alpha}{224}\\ &-\frac{\alpha^3}{288}-\frac{\beta^3}{288}-\frac{\gamma^3}{2880}-\frac{\alpha^2\beta}{288}-\frac{\alpha\beta^2}{288}-\frac{\alpha^2\gamma}{480}-\frac{\alpha\gamma^2}{960}-\frac{\beta^2\gamma}{480}-\frac{\beta\gamma^2}{960}\\ &-\frac{\alpha\beta\gamma}{360}+\frac{\alpha^4}{704}+\frac{\beta^4}{704}+\frac{\gamma^4}{10560}+\frac{\alpha^3\beta}{704}+\frac{\alpha^2\beta^2}{704}+\frac{\alpha\beta^3}{704}+\frac{\alpha^3\gamma}{1056}\\ &+\frac{\alpha^2\gamma^2}{1760}+\frac{\alpha\gamma^3}{3520}+\frac{\beta^3\gamma}{1056}+\frac{\beta^2\gamma^2}{1760}+\frac{\beta\gamma^3}{3520}+\frac{\alpha^2\beta\gamma}{704}+\frac{\alpha\beta^2\gamma^2}{704}+\frac{3\alpha\beta\gamma^2}{3520}\Big)\end{aligned}$$

5.1.2 Computation of the Non-Diagonal Components of the Matrices M and N

As seen in Paragraph 3.4.4:

$$M^{ij} = \int_{T_1}\langle d\mu^j, d\mu^i\rangle + \int_{T_2}\langle d\mu^j, d\mu^i\rangle$$
$$N^{ij} = \int_{T_1}\mu^j\mu^i + \int_{T_2}\mu^j\mu^i$$

For the components of the matrix M:

$$\begin{aligned}&\int_{T_k}\langle d\mu^j, d\mu^i\rangle\\ &=\frac{-1}{\Gamma^{1/2}}\int_0^1\int_0^{1-u}\frac{\alpha-\beta+\gamma+\alpha\gamma+u\gamma(-\alpha-\beta+\gamma)+(1-u-v)\alpha(\alpha-\beta-\gamma)+(1-u-v)u\Lambda}{\big(1+2\beta u(1-u-v)+2\alpha v(1-u-v)+2\gamma uv\big)^{1/2}}dvdu\\ &\approx\frac{-1}{\Gamma^{1/2}}\Big(\frac{\alpha}{2}-\frac{\beta}{2}+\frac{\gamma}{2}+\frac{\alpha^2}{12}+\frac{\gamma^2}{12}-\frac{\alpha\beta}{12}-\frac{\beta\gamma}{12}+\frac{\gamma\alpha}{6}-\frac{\alpha^3}{180}-\frac{\beta^3}{360}-\frac{\gamma^3}{180}\\ &+\frac{\alpha\beta^2}{120}-\frac{\alpha^2\gamma}{90}-\frac{\alpha\gamma^2}{90}+\frac{\beta^2\gamma}{120}-\frac{\alpha\beta\gamma}{180}+\frac{\alpha^4}{1120}+\frac{\beta^4}{1120}+\frac{\gamma^4}{1120}-\frac{\alpha\beta^3}{560}-\frac{\beta^3\gamma}{560}\\ &+\frac{\alpha^2\gamma^2}{560}+\frac{\alpha^3\gamma}{560}+\frac{\alpha\gamma^3}{560}+\frac{\alpha^2\beta\gamma}{840}+\frac{\alpha\beta^2\gamma}{1680}+\frac{\alpha\beta\gamma^2}{840}-\frac{\alpha^5}{5040}-\frac{\beta^5}{3360}-\frac{\gamma^5}{5040}\\ &+\frac{\alpha\beta^4}{2016}+\frac{\beta^4\gamma}{2016}-\frac{\alpha^4\gamma}{2520}-\frac{\alpha^3\gamma^2}{2520}-\frac{\alpha^2\gamma^3}{2520}-\frac{\alpha\gamma^4}{2520}-\frac{\alpha^3\beta\gamma}{3360}-\frac{\alpha^2\beta^2\gamma}{5040}-\frac{\alpha\beta^3\gamma}{10080}\\ &-\frac{\alpha\beta^2\gamma^2}{5040}-\frac{\alpha\beta\gamma^3}{3360}-\frac{\alpha^2\beta\gamma^2}{2520}+\frac{\alpha^6}{3456}-\frac{5\beta^6}{38016}+\frac{\gamma^6}{3456}-\frac{\alpha\beta^5}{6336}-\frac{\beta^5\gamma}{6336}+\frac{\alpha^5\gamma}{1728}\\ &+\frac{\alpha^4\gamma^2}{1728}+\frac{\alpha^3\gamma^3}{1728}+\frac{\alpha^2\gamma^4}{1728}+\frac{\alpha\gamma^5}{1728}+\frac{\alpha^4\beta\gamma}{2160}+\frac{\alpha^3\beta^2\gamma}{2880}+\frac{\alpha^2\beta^3\gamma}{4320}+\frac{\alpha\beta^4\gamma}{8640}+\frac{\alpha\beta^3\gamma^2}{4320}\\ &+\frac{\alpha\beta^2\gamma^3}{2880}+\frac{\alpha\beta\gamma^4}{2160}+\frac{\alpha^2\beta\gamma^3}{1440}+\frac{\alpha^3\beta\gamma^2}{1440}+\frac{\alpha^2\beta^2\gamma^2}{1920}\Big)\end{aligned}$$

For the components of the matrix N:

$$\int_{T_k} \mu^j \mu^i = \int_0^1\int_0^{1-u} \frac{\Gamma^{1/2} u(1-u-v)}{\big(1+2\beta u(1-u-v)+2\alpha v(1-u-v)+2\gamma uv\big)^{3/2}} dvdu$$

$$\approx \Gamma^{1/2}\Big(\frac{1}{24}-\frac{\alpha}{120}-\frac{\beta}{60}-\frac{\gamma}{120}+\frac{\alpha^2}{448}+\frac{3\beta^2}{448}+\frac{\gamma^2}{448}+\frac{\alpha\beta}{224}+\frac{\beta\gamma}{224}+\frac{\gamma\alpha}{336}$$
$$-\frac{\alpha^3}{1440}-\frac{\beta^3}{360}-\frac{\gamma^3}{1440}-\frac{\alpha^2\beta}{720}-\frac{\alpha\beta^2}{480}-\frac{\alpha^2\gamma}{960}-\frac{\alpha\gamma^2}{960}-\frac{\beta^2\gamma}{480}-\frac{\beta\gamma^2}{720}$$
$$-\frac{\alpha\beta\gamma}{480}+\frac{\alpha^4}{4224}+\frac{5\beta^4}{4224}+\frac{\gamma^4}{4224}+\frac{\alpha^3\beta}{2112}+\frac{\alpha^2\beta^2}{1408}+\frac{\alpha\beta^3}{1056}+\frac{\alpha^3\gamma}{2640}$$
$$+\frac{3\alpha^2\gamma^2}{7040}+\frac{\alpha\gamma^3}{2640}+\frac{\beta^3\gamma}{1056}+\frac{\beta^2\gamma^2}{1408}+\frac{\beta\gamma^3}{2112}+\frac{3\alpha^2\beta\gamma}{3520}+\frac{\alpha\beta^2\gamma^2}{880}+\frac{3\alpha\beta\gamma^2}{3520}\Big)$$

5.2 Test Case

It is always necessary to test a program with cases for which the exact solutions are well-known in order to see if the approximated solutions given by the program are close to the exact solutions. This is unfortunately not possible here, since no surface exists for which the eigenvalues and eigenfunctions are analytically computable. However, for the surface we present hereafter, some results are known.

5.2.1 The Surface F_2

It is a well-known fact that the minimal n-gon representing a Riemann surface of genus g is a $4g$-gon. On Figure 5.2, we provide two representations of the F_2 surface, one with the Fenchel-Nielsen parameters and the associated right-angled hexagons, the other as an octagon. The surface F_2 is the surface defined by the most symmetric octagon (all the triangles drawn in black on the figure are equilateral). To obtain the hexagons from the octagon, it is necessary to cut some parts of the octagon and glue them onto other places.

Using trigonometric identities in hyperbolic geometry (See [Bus92] pages 33 and 34), one can compute the length and twist (Fenchel-Nielsen) parameters l_i and t_i $(i = 1, 2, 3)$ of the two identical Y-Pieces. All the l_i are the same and correspond to the double of the length of the geodesic arc AD on Figure 5.2. All the t_i are also the same, and can be computed as $\frac{AE}{AD}$, where EF represents the common perpendicular to BC and AD. Triangle ABC is equilateral with angles $\frac{\pi}{4}$, thus:

$$\cosh AD = \sqrt{2}+1$$

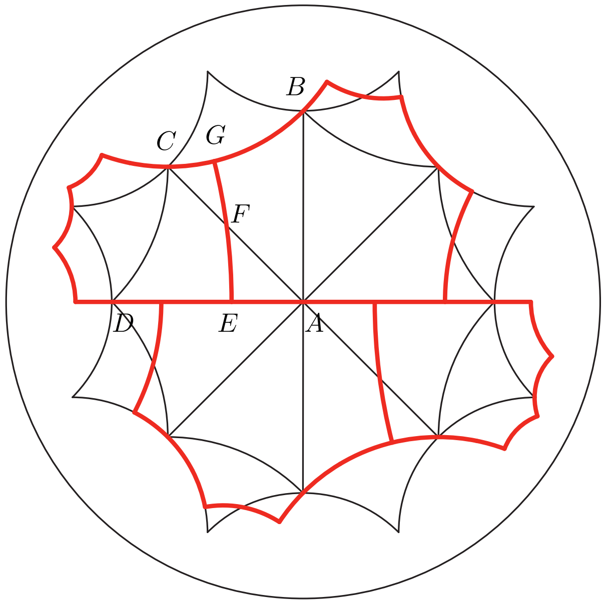

Figure 5.2: F_2 Surface

Triangle AEF is right-angled in E and, by symmetry, F is the center of AC, then:

$$\tanh AE = \frac{\sqrt{2}}{2} \tanh AF$$

Finally, the Fenchel-Nielsen parameters are:

$$l_i = 2\operatorname{arccosh}(\sqrt{2}+1)$$

$$t_i = \frac{\operatorname{arctanh}\left(\frac{\sqrt{2}}{2}\tanh(\frac{\operatorname{arccosh}(1+\sqrt{2})}{2})\right)}{\operatorname{arccosh}(\sqrt{2}+1)}$$

To achieve the description of the surface, we indicate on Figure 5.3 the gluing scheme: all the repeated points are identified.

5.2.2 Eigenvalues of the Surface F2

Jenni studied this surface in his Phd thesis [Jen81] and proved that the multiplicity of the first eigenvalue λ_1 is 3 and that:

$$3.83 \leq \lambda_1 \leq 3.85$$

This theoretical result allows us to test if the first three eigenvalues we calculate with our program tend to a common value between the preceding lower and upper bounds.

In this example (as well as on any surface), we can also test if the order of convergence is h^2 as expected. When we refine the triangulation, we actually create an increasing sequence (for the inclusion) of finites function subspaces:

$$V_h \subset V_{\frac{h}{2}} \subset V_{\frac{h}{4}} \subset V_{\frac{h}{8}}$$

From the formula 3.6 of the eigenvalues characterization, we deduce that for[2] $1 \leq m \leq I$:

$$\lambda_{m,h} \geq \lambda_{m,\frac{h}{2}} \geq \lambda_{m,\frac{h}{4}} \geq \lambda_{m,\frac{h}{8}}$$

With the beta-version of the program, we are unfortunately limited to four successive refinements. With more refinement, Mathematica is unable to deal with so many triangles.

5.2.3 Triangulation of F_2

In Figures 5.3, 5.4, 5.5 and 5.6, we present a sequence of four successive refinements of the triangulation. The initial triangulation is obtained with the algorithm presented in Chapter 2 by subdividing the shortest edge into two parts. It is then successively refined, creating four triangles from one as described in Paragraph 2.4.

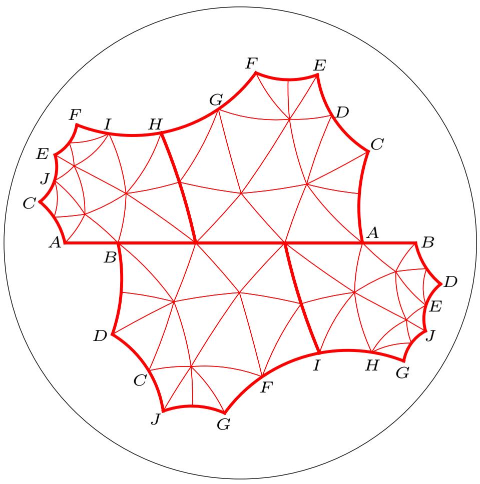

Figure 5.3: Initial triangulation. Number of triangles: 64

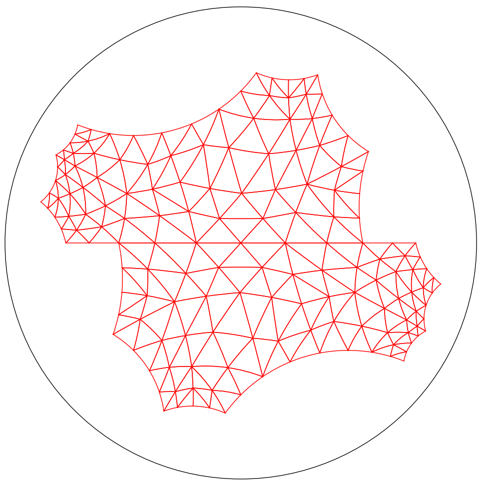

Figure 5.4: First refinement. Number of triangles: 256

[2]I is the dimension of V_h

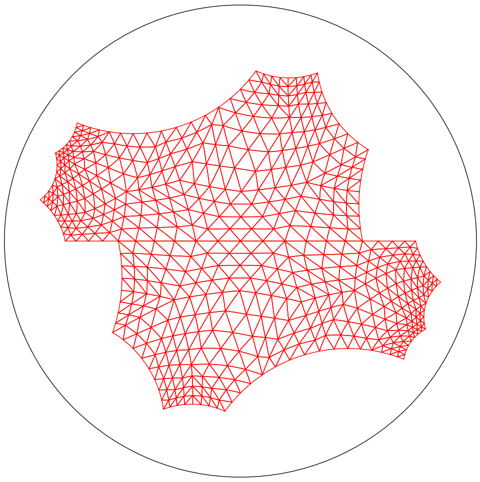

Figure 5.5: Second refinement. Number of triangles: 1024

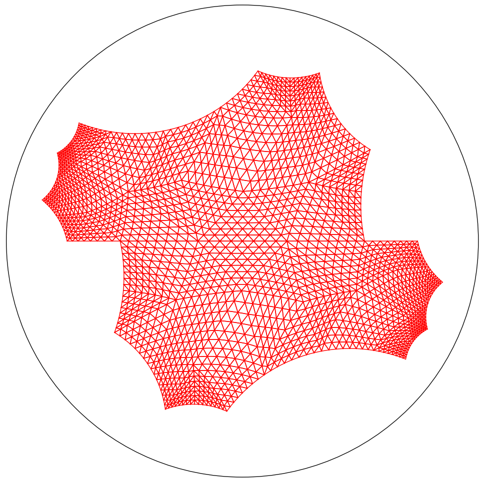

Figure 5.6: Third refinement. Number of triangles: 4092

5.2.4 Eigenvalues of F_2

We compute the eigenvalues on the finite function spaces associated with the triangulations of Figures 5.3, 5.4, 5.5 and 5.6 and we summarize the results in the following tables. $n-1$ represents the number of refinements of the initial triangulation and for an easier reading, we denote λ_{1k} $(k=1,2,3)$ the three first eigenvalues in $V_{h,0}$ instead of $\lambda_{k,\frac{h}{2^{n-1}}}$ since they correspond to the eigenvalue λ_1 in $H_0^1(X)$ (same for higher eigenvalues). For the first eigenvalue, we obtain:

n	λ_{11}	λ_{12}	λ_{13}
1	4.4280	4.4860	4.5624
2	4.0033	4.0066	4.0139
3	3.8804	3.8810	3.8825
4	3.8493	3.8494	3.8498

For the second eigenvalue:

n	λ_{21}	λ_{22}	λ_{23}	λ_{24}
1	6.5067	6.5958	6.8580	7.3560
2	5.6453	5.6698	5.7067	5.7704
3	5.4268	5.4325	5.4409	5.4545
4	5.3719	5.3733	5.3754	5.3787

For the third eigenvalue:

n	λ_{31}	λ_{32}
1	10.586	11.216
2	8.9321	8.9333
3	8.4186	8.4229
4	8.2917	8.2931

For the seventh eigenvalue:

n	λ_{71}	λ_{72}	λ_{73}	λ_{74}
1	32.146	35.392	36.343	41.554
2	24.097	24.214	24.804	24.852
3	21.436	21.454	21.575	21.584
4	20.749	20.753	20.782	20.785

To verify if the order of convergence for the eigenvalues is in h^2, we plot these results on the following curves and find, with the software Igor Pro, an interpolating function of the type $A + \frac{B}{n^2}$ which fits these points.

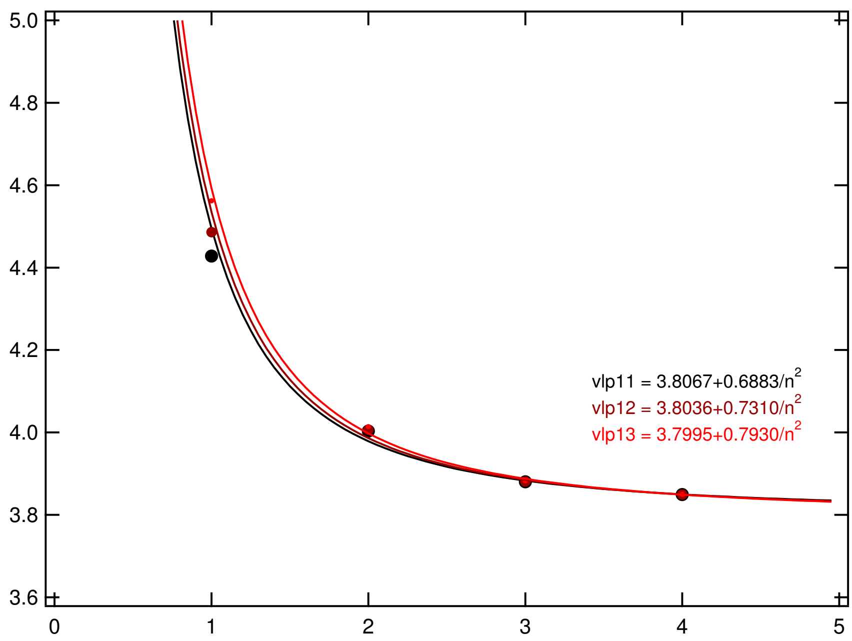

Figure 5.7: The three first approximate eigenvalues converging to λ_1

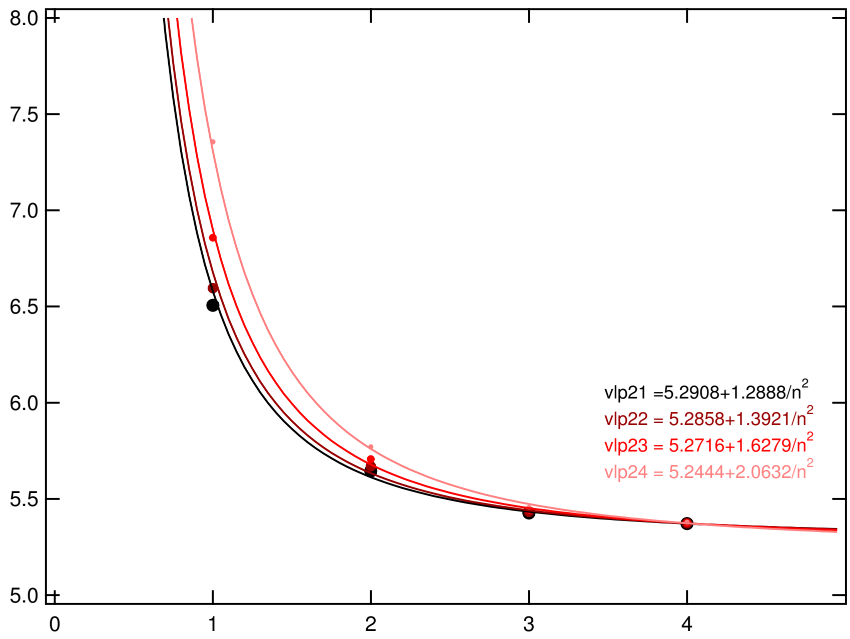

Figure 5.8: The four approximate eigenvalues converging to λ_2

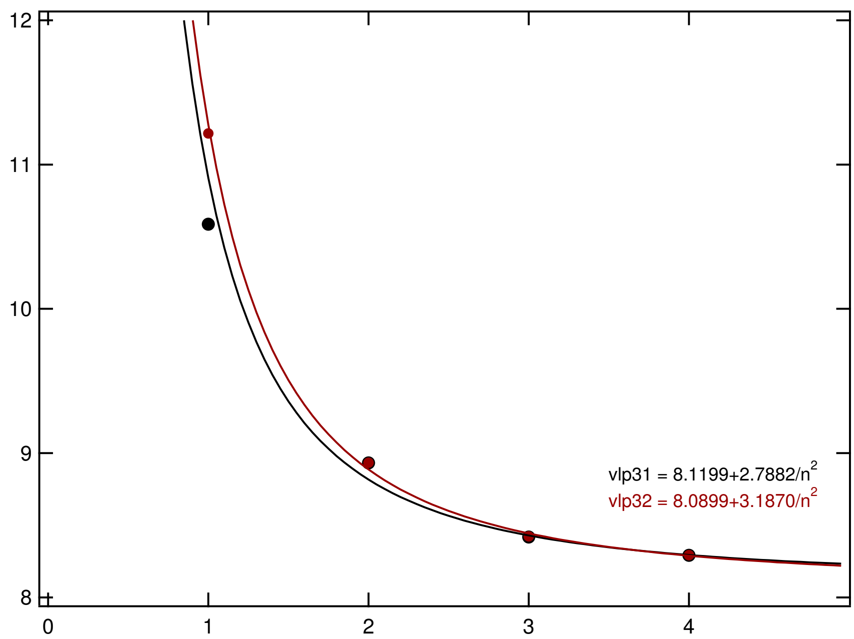

Figure 5.9: The two approximate eigenvalues converging to λ_3

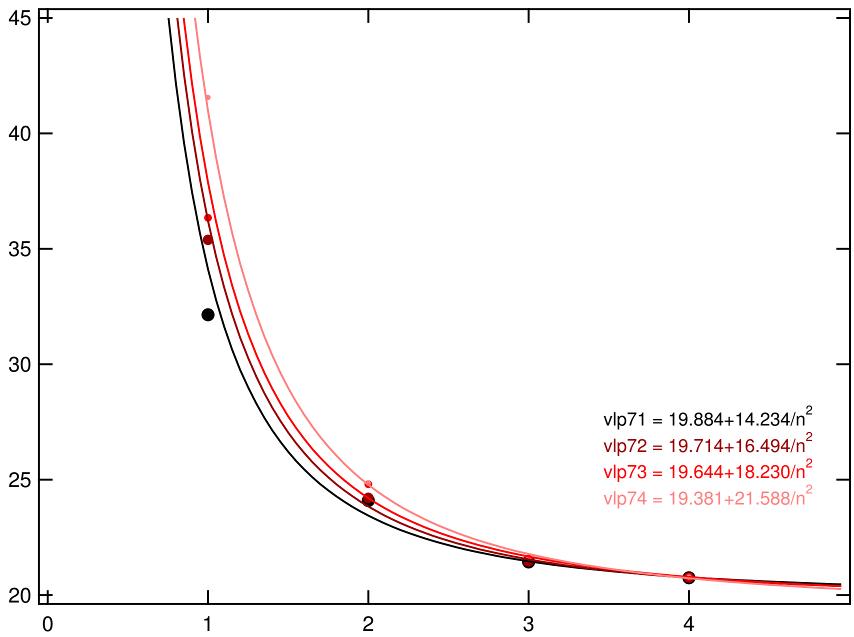

Figure 5.10: The four approximate eigenvalues converging to λ_7

Since we do not know the values of the exact eigenvalue represented by the coefficient A, it could be possible to find other functions, changing A, B and the power of n, which fit also quite well these points. However, we know that the first eigenvalue is between 3.83 and 3.85. Using this fact, we can observe that there is no better fitting function for the first eigenvalue than the one of the type $A + \frac{B}{n^2}$.

To achieve the interpretation of these results, we plot in the next figures $\ln(\lambda_{ik} - A)$ in function of $\ln n$ for each eigenvalue. We can notice that the fitting curves are lines with a gradient close to -2, which confirms that the order of convergence for the eigenvalues is in h^2.

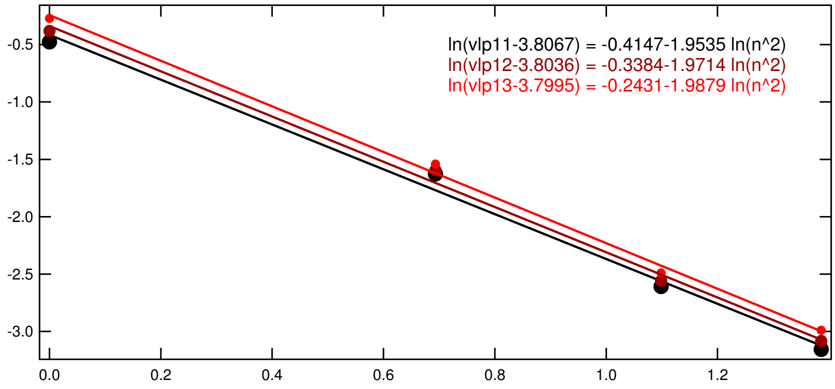

Figure 5.11: λ_{1k} in logarithmic scale

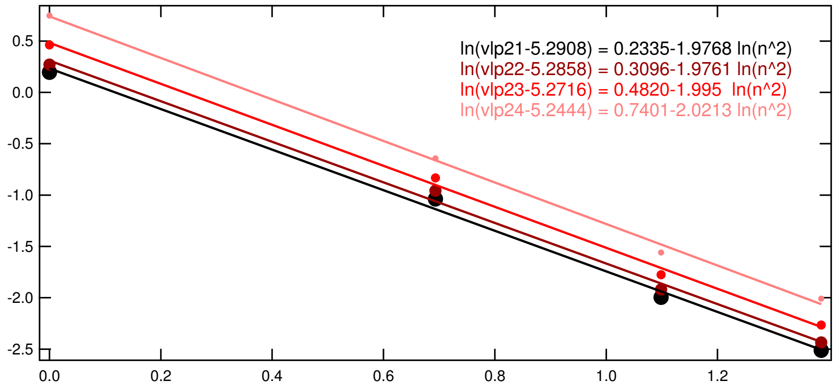

Figure 5.12: λ_{2k} in logarithmic scale

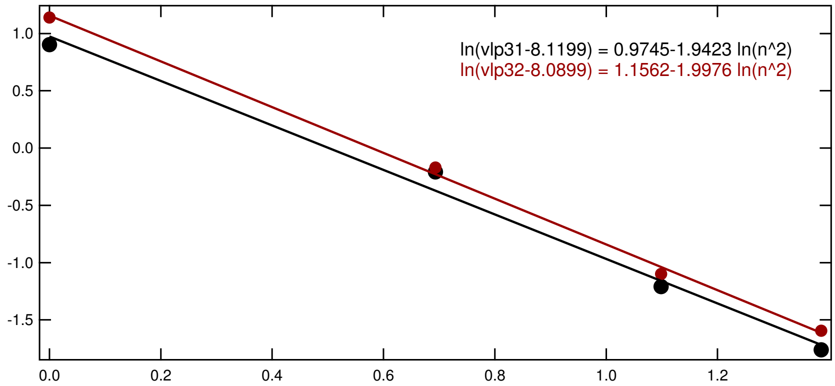

Figure 5.13: λ_{3k} in logarithmic scale

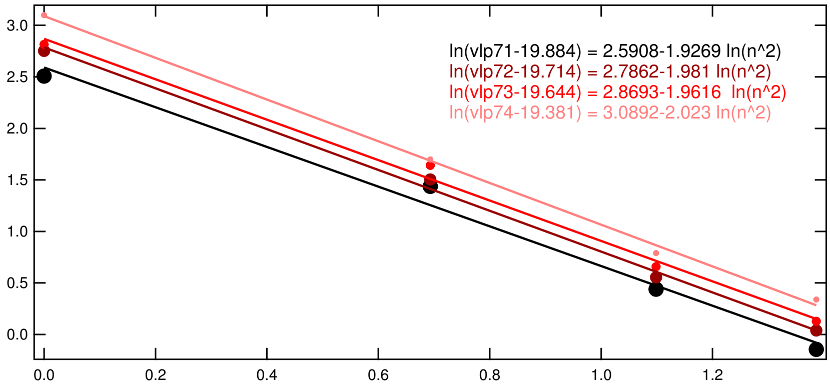

Figure 5.14: λ_{7k} in logarithmic scale

Conclusion and Outlook

Theorems 42 and 46 in Chapter 4 show that we have reached the goal we set, that is, to create a method which can calculate an approximation of the eigenfunctions and eigenvalues on the surface while having control on the convergence speed, and which is invariant under the isometries of the surface. The results in Chapter 5 show, moreover, that the program runs as expected on the examples we calculate.

Let us zoom out and take a global look at this work and its main points. Hyperbolic Geometry provides tools for the triangulation and the barycentric coordinates, which allow us to define and transform the Spectral Problem on a finite functions space into a solvable algebraic problem. The essentially hyperbolic part is actually the triangulation since the constant -1 curvature provides the tools presented in Appendix A. This may not seem so crucial for the definition of the barycentric coordinates, since it is possible to define intrinsic barycentric coordinates on a surface, especially if the size of the triangles decreases. Hyperbolic geometry, however, allows to derive a simple expression for them and the associated metric tensor. The hyperbolic characteristic appears also in the Lagrange Interpolation Theorem 39, where the fact that the derivatives of the components of the metric tensor are terms of order $O(h^4)$ (leading to conclude that the Christoffel symbols are terms of order $O(h^2)$) allows us to estimate the error of the interpolation.

Hyperbolic geometry hence provides very useful tools, but is only necessary for the convergence of the approximation method. We could thus imagine to generalize our method to any surface with a Riemannian metric tensor, defining some kinds of equivalence classes of coordinates charts for which the convergence theorems hold.

Recalling the Ddoziuk's article [Dod76] at the origin of this work, another development could be to show similar results for the Spectral Problem expressed with 1- and 2-forms, or even for manifolds of higher dimension.

Following the same idea of generalization, albeit in a more concrete manner, it should not prove difficult to use our results directly to a PDE Problem with boundaries conditions (*e.g.* type Dirichlet).

Finally, we want to point out the originality of this work, in the sense that it mixes several components of mathematics: Riemannian geometry, functional analysis, numerical analysis as well as programming. Normally there is not much communication between these disciplines, and a certain degree of intellectual flexibility was necessary to assimilate the knowledge of these different branches of mathematics and build bridges between them. Not an easy task, but nevertheless exciting!

Appendix A

Matrix Model

The very short presentation of the Matrix Model in paragraph 3.1 is not developed enough to explain all the tools required to write the triangulation algorithm presented in Chapter 2. We showed how the points and the geodesics of $\mathbb{H}$ can be represented by matrices. We now need to explain how to calculate a geodesic matrix from two point matrices. We also want to triangulate the interior of a domain and thus need to define the concept of right- and left-hand side of a geodesic. This will be done by orienting them. We also have to compute the distance between two points, and finally to be able to translate a point along an oriented geodesic. We recall that this model was originally discussed by Fenchel in [Fen89] and further developed by Semmler in [ADBS11]. Our presentation is strongly based on this last article, particularly Paragraphs A.1 and A.3.

A.1 Points and Geodesics

A.1.1 Möbius Transformations

It is well-know that the isometries of $\mathbb{H}$ are the Möbius transformations preserving $\mathbb{H}$. They are of the following type:

$$z \in \mathbb{H} \mapsto \frac{az+b}{cz+d} \quad \text{if } \det \begin{pmatrix} a & b \\ c & d \end{pmatrix} > 0$$
$$z \in \mathbb{H} \mapsto \frac{a\bar{z}+b}{c\bar{z}+d} \quad \text{if } \det \begin{pmatrix} a & b \\ c & d \end{pmatrix} < 0$$

It seems natural to associate a matrix of $\mathrm{GL}(2, \mathbb{R})$ to the corresponding Möbius transformation. Note also that multiplying a matrix by a constant yields to the same Möbius transformation.

A.1.2 Points and Geodesics

A point of $\mathbb{H}$ is identified with the half-turn around itself and its corresponding Matrix in $\mathrm{GL}(2, \mathbb{R})$. For a point $p = r + is \in \mathbb{H}$, the corresponding normalized matrix is:

$$p = \frac{1}{s} \begin{pmatrix} -r & r^2 + s^2 \\ -1 & r \end{pmatrix} \tag{A.1}$$

The letter p denotes either the geometric point in $\mathbb{H}$ or the Möbius transformation corresponding to the half-turn around it, or its corresponding matrix (usually normalized but not always). Observe that we chose the bottom-left component of the matrix to be -1. One may check that indeed the Möbius transformation given by this matrix keeps the point $r + is$ fixed and that its square is the matrix -1 (1 being the identity matrix), which corresponds to the identity map.

A geodesic in $\mathbb{H}$ is identified with the symmetry around itself and the corresponding matrix in $\mathrm{GL}(2, \mathbb{R})$. For a geodesic γ defined by the Euclidean circle with center $\rho \in \mathbb{R}$ and radius μ, the corresponding normalized matrix is:

$$\gamma = \frac{1}{\mu} \begin{pmatrix} \rho & -\rho^2 + \mu^2 \\ 1 & -\rho \end{pmatrix} \tag{A.2}$$

The letter γ denotes either the geometric geodesic in $\mathbb{H}$ or the Möbius transformation corresponding to the symmetry around it, or its corresponding matrix (usually normalized but not always). Here also, one may check that the Möbius transformation given by this matrix keeps the geodesic γ invariant and that its square is the identity matrix.

Remark that these matrices represent the null-trace subspace of $\mathrm{GL}(2, \mathbb{R})$, denoted $\mathrm{T0}(2, \mathbb{R})$. A basis of this subspace is given by the three following matrices:

$$I = \begin{pmatrix} 1 & 0 \\ 0 & -1 \end{pmatrix}, \quad J = \begin{pmatrix} 0 & 1 \\ 1 & 0 \end{pmatrix}, \quad K = \begin{pmatrix} 0 & 1 \\ -1 & 0 \end{pmatrix}$$

With the following properties:

$$I^2 = J^2 = -K^2 = 1$$
$$IJ = -JI = K, \quad JK = -KJ = -I, \quad KI = -IK = -J$$

As for the trace we define a new trace operator for a matrix A of $\mathrm{GL}(2, \mathbb{R})$: $\operatorname{tr} A = \frac{1}{2} \operatorname{trace} A$. It is also straight-forward to verify the properties:

Proposition 47. For $A \in \mathrm{T0}(2\mathbb{R})$:

$$\det A = -\operatorname{tr} A^2$$
$$A^2 = \operatorname{tr} A^2 \ 1$$

The representation of the Möbius transformations by a matrix has a several useful properties. We present some of them in what follows.

A.1.3 Action of Isometries on Points and Geodesics

Proposition 48. Given a point p, a geodesic γ and an isometry of $\mathbb{H}$ A such that $\det A > 0$. Then:

$$A(p) = ApA^{-1}$$
$$A(\gamma) = A\gamma A^{-1}$$

where A is seen on the left of the equality as a Möbius transformation and on the right as a matrix.

Proof. It is always possible to isometrically move the point p onto i and to conjugate A accordingly. Similarly, we may move γ onto γ_0, the vertical geodesic at the origin. Thus we may assume that:

$$p = \begin{pmatrix} 0 & 1 \\ -1 & 0 \end{pmatrix}, \quad \gamma = \gamma_0 = \begin{pmatrix} 1 & 0 \\ 0 & -1 \end{pmatrix}, \quad A = \begin{pmatrix} a & b \\ c & d \end{pmatrix}$$

where A is supposed to have been normalized ($\det A = 1$). Let us calculate the image of p:

$$A(p) = \frac{ai+b}{ci+d} = \frac{ac+db+i}{c^2+d^2}$$

Moreover:

$$ApA^{-1} = \begin{pmatrix} -db-ac & b^2+a^2 \\ -d^2-c^2 & db+ac \end{pmatrix}$$

Hence, both calculations lead to the same image point.
Let us now calculate the image of γ. $A(0) = \frac{b}{d}$ and $A(\infty) = \frac{a}{c}$. The image of γ is thus the geodesic with centre $\rho = \frac{1}{2}\left(\frac{b}{d} + \frac{a}{c}\right)$ and radius $\nu = \frac{1}{2|dc|}$.
Moreover:

$$A\gamma A^{-1} = \begin{pmatrix} ad+bc & -2ba \\ 2dc & -ad-bc \end{pmatrix}$$

Again, both calculations lead to the same image geodesic. $\square$

Remark. If $\det(A) < 0$, then:

$$A(p) = -ApA^{-1}$$
$$A(\gamma) = A\gamma A^{-1}$$

As in the preceding proposition, we juggle between the Möbius transformation and matrix representations for further calculations, choosing the most appropriated.

A.2 Orientation of the Matrices of $\mathrm{T0}(2,\mathbb{R})$

A.2.1 Orientation of the Geodesics

The domain we want to triangulate is a geodesic polygonal domain and it is thus necessary to know the interior and the exterior of the domain. A way to do so is to define an orientation for the geodesics, and consequently the right- and left-hand side of the geodesic.

Given a matrix γ with $\det\gamma < 0$ and $\operatorname{tr}\gamma = 0$. Such a matrix is called a geodesic matrix, since, up to normalization, it is of the same type as described in the preceding paragraph. Let us now define:

$$\alpha = \alpha_\gamma = a\,1 + \gamma \tag{A.3}$$

with $a \in \mathbb{R}$ chosen such that $\det\alpha = 1$. This leads to: $a = \pm\sqrt{1 + \operatorname{tr}\gamma^2}$. Here lies the choice of the orientation of γ. We choose:

$$a = +\sqrt{1 + \operatorname{tr}\gamma^2}$$

We now have to explain why this may be interpreted as an orientation of the geodesic. One of the many useful properties of the Matrix Model is:

Proposition 49. Given a point p and a geodesic γ:

$$p \in \gamma \quad \Leftrightarrow \quad p\gamma = -\gamma p \quad \Leftrightarrow \quad \operatorname{tr}(p\gamma) = 0$$

Proof. Move γ isometrically to γ_0 and consider a point $p = r + is$, then:

$$\gamma = \begin{pmatrix} 1 & 0 \\ 0 & -1 \end{pmatrix}, \qquad p = \frac{1}{s}\begin{pmatrix} -r & r^2+s^2 \\ -1 & r \end{pmatrix}$$
$$p\gamma = \frac{1}{s}\begin{pmatrix} -r & -r^2-s^2 \\ -1 & -r \end{pmatrix}, \qquad \gamma p = \frac{1}{s}\begin{pmatrix} -r & r^2+s^2 \\ 1 & -r \end{pmatrix}$$

and the results follow immediately. □

Given a point p on a geodesic γ. The above $\alpha = \alpha_\gamma$ is an isometry of $\mathbb{H}$ with positive determinant. Let us define q the image of p by α: $q = \alpha p \alpha^{-1}$. q actually lies on γ because:

$$\begin{aligned} \operatorname{tr}(q\gamma) &= \operatorname{tr}(\alpha p \alpha^{-1}\gamma) \\ &= \operatorname{tr}(p\alpha^{-1}\gamma\alpha) \\ &= \operatorname{tr}(p\alpha^{-1}\alpha\gamma) \\ &= \operatorname{tr}(p\gamma) = 0 \end{aligned}$$

This leads to the definition of the orientation of a geodesic:

Definition 50. Given a geodesic γ, a point p lying on γ and q the image of p by α_γ. We say that γ is oriented from p to q.

Remark. Next proposition shows that this definition is independent of the choice of the point p.

Note that the geodesic orientation is only visible in α: γ and $-\gamma$ represent indeed the same Moebius transformation or geometrical geodesic and a is the same for γ and $-\gamma$, but α_γ and $\alpha_{-\gamma}$ are not the same.

Proposition 51. Given a geodesic γ oriented from a point p to its image q by α. Consider now an isometry A of $\mathbb{H}$ with $\det A = 1$. The image $\gamma' = A\gamma A^{-1}$ is oriented from $p' = ApA^{-1}$ to $q' = AqA^{-1}$.

Proof. Let us calculate $\alpha' = \alpha_{\gamma'}$:

$$\begin{aligned}\alpha' &= \sqrt{1+\operatorname{tr}\gamma'^2}\ 1+\gamma' \\ &= \sqrt{1+\operatorname{tr}(A\gamma A^{-1}A\gamma A^{-1})}\ 1\ +\gamma' \\ &= \sqrt{1+\operatorname{tr}\gamma^2}\ 1+A\gamma A^{-1} \\ &= A\alpha A^{-1}\end{aligned}$$

Thus:

$$\alpha' p' \alpha'^{-1} = A\alpha A^{-1}ApA^{-1}A\alpha^{-1}A^{-1} = AqA^{-1} = q'$$

□

In particular, if $\lambda \in \mathbb{R}$, then $\lambda\gamma$ has the orientation of γ "multiplied" by the sign of λ. Let us study a basic example with the vertical geodesic at the origin γ_0. i lies on γ_0 and $a = \sqrt{2}$, thus:

$$\alpha_{\gamma_0} = \begin{pmatrix} 1+\sqrt{2} & 0 \\ 0 & -1+\sqrt{2} \end{pmatrix}$$

The image of i by α_{γ_0} is[1]:

$$q = \frac{(1+\sqrt{2})i}{(-1+\sqrt{2})} = \left(1+\sqrt{2}\right)^2 i$$

which is above i. On the other hand:

$$\alpha_{-\gamma_0} = \begin{pmatrix} -1+\sqrt{2} & 0 \\ 0 & 1+\sqrt{2} \end{pmatrix}$$

[1]we calculate here using the Möbius transformation representation

And the image of i by $\alpha_{-\gamma_0}$ is:

$$q = \frac{(-1+\sqrt{2})i}{(1+\sqrt{2})} = \big(-1+\sqrt{2}\big)^2 i$$

which is below i. Hence, we can affirm that γ_0 is bottom-up oriented, whereas $-\gamma_0$ is top-down oriented.

A.2.2 Orientation of the Points

As a point matrix p and its opposite $-p$ represent the same half turn around the point, a similar argumentation can be carried out for the points, leading to the definition of a positive and negative orientation for a point. However, the motivation for the geodesic orientation was to have a tool to define right- and left-hand side about it. This is needed to determine the interior of the domains we want to triangulate. An orientation of points provides no advantage for this, and thus a point matrix will always be given with its bottom-left component being negative and the up-right component being positive.

A.3 Wedge Operator and Distances

A powerful advantage of this Matrix Model is the following operator that computes the geodesic matrix from two points, the point matrix from two intersecting geodesics, etc.

Definition 52. Given two matrices A and B of $\mathrm{T0}(2,\mathbb{R})$, we define:

$$A \wedge B = \frac{1}{2}(AB - BA) \tag{A.4}$$

Proposition 53. Let p, q, γ, σ be two different point matrices and two different geodesic matrices respectively, then:

i) $p \wedge q$ represents the geodesic through p and q, oriented from p to q.

ii) $p \wedge \gamma$ represents the geodesic through p perpendicular to γ oriented to the left from γ.

iii) If γ and σ don't intersect, $\gamma \wedge \sigma$ represents the common perpendicular geodesic to γ and σ.

iv) If γ and σ intersect, $\gamma \wedge \sigma$ represents the intersection point.

Proof. In Proposition 51, we proved that the image by an isometry of a geodesic oriented from p to q has the same orientation as the geodesic oriented from p' to q', the images of p and q. This allows us to move the geodesics for the demonstration. We will in particular use the vertical geodesic at the origin γ_0.

i) Given $p = is$ and $q = it$ on $\gamma_0 = \begin{pmatrix} 1 & 0 \\ 0 & -1 \end{pmatrix}$:

$$p = \begin{pmatrix} 0 & s \\ -1/s & 0 \end{pmatrix}, \quad q = \begin{pmatrix} 0 & t \\ -1/t & 0 \end{pmatrix}, \quad p \wedge q = \frac{1}{2} \begin{pmatrix} -\frac{s}{t} + \frac{t}{s} & 0 \\ 0 & -\frac{t}{s} + \frac{s}{t} \end{pmatrix}$$

If $t > s$, then $-\frac{s}{t} + \frac{t}{s} > 0$ and $p \wedge q$ has the same orientation as γ_0. If $t < s$, then $-\frac{s}{t} + \frac{t}{s} < 0$ and $p \wedge q$ has the opposite orientation as γ_0. In both cases, $p \wedge q$ has the orientation from p to q.

ii) Move isometrically γ to γ_0 and consider $p = r + is$:

$$p \wedge \gamma = \frac{1}{s} \begin{pmatrix} 0 & -r^2 - s^2 \\ -1 & 0 \end{pmatrix}$$

It is obviously a geodesic matrix with radius $\sqrt{r^2 + s^2}$ and centre 0. Let us now calculate $\alpha = \alpha(p \wedge \gamma)$ and the image by α of the point $q = i\sqrt{r^2 + s^2}$ lying on γ and $p \wedge \gamma$. $a(p \wedge \gamma) = \sqrt{1 - \det p \wedge \gamma} = \sqrt{2 + \frac{r^2}{s^2}}$, thus:

$$\alpha = \begin{pmatrix} \sqrt{2 + \frac{r^2}{s^2}} & -\frac{r^2+s^2}{s} \\ -\frac{1}{s} & \sqrt{2 + \frac{r^2}{s^2}} \end{pmatrix}$$

Finally:

$$\begin{aligned} q' &= \alpha(q) \\ &= \frac{\sqrt{2 + \frac{r^2}{s^2}}\, i\sqrt{r^2 + s^2} - \frac{r^2+s^2}{s}}{-\frac{1}{s}\, i\sqrt{r^2 + s^2} + \sqrt{2 + \frac{r^2}{s^2}}} \\ &= \frac{1}{3 + 2\frac{r^2}{s^2}} \Big(-2\frac{r^2 + s^2}{s} \sqrt{2 + \frac{r^2}{s^2}} + i(\dots) \Big) \end{aligned}$$

q' thus lies on the left of γ and $p \wedge \gamma$ is thus oriented to the left.

iii) If γ and σ don't intersect, we can move them such that the common perpendicular geodesic is γ_0. In this situation:

$$\gamma = \begin{pmatrix} 0 & \mu \\ 1/\mu & 0 \end{pmatrix}, \quad \sigma = \begin{pmatrix} 0 & \nu \\ 1/\nu & 0 \end{pmatrix}, \quad \gamma \wedge \sigma = \frac{1}{2} \begin{pmatrix} \frac{\mu}{\nu} - \frac{\nu}{\mu} & 0 \\ 0 & \frac{\nu}{\mu} - \frac{\mu}{\nu} \end{pmatrix}$$

We remark that $\det(\gamma \wedge \sigma) < 0$, thus $\gamma \wedge \sigma$ is a geodesic matrix. It is here also possible to determine the orientation of $\gamma \wedge \sigma$ in function of the orientations of γ and σ, but we would have to define the relative orientation of a geodesic from another. We do not explain it in details here. Nevertheless, with the definitions of γ and σ, it is obvious that they are "oriented in the same direction". In this case, $\gamma \wedge \sigma$ has the same orientation of γ_0 if $\frac{\mu}{\nu} - \frac{\nu}{\mu} > 0 \Leftrightarrow \mu > \nu$, that is $\gamma \wedge \sigma$ is oriented from σ to γ.

iv) If γ and σ intersect, we can move them such that γ lies on γ_0 and the intersection point is i.

$$\gamma = \begin{pmatrix} 1 & 0 \\ 0 & -1 \end{pmatrix}, \sigma = \frac{1}{\mu} \begin{pmatrix} \rho & -\rho^2 + \mu^2 \\ 1 & -\rho \end{pmatrix}, \gamma \wedge \sigma = \frac{1}{\mu} \begin{pmatrix} 0 & -\rho^2 + \mu^2 \\ -1 & 0 \end{pmatrix}$$

with $1 + \rho^2 = \mu^2$ (Pythagorus' Theorem in the triangle i, 0 and the centre ρ of the geodesic σ). $\gamma \wedge \sigma$ is thus i.

$\square$

Let us write down some useful properties of the wedge operator:

Proposition 54. For $W, X, Y, Z \in T0(2, \mathbb{R})$ (indifferently point or geodesic matrices), the following identities hold:

$$\begin{aligned} X \wedge (Y \wedge Z) &= \operatorname{tr}(XY)\, Z - \operatorname{tr}(XZ)\, Y && \text{(A.5)} \\ \operatorname{tr}((X \wedge Y)(Z \wedge W)) &= \operatorname{tr}(XW) \operatorname{tr}(YZ) - \operatorname{tr}(XZ) \operatorname{tr}(YW) && \text{(A.6)} \\ -\det(\operatorname{tr}(X_i Y_j)) &= \operatorname{tr}((X_1 \wedge X_2) X_3) \operatorname{tr}((Y_1 \wedge Y_2) Y_3) && \text{(A.7)} \end{aligned}$$

where $\det(\operatorname{tr}(X_i Y_j))$ is the determinant of the 3×3 matrix with components $\operatorname{tr}(X_i Y_j)$.

Proof. It suffices to verify these identities for the basis elements I, J, K, using the fact that:

$$I \wedge J = K, \quad J \wedge K = -I, \quad K \wedge I = -J$$

$\square$

Proposition 55. Let p, q, γ, σ be two different point matrices and two different geodesic matrices respectively, then:

i) The distance between p and q is given by:

$$\cosh \operatorname{dist}(p,q) = \frac{|\operatorname{tr}(pq)|}{\sqrt{\operatorname{tr} p^2 \operatorname{tr} q^2}} \tag{A.8}$$

ii) The oriented distance between p and γ is given by:

$$\sinh \operatorname{dist}(p,\gamma) = \frac{\operatorname{tr}(p\gamma)}{\sqrt{-\operatorname{tr} p^2 \operatorname{tr} \gamma^2}} \tag{A.9}$$

iii) If γ and σ don't intersect, the distance between γ and σ is given by:

$$\cosh \operatorname{dist}(\gamma,\sigma) = \frac{|\operatorname{tr}(\gamma\sigma)|}{\sqrt{\operatorname{tr} \gamma^2 \operatorname{tr} \sigma^2}} \tag{A.10}$$

iv) If γ and σ intersect, the angle $\sphericalangle(\gamma,\sigma)$ between γ and σ is given by:

$$\cos \sphericalangle(\gamma,\sigma) = \frac{\operatorname{tr}(\gamma\sigma)}{\sqrt{\operatorname{tr} \gamma^2 \operatorname{tr} \sigma^2}} \tag{A.11}$$

Proof. The proof is quite technical and is partially presented in [ADBS11] and we do not go into any detail here. □

We now have almost all the tools necessary for the triangulation. Recall however that in the triangulation algorithm, we sometimes have to create new points. These new points are either points at a distance ε from two other points or points at the intersection of two circles. This leads to the last tool we need: to translate a point along a geodesic.

A.4 Translations Along a Geodesic

When we defined α for a geodesic γ (see Formula A.3), we remarked that it represents a translation along γ. Inspired by this fact we define for a normalized geodesic matrix γ:

$$T = \cosh \frac{d}{2}\, 1 + \sinh \frac{d}{2}\, \gamma \tag{A.12}$$

Given a point p lying on γ, then:

$$\begin{aligned}
q &= TpT^{-1} \\
&= (\cosh\frac{d}{2}1 + \sinh\frac{d}{2}\gamma)p(\cosh\frac{d}{2}1 - \sinh\frac{d}{2}\gamma) \\
&= \cosh^2\frac{d}{2}p + 2\cosh\frac{d}{2}\sinh\frac{d}{2}\gamma\wedge p - \sinh^2\frac{d}{2}\gamma p\gamma \\
&= (-1 + 2\cosh^2\frac{d}{2})\,p + 2\cosh\frac{d}{2}\sinh\frac{d}{2}\gamma\wedge p \\
&= \cosh d\, p + \sinh d\,\gamma\wedge p
\end{aligned}$$

where we used Proposition 49 and $\det\gamma = -1$ to state the line 4. It is now easy to prove that $q \in \gamma$; we do the calculation moving γ to γ_0 and p to i:

$$\gamma = \begin{pmatrix} 1 & 0 \\ 0 & -1 \end{pmatrix}, \quad p = \begin{pmatrix} 0 & 1 \\ -1 & 0 \end{pmatrix}, \quad \gamma\wedge p = \begin{pmatrix} 0 & 1 \\ 1 & 0 \end{pmatrix}$$

And thus:

$$q = \begin{pmatrix} 0 & \cosh d + \sinh d \\ -\cosh d + \sinh d & 0 \end{pmatrix}$$

Hence $q \in \gamma$ and as $\cosh d + \sinh d \geq 1$, p has been moved toward the orientation of γ. Finally, let us suppose that p is normalized and calculate the distance between p and q:

$$\mathrm{tr}(pq) = \cosh d\,\mathrm{tr}\,p^2 + \sinh d\,\mathrm{tr}(p(\gamma\wedge p)) = -\cosh d$$

The operator T thus represents the translation of distance d along γ toward the orientation of γ.

A.5 Barycentric Coordinates

Another reason for the use of the Matrix Model was the definition of the barycentric coordinates of a point inside a triangle of the triangulation. The idea is to give a meaning to an expression of the form $(1-s-t)p_0 + sp_1 + tp_2$ where p_0, p_1, p_2 are three normalized point matrices. We want to show that such an expression represents a unique point inside the geodesic triangle $p_0p_1p_2$. The proof we present here is very geometric and requires that we see the surface as a portion of the hyperboloid $\mathcal{H}$ of $\mathbb{R}^3$:

$$\mathcal{H} = \{(x, y, z) \in \mathbb{R}^3, z > 0 \mid x^2 + y^2 - z^2 = -1\}$$

We can establish a correspondence between a point $P = (x, y, z) \in \mathbb{R}^3, z > 0$ and the matrix[2] $P \in T0(2, \mathbb{R})$:

$$P = xI + yJ + zK$$

And reciprocally if the matrix P has a positive determinant. We will show that normalizing the matrix P actually represents the central projection of $P \in \mathbb{R}^3$ onto the hyperboloid $\mathcal{H}$. The projection p of P onto $\mathcal{H}$ is indeed given by the mapping:

$$P \mapsto p = \frac{P}{\lambda} \quad \text{where} \quad \lambda = \sqrt{z^2 - y^2 - x^2}$$

Moreover, the normalization of the matrix P is:

$$p = \frac{P}{\sqrt{\det P}}$$

where:

$$\det P = -\operatorname{tr} P^2 = -\operatorname{tr}((xI + yJ + zK)(xI + yJ + zK)) = -x^2 - y^2 + z^2$$

Hence, the projection on $\mathcal{H}$ and the normalization of a point matrix are the same operation.

Theorem 56. *Consider three points $p_0, p_1, p_2 \in \mathbb{H}$ and the linear combination $(1-s-t)p_0 + sp_1 + tp_2$, where $s, t \in [0, 1]$ and $s + t \leq 1$, then the normalized matrix :*

$$p = \frac{\big((1-s-t)p_0 + sp_1 + tp_2\big)}{\sqrt{\det\big((1-s-t)p_0 + sp_1 + tp_2\big)}} \tag{A.13}$$

is a point lying on the geodesic triangle $p_0p_1p_2$ and this decomposition is unique.

Proof. The first thing to prove is that the linear combination $P = (1-s-t)p_0 + sp_1 + tp_2$ has a positive determinant. Decompose p_0, p_1, p_2 on the basis I, J, K: $p_i = a_iI + b_iJ + c_iK$. The trace of P is still zero, and thus (observing

[2]as for the points of $\mathbb{H}$ and matrices, we use the same notation for points in $\mathbb{R}^3$ and their corresponding matrix

that $\operatorname{tr}(I^2) = 1$, $\operatorname{tr}(IJ) = 0$, etc):

$$\begin{aligned}
\det P &= -\operatorname{tr} P^2 \\
&= -((1-s-t)a_0 + sa_1 + ta_2)^2 - ((1-s-t)b_0 + sb_1 + tb_2)^2 \\
&\quad + ((1-s-t)c_0 + sc_1 + tc_2)^2 \\
&= (1-s-t)^2 + s^2 + t^2 + 2(1-s-t)s(-a_0a_1 - b_0b_1 + c_0c_1) \\
&\quad + 2st(-a_1a_2 - b_1b_2 + c_1c_2) + 2t(1-s-t)(-a_2a_0 - b_2b_0 + c_2c_0) \\
&= (1-s-t)^2 + s^2 + t^2 - 2(1-s-t)s \operatorname{tr} p_0p_1 - 2st \operatorname{tr} p_1p_2 \\
&\quad - 2t(1-s-t)\operatorname{tr} p_2p_0 \\
&> 0
\end{aligned}$$

Recall that $-\operatorname{tr} p_ip_j = \cosh \operatorname{dist}(p_i, p_j)$ if p_i and p_j are normalized.

Moreover, as mentioned in the introduction of this paragraph, P can be seen as a point in $\mathbb{R}^3$. As well as p_0, p_1, p_2 which also lie on $\mathcal{H}$ because they are normalized matrices. P is thus a point in the euclidean triangle $p_0p_1p_2 \subset \mathbb{R}^3$. It is known that the geodesics of $\mathcal{H}$ are intersections of $\mathcal{H}$ with planes through the origin O. The intersection of the tetrahedron $Op_0p_1p_2$ with $\mathcal{H}$ is thus the geodesic triangle $p_0p_1p_2 \subset \mathcal{H}$, and the normalized matrix $p = \frac{P}{\sqrt{\det P}}$ is the projection of P on this geodesic triangle. $\square$

Remark. As a digression and following the preceding reflexion, a linear combination of the type $P = (1-t)p_0 + tp_1$ represents a point lying on the geodesic arc between p_0 and p_1. In this case, the formula we obtain for the translation along a geodesic can provide a parameterization for t such that the normalized linear combination is a geodesic parameterization. The translation of p_0 of distance d along the geodesic $\gamma = \frac{p_0 \wedge p_1}{\sqrt{-\det p_0 \wedge p_1}}$ is:

$$p = \cosh d\, p_0 + \sinh d\, \frac{(p_0 \wedge p_1) \wedge p_0}{\sqrt{-\det p_0 \wedge p_1}}$$

Let us calculate the determinant $-\det p_0 \wedge p_1$ (See Proposition 54 for the formulae we use). d_{01} represents the distance between p_0 and p_1:

$$\begin{aligned}
-\det p_0 \wedge p_1 &= \operatorname{tr}(p_0 \wedge p_1)^2 \\
&= (\operatorname{tr}(p_0p_1))^2 - \operatorname{tr} p_0^2 \operatorname{tr} p_1^2 \\
&= \cosh^2 d_{01} - 1 \\
&= \sinh^2 d_{01}
\end{aligned}$$

Thus:

$$\begin{aligned}
p &= \cosh d\, p_0 + \frac{\sinh d}{\sinh d_{01}}(p_0 \wedge p_1) \wedge p_0 \\
&= \frac{\cosh d \sinh d_{01} - \sinh d \cosh d_{01}}{\sinh d_{01}}\, p_0 + \frac{\sinh d}{\sinh d_{01}}\, p_1
\end{aligned}$$

Identifying this last expression with:

$$\frac{1-t}{\sqrt{\det P}}\,p_0 + \frac{t}{\sqrt{\det P}}\,p_1$$

we get:

$$\begin{aligned}
& \frac{1-t}{t} = \left(\frac{\cosh d \sinh d_{01} - \sinh d \cosh d_{01}}{\sinh d_{01}}\right)\frac{\sinh d_{01}}{\sinh d} \\
\Leftrightarrow \qquad & t(d) = \frac{\sinh d}{\cosh d \sinh d_{01} - \sinh d(\cosh d_{01} - 1)}
\end{aligned}$$

A.6 Hyperbolic Triangles

For several proofs in chapter 4, the radii of the circumcircle and inscribed circle appear, in particular the quotient of them. This is what we want to calculate in this paragraph. For a triangle of the triangulation $T_j = P_{j,0}P_{j,1}P_{j,2}$, we use the notations defined on a triangle (see Notations) which we recall here: $A = P_{j,1}, B = P_{j,2}, C = P_{j,0}$; a, b, c are the lengths of the respective geodesic arcs BC, CA, AB and α, β, γ are:

$$\begin{aligned}
\alpha &= \cosh a - 1 \\
\beta &= \cosh b - 1 \\
\gamma &= \cosh c - 1
\end{aligned}$$

A.6.1 Circumcircle

To calculate the radius of the circumcircle, we first find its centre as the intersection of the perpendicular bisectors of each edge of the triangle and then compute the distance from this centre to every vertex of the triangle. With the Matrix Model, it becomes very easy since the matrix of the perpendicular bisector of the edge AB is[3] (See [ADBS11] p. 51):

$$A - B$$

The centre of the circumcircle is thus:

$$\begin{aligned}
P &= (A - B) \wedge (B - C) \\
&= A \wedge B + B \wedge C + C \wedge A
\end{aligned}$$

[3] A and B must be normalized

And then, the radius of the circumcircle is:

$$\cosh R = \frac{|\operatorname{tr} PA|}{\sqrt{\operatorname{tr} P^2 \operatorname{tr} A^2}}$$

Let us calculate the numerator (See Proposition 54 for the rules used):

$$\begin{aligned}
-\operatorname{tr} PA &= -\operatorname{tr}((B \wedge C).A) \\
&= \big(1 + 2\cosh a \cosh b \cosh c - \cosh^2 a - \cosh^2 b - \cosh^2 c\big)^{1/2} \\
&= (-\alpha^2 - \beta^2 - \gamma^2 + 2\alpha\beta + 2\beta\gamma + 2\gamma\alpha + 2\alpha\beta\gamma)^{1/2} \\
&= \Gamma^{1/2}
\end{aligned}$$

For the denominator:

$$\begin{aligned}
\operatorname{tr} P^2 &= \operatorname{tr}((C \wedge A)^2) + 2\operatorname{tr}((A \wedge B).(B \wedge C)) + (\text{cyclic terms}) \\
&= (\operatorname{tr}(CA))^2 - \operatorname{tr} C^2 \operatorname{tr} A^2 + 2\operatorname{tr} AC \operatorname{tr} B^2 - 2\operatorname{tr} AB \operatorname{tr} BC + (\text{c. t.}) \\
&= \cosh^2 b - 1 + 2\cosh b - 2\cosh c \cosh a + (\text{c. t.}) \\
&= \alpha^2 + \beta^2 + \gamma^2 - 2\alpha\beta - 2\beta\gamma - 2\gamma\alpha
\end{aligned}$$

Finally:

$$\sinh^2 R = \frac{2\alpha\beta\gamma}{-\alpha^2 - \beta^2 - \gamma^2 + 2\alpha\beta + 2\beta\gamma + 2\gamma\alpha} = \frac{2\alpha\beta\gamma}{\Lambda} \tag{A.14}$$

A.6.2 Inscribed Circle

Similarly to the circumcircle, we first find the centre of the inscribed circle as the intersection of the bisectors at each vertex of the triangle and then compute the distance from this centre to every edge of the triangle. The matrix of the bisector at the edge B is:

$$\frac{A \wedge B}{\sqrt{\operatorname{tr}(A \wedge B)^2}} - \frac{B \wedge C}{\sqrt{\operatorname{tr}(B \wedge C)^2}}$$

The centre of the inscribed circle is thus:

$$Q = \Big(\frac{A \wedge B}{\sqrt{\operatorname{tr}(A \wedge B)^2}} - \frac{B \wedge C}{\sqrt{\operatorname{tr}(B \wedge C)^2}}\Big) \wedge \Big(\frac{B \wedge C}{\sqrt{\operatorname{tr}(B \wedge C)^2}} - \frac{C \wedge A}{\sqrt{\operatorname{tr}(C \wedge A)^2}}\Big)$$

Since a point matrix can be multiplied by a factor without changing its associated point, we use Formulae A.5, A.7 and multiply the last expression by $-\frac{\sinh a \sinh b \sinh c}{\sqrt{2\cosh a \cosh b \cosh c}}$, which becomes:

$$Q = \sinh a\, A + \sinh b\, B + \sinh c\, C$$

And then, the radius of the inscribed circle ρ is given by:

$$\sinh\rho = \frac{|\operatorname{tr}(Q.(A\wedge B))|}{\sqrt{-\operatorname{tr}Q^2\operatorname{tr}(A\wedge B)^2}}$$

With:

$$\begin{aligned}\operatorname{tr}(Q.(A\wedge B)) &= \sqrt{\operatorname{tr}(A\wedge B)^2}\ \operatorname{tr}(C.(A\wedge B))\\ &= \sqrt{\operatorname{tr}(A\wedge B)^2}\,\Gamma^{1/2}\end{aligned}$$

And:

$$\begin{aligned}-\operatorname{tr}Q^2 &= -\sinh^2 a\operatorname{tr}A^2 - 2\sinh b\sinh c\operatorname{tr}BC + \text{(cyclic terms)}\\ &= \sinh^2 a + 2\sinh b\sinh c\cosh a + \text{(c. t.)}\\ &= \alpha(\alpha+2)+\beta(\beta+2)+\gamma(\gamma+2)+\sqrt{\alpha(\alpha+2)}\sqrt{\beta(\beta+2)}(\gamma+1)\\ &\quad+\sqrt{\beta(\beta+2)}\sqrt{\gamma(\gamma+2)}(\alpha+1)+\sqrt{\gamma(\gamma+2)}\sqrt{\alpha(\alpha+2)}(\beta+1)\end{aligned}$$

And finally:

$$\sinh^2\rho = \frac{-\alpha^2-\beta^2-\gamma^2+2\alpha\beta+2\beta\gamma+2\gamma\alpha+2\alpha\beta\gamma}{\alpha(\alpha+2)+\sqrt{\alpha(\alpha+2)}\sqrt{\beta(\beta+2)}(\gamma+1)+\text{(c. t.)}} \tag{A.15}$$

A.6.3 Quotient of the Radii

The quotient of the of the circumcircle radius to the inscribed circle radius is an image of the regularity of the triangulation. Theorems 42 and 46 concerning the convergence of the eigenvalues and eigenfunctions require an estimate of the quotient of the sinh of the radii. Here we calculate a lower and an upper bounds for the quotient:

$$q(\alpha,\beta,\gamma) = \frac{\sinh^2 R(\alpha,\beta,\gamma)}{\sinh^2\rho(\alpha,\beta,\gamma)}$$

For a given triangle let us fix an edge (say γ) and consider whether it is possible to find another triangle in the same circumcircle for which $q(\alpha,\beta,\gamma)$ is greater. When γ and R are fixed, β becomes a function of α and q depends only on the variable α. Abusing the notation we will still denote the quotient by q even if is a function of one variable: $q(\alpha) = q(\alpha,\beta(\alpha),\gamma)$. Let us compute the derivative of $q(\alpha)$:

$$\frac{dq}{d\alpha}(\alpha) = \frac{\partial q}{\partial\alpha}(\alpha,\beta(\alpha),\gamma) + \frac{\partial q}{\partial\beta}(\alpha,\beta(\alpha),\gamma)\frac{d\beta}{d\alpha}$$

For the calculation[4] of the derivative of $\beta(\alpha)$, recall that we supposed R and γ to be fixed. As R normally depends on α, β and γ:

$$\begin{aligned}\frac{d\beta}{d\alpha}(\alpha,\beta,\gamma) &= -\frac{\frac{\partial \sinh^2 R}{\partial\alpha}}{\frac{\partial \sinh^2 R}{\partial\beta}} \\ &= -\frac{(\alpha-\beta+\gamma)\beta}{(\alpha-\beta+\gamma)\alpha}\end{aligned}$$

Thus:

$$\frac{dq}{d\alpha}(\alpha) = \frac{N}{D}$$

where:

$$\begin{aligned}N \;=\; & 4\beta\gamma\Big[\big(\alpha-\beta\big)\Big(\big(\alpha+\beta+3\gamma+\alpha\beta+\beta\gamma+\gamma^2\big)\sqrt{\alpha(\alpha+2)}\sqrt{\beta(\beta+2)} \\ & +\big(\alpha+\beta+\gamma+3\big)\sqrt{\gamma(\gamma+2)}\big(\alpha\sqrt{\beta(\beta+2)}+\beta\sqrt{\alpha(\alpha+2)}\big) \\ & +\alpha\beta\big(1+\gamma\big)\big(\alpha+\beta+\gamma+4\big)\Big)+\sqrt{\gamma(\gamma+2)}\Big(\alpha\sqrt{\beta(\beta+2)}-\beta\sqrt{\alpha(\alpha+2)}\Big)\Big]\end{aligned}$$

and:

$$D = \big(-\alpha+\beta+\gamma\big)\Gamma(\Gamma-2\alpha\beta\gamma)\sqrt{\alpha(\alpha+2)}\sqrt{\beta(\beta+2)}$$

Obviously the sign of the derivative of q depends only on the sign of the term $\alpha-\beta$ and $-\alpha+\beta+\gamma$. R and γ being fixed, q thus increases with α until $\alpha=\beta$ and decreases until $\alpha=\beta+\gamma$. The case $\alpha=\beta+\gamma$ actually corresponds to BC being a diameter of the circumcircle (See the next Paragraph A.6.4). The variations of the quotient q are the same as in euclidean geometry.

As the quotient $q(\alpha,\beta,\gamma)$ is symmetric over the permutation α,β, we can conclude that it increases when α decreases until the limit $a=\varepsilon$. Applying the same argumentation when we fix $a=\varepsilon$, we can conclude that for a given circumcircle radius R, the quotient $q(\alpha,\beta,\gamma)$ is maximal for $a=b=\varepsilon$ ($\Leftrightarrow\ \alpha=\beta=\cosh\varepsilon-1$). We can also note that q increases when the circumcircle increases, and finally the maximum of q is reached for $a=\varepsilon$, $b=\varepsilon$ and c such that $R=\varepsilon$, that is:

$$q_{\max}(\varepsilon) = q\big(\cosh\varepsilon-1, \cosh\varepsilon-1, \cosh(2\,\mathrm{arccosh}\tfrac{\cosh\varepsilon}{\cosh\varepsilon/2})-1\big)$$

Moreover, we know that the shortest edge of an hexagon must be smaller than arccosh 2. As ε is itself smaller than a third of this shortest edge, it is possible to find a parabolic upper bound for the quotient q for ε between 0

[4]all these calculations are performed with symbolic mathematical software

and $\frac{\operatorname{arccosh} 2}{3}$. In the following inequalities $q_{\max}(0)$ is actually to be understood as a limit value.

$$\begin{aligned}
q_{\max}(\varepsilon) &\leq q_{\max}(0) + \left(q_{\max}\left(\tfrac{\operatorname{arccosh} 2}{3}\right) - q_{\max}(0)\right)\tfrac{9\,\varepsilon^2}{\operatorname{arccosh}^2 2} \\
&\leq \tfrac{4}{3(\sqrt{3}-2)^2} + \left(q_{\max}\left(\tfrac{\operatorname{arccosh} 2}{3}\right) - \tfrac{4}{3(\sqrt{3}-2)^2}\right)\tfrac{9\,\varepsilon^2}{\operatorname{arccosh}^2 2}
\end{aligned}$$

$q_{\max}(\frac{\operatorname{arccosh} 2}{3}) \approx 20.06$ and $q_{\max}(0) = \frac{4}{3(\sqrt{3}-2)^2} \approx 18.57$, thus:

$$\frac{4}{3(\sqrt{3}-2)^2} \leq q_{\max}(\varepsilon) \leq \frac{4}{3(\sqrt{3}-2)^2} + 7.73\varepsilon^2$$

We calculate this upper bound to have an idea of the terms $O(h^2)$ when we make an expansion with respect to h (h is the diameter of the triangulation). As $\frac{h}{2} < \varepsilon$:

$$\frac{4}{3(\sqrt{3}-2)^2} \leq q_{\max}(h) \leq \frac{4}{3(\sqrt{3}-2)^2} + 1.94h^2 \tag{A.16}$$

We remark that even if h is not so small, the terms $O(h)$ from this quotient stay very small ($O(h^2) \leq 1.49$ for $h = 2\frac{\operatorname{arccosh} 2}{3}$). Notice also that if we make the same calculation in the euclidean case, the quotient $\frac{R}{\rho}$ is a constant equal to $\frac{4}{3(\sqrt{3}-2)^2}$ (which is in fact actually not surprising).

As a remark, with the same argumentation, it is possible to prove that the quotient q is minimal for an equilateral triangle, and:

$$q_{\min}(0) = 4 \leq q_{\min}(\varepsilon) \leq q_{\min}(\tfrac{\operatorname{arccosh} 2}{3}) \leq 4.2$$

where of course $q_{\min}(\varepsilon) = q(\cosh\varepsilon - 1, \cosh\varepsilon - 1, \cosh\varepsilon - 1)$ and $q_{\min}(0)$ is also to be understood as a limit value.

A.6.4 About Some Recurrent Formulae

We have seen in different paragraphs that some formulae appear quite often. For example $\Gamma = -\alpha^2 - \beta^2 - \gamma^2 + 2\alpha\beta + 2\beta\gamma + 2\gamma\alpha + 2\alpha\beta\gamma$ and $\Lambda = -\alpha^2 - \beta^2 - \gamma^2 + 2\alpha\beta + 2\beta\gamma + 2\gamma\alpha$ or the expression $\alpha - \beta - \gamma$. We would like to give them a geometrical meaning.

We begin with the last expression. $\alpha - \beta - \gamma = 0$ actually corresponds to BC being a diameter of the circumcircle. If we denote D the midpoint of BC and d the distance between D and A:

$$\begin{aligned}
\cosh d &= \frac{-\operatorname{tr}((B+C)A)}{\sqrt{\operatorname{tr}(B+C)^2 \operatorname{tr} A^2}} \\
&= \frac{\cosh c + \cosh b}{\sqrt{2(1+\cosh a)}}
\end{aligned}$$

If we want D to be the centre of the circumcircle, then $2d = a$, and thus:

$$\begin{array}{lrcl} & \cosh\frac{a}{2}\sqrt{2(1+\cosh a)} & = & \cosh b + \cosh c \\ \Leftrightarrow & \cosh a + 1 & = & \cosh b + \cosh c \\ \Leftrightarrow & \alpha & = & \beta + \gamma \end{array}$$

Move isometrically the triangle such that the centre of the circumcircle lies on the origin of $\mathbb{D}$, we can thus conclude that if $\alpha \leq \beta+\gamma$ then the euclidean triangle ABC is acute, whereas if $\alpha \geq \beta+\gamma$ then the euclidean triangle ABC is obtuse. In other words if $\alpha \geq \beta+\gamma$, then the vertices of the triangle are in a same half of the circumcircle, whereas they are not if $\alpha \leq \beta+\gamma$.

We now want to explain the geometrical meaning of the two other expressions: Γ and Λ . In every calculations we made they were assumed to be positive. To prove the meaning of these assumptions, we have to think of the triangle inequality, which also holds for hyperbolic triangles. As we have supposed that a corresponds to the longest edge of the triangle, the triangle inequality reads:

$$a \leq b + c$$

From the preceding study of the sign of $\alpha - \beta - \gamma$, there are two cases for α, β, γ; either they satisfy also the triangle inequality, or not.

If $\alpha \leq \beta + \gamma$, then it is very simple:

$$\begin{aligned} \Lambda &= -\alpha^2 - \beta^2 - \gamma^2 + 2\alpha\beta + 2\beta\gamma + 2\gamma\alpha \\ &= \alpha(\beta-\alpha) + \beta(\gamma-\beta) + \gamma(\alpha-\gamma) + \alpha\beta + \beta\gamma + \gamma\alpha \\ &\geq 0 \end{aligned}$$

because of the triangle inequality on α, β, γ: $|\alpha(\beta-\alpha)| \leq \alpha\gamma$, etc. It becomes then obvious for Γ:

$$\Gamma = \Lambda + 2\alpha\beta\gamma \geq 0$$

If $\alpha \geq \beta + \gamma$, it is a bit more complicated, but also more interesting. We have to go back to the first triangle inequality:

$$\begin{array}{lrcl} & a & \leq & b + c \\ \Leftrightarrow & \cosh a & \leq & \cosh b \cosh c + \sinh b \sinh c \\ \Leftrightarrow & \alpha & \leq & \beta\gamma + \beta + \gamma + \sqrt{\beta(\beta+2)}\sqrt{\gamma(\gamma+2)} \end{array}$$

With the hypothesis $\alpha \geq \beta + \gamma$, we have $|\alpha - \beta - \gamma - \beta\gamma| \leq \beta\gamma$. Then:

$$\begin{array}{lrcl} & (\alpha-\beta-\gamma-\beta\gamma)^2 & \leq & \beta(\beta+2)\gamma(\gamma+2) \\ \Leftrightarrow & \alpha^2 + \beta^2 + \gamma^2 - 2\alpha\beta - 2\beta\gamma - 2\gamma\alpha - 2\alpha\beta\gamma & \leq & 0 \\ \Leftrightarrow & \Gamma & \geq & 0 \end{array}$$

As this last inequality is sharp, it is not true that Λ is always positive. To explain its geometrical meaning, we have to have a look at the expression of the radius of circumcircle of the triangle (Equation A.14):

$$\sinh^2 R = \frac{2\alpha\beta\gamma}{-\alpha^2 - \beta^2 - \gamma^2 + 2\alpha\beta + 2\beta\gamma + 2\gamma\alpha}$$

When Λ is null, then the radius becomes infinite. Geometrically, in $\mathbb{D}$, the circumcircle of the triangle is tangent to the unit disc. In the hyperboloid model, the circumcircle is actually a parabola, thus, not a circle anymore.

As a last remark, we point out that from the trigonometry formulae in hyperbolic triangles:

$$\begin{aligned}\sinh a \sinh b \cos\phi &= \cosh a + \cosh b - \cosh c \\ &= \alpha\beta + \alpha + \beta - \gamma\end{aligned}$$

Where ϕ is the angle between the edges of length a and b. It is thus easy to prove that:

$$\Gamma = (\sinh a \sinh b \sin\phi)^2 \tag{A.17}$$

Appendix B

Commutativity of $\sharp$ and D

Proposition 57. Given $= v^i \partial_i$ a vector field and $\theta = \theta^i dx^i$ a 1-form. Then:

$$D_v {}^\sharp\theta = {}^\sharp D_v \theta$$

Proof. From the linearity of the covariant derivative, it suffices to prove the proposition on the basis vector fields in a coordinate charts. Let us suppose that $v = \partial_i$.

$$\begin{aligned}
(D_{\partial_i} {}^\sharp\theta)^k &= \frac{\partial}{\partial x^i}(G^{km}\theta_m) + \Gamma^k_{ij} G^{jn}\theta_n \\
&= \frac{\partial G^{km}}{\partial x^i}\theta_m + G^{km}\frac{\partial \theta_m}{\partial x^i} + \Gamma^k_{ij} G^{jn}\theta_n \\
&= G^{km}\frac{\partial \theta_m}{\partial x^i} - G^{kn} G_{nl}\frac{\partial G^{lm}}{\partial x^i}\theta_m + \frac{1}{2} G^{kn}\Big(\frac{\partial G_{im}}{\partial x^j} + \frac{\partial G_{jm}}{\partial x^i} - \frac{\partial G_{ij}}{\partial x^m}\Big) G^{jn}\theta_n \\
&= G^{km}\frac{\partial \theta_m}{\partial x^i} - G^{km}\frac{\partial G_{mj}}{\partial x^i} G^{jn}\theta_n + \frac{1}{2} G^{km}\Big(\frac{\partial G_{im}}{\partial x^j} + \frac{\partial G_{jm}}{\partial x^i} - \frac{\partial G_{ij}}{\partial x^m}\Big) G^{jn}\theta_n \\
&= G^{km}\frac{\partial \theta_m}{\partial x^i} + \frac{1}{2} G^{km}\Big(\frac{\partial G_{im}}{\partial x^j} - \frac{\partial G_{jm}}{\partial x^i} - \frac{\partial G_{ij}}{\partial x^m}\Big) G^{jn}\theta_n \\
&= G^{km}\frac{\partial \theta_m}{\partial x^i} - G^{km}\Gamma^n_{im}\theta_n \\
&= G^{km}(D_{\partial_i}\theta)_m \\
&= ({}^\sharp D_{\partial_i}\theta)^k
\end{aligned}$$

$\square$

Appendix C

Study of $G^{ij}(x)$ and $\Gamma_{ij}^k(x)$ on a Triangle

The aim of this appendix is to find an expansion in terms of the diameter of the trangulation h for the components of the inverse of the metric tensor G^{ij}, as well as for the Christoffel symbols Γ_{ij}^k. We make the assumption that the triangle we consider has a circumcircle (this is the case for all triangles in the triangulation we make in this thesis). By A.6.4, we then have $\Lambda > 0$ (and $\Gamma > 0$).

We recall the expression of the components G^{ij}. As before, we denote (u, v) the coordinate system. For a triangle $T_j = P_{j,0}P_{j,1}P_{j,2}$, we redefine the name of the vertices and use the usual notations for a triangle (see Chapter Notations). For $x = (u, v)$ in the triangle T_j (See Paragraph 3.2.2), that is, $0 \leq u, v \leq 1$ and $0 \leq 1 - u + v \leq 1$:

$$
\begin{aligned}
G^{11}(u,v) &= \frac{1}{\Gamma}\Big(1 + 2\beta u(1-u-v) + 2\alpha v(1-u-v) + 2\gamma uv\Big).\\
&\quad \Big(\alpha(\alpha+2) - 2u\alpha(\alpha-\beta-\gamma) - u^2\Lambda\Big)\\
G^{12}(u,v) &= \frac{1}{\Gamma}\Big(1 + 2\beta u(1-u-v) + 2\alpha v(1-u-v) + 2\gamma uv\Big).\\
&\quad \Big(-\alpha\beta - \alpha - \beta + \gamma - u\beta(-\alpha+\beta-\gamma) - v\alpha(\alpha-\beta-\gamma) - uv\Lambda\Big)\\
G^{22}(u,v) &= \frac{1}{\Gamma}\Big(1 + 2\beta u(1-u-v) + 2\alpha v(1-u-v) + 2\gamma uv\Big).\\
&\quad \Big(\beta(\beta+2) - 2v\beta(-\alpha+\beta-\gamma) - v^2\Lambda\Big)
\end{aligned}
$$

The variables u and v lie in the triangle $S = \{(u, v), u, v \geq 0, u + v \leq 1\}$. We begin with the study of G^{12} because we can not find lower and upper bounds for it as precisely as for the other components. Next, we study G^{11}. G^{22} is very similar to G^{11} and we do not present all the details and just give the results.

C.1 G^{12}

$$G^{12}(u,v) = \frac{1}{\Gamma}\Big(1+2\beta u(1-u-v)+2\alpha v(1-u-v)+2\gamma uv\Big).$$
$$\Big(-\alpha\beta-\alpha-\beta+\gamma-u\beta(-\alpha+\beta-\gamma)-v\alpha(\alpha-\beta-\gamma)-uv\Lambda\Big)$$

We first point out that G^{12} is a product of two quadratic polynomials:

$$G^{12} = \frac{1}{\Gamma}\,\Phi(u,v)\mathrm{P}(u,v)$$

where:

$$\mathrm{P}(u,v) = -\alpha\beta-\alpha-\beta+\gamma-u\beta(-\alpha+\beta-\gamma)-v\alpha(\alpha-\beta-\gamma)-uv\Lambda$$

It is not easy to study the behavior of G^{12} by finding all the critical points (where the partial derivatives vanish), etc. We thus find lower and upper bounds for it by finding them for the two quadratic polynomials. $\Phi(u,v)$ and $\mathrm{P}(u,v)$ have the same critical point:

$$u_0 = \frac{\alpha(-\alpha+\beta+\gamma)}{\Lambda}$$
$$v_0 = \frac{\beta(\alpha-\beta+\gamma)}{\Lambda}$$

We apply the Monge Theorem for a function of two variables:

$$\frac{\partial^2\Phi}{\partial u^2}(u_0,v_0)\frac{\partial^2\Phi}{\partial v^2}(u_0,v_0) - \frac{\partial^2\Phi}{\partial u\partial v}(u_0,v_0)\frac{\partial^2\Phi}{\partial u\partial v}(u_0,v_0) = 4\Lambda > 0$$
$$\frac{\partial^2\mathrm{P}}{\partial u^2}(u_0,v_0)\frac{\partial^2\mathrm{P}}{\partial v^2}(u_0,v_0) - \frac{\partial^2\mathrm{P}}{\partial u\partial v}(u_0,v_0)\frac{\partial^2\mathrm{P}}{\partial u\partial v}(u_0,v_0) = -\Lambda^2 < 0$$

Φ is thus a concave elliptic paraboloid with a maximum in (u_0,v_0) whereas P is a hyperbolic paraboloid with a saddle point in (u_0,v_0). For Φ:

$$\Phi(u_0,v_0) = \frac{\Gamma}{\Lambda} = 1+\sinh^2 R$$
$$\Phi(0,0) = 1$$
$$\Phi(1,0) = 1$$
$$\Phi(0,1) = 1$$

Thus, for $(u,v) \in S$:
$$1 \leq \Phi(u,v) \leq 1 + \sinh^2 R$$

For P, the extremum (denoted extr in the fourth equation) is either at a vertex of S or on the side $(u, 1-u)$:

$$\begin{aligned}
\mathrm{P}(0,0) &= -\alpha - \beta + \gamma - \alpha\beta \\
\mathrm{P}(1,0) &= -\alpha - \beta + \gamma - \beta(\beta - \gamma) \\
\mathrm{P}(0,1) &= -\alpha - \beta + \gamma - \alpha(\alpha - \gamma) \\
\operatorname*{extr}_{u\in[0,1]} \mathrm{P}(u, 1-u) &= (-\alpha - \beta + \gamma)\Big(-4 + \frac{8\alpha\beta\gamma}{\Lambda} + \frac{\gamma^2(-\alpha-\beta+\gamma)}{\Lambda}\Big)
\end{aligned}$$

Thus, for $(u,v) \in S$:

$$k(-\alpha-\beta+\gamma) - O(h^4) \leq \mathrm{P}(u,v) \leq k'(-\alpha-\beta+\gamma) + O(h^4)$$

where k, k' are 1 or -4 and $O(h^4)$ is one of the terms after $-\alpha-\beta+\gamma$ in the preceding equations. Now we can conclude for G^{12}. For $(u,v) \in S$:

$$\begin{aligned}
\frac{1}{\Gamma} \min_{(u,v)\in S} \Phi(u,v) \min_{(u,v)\in S} \mathrm{P}(u,v) \leq G^{12}(u,v) &\leq \frac{1}{\Gamma} \max_{(u,v)\in S} \Phi(u,v) \max_{(u,v)\in S} \mathrm{P}(u,v) \\
\frac{k(-\alpha-\beta+\gamma)}{\Gamma} - O(1) \leq G^{12}(u,v) &\leq \frac{k'(-\alpha-\beta+\gamma)}{\Gamma} + O(1)
\end{aligned}$$

C.2 G^{11}

$$\begin{aligned}
G^{11}(u,v) = \frac{1}{\Gamma}&\Big(1 + 2\beta u(1-u-v) + 2\alpha v(1-u-v) + 2\gamma uv\Big). \\
&\Big(\alpha(\alpha+2) - 2u\alpha(\alpha-\beta-\gamma) - u^2\Lambda\Big)
\end{aligned}$$

G^{11} is also a product of two quadratic polynomials:

$$G^{11}(u,v) = \frac{1}{\Gamma}\Phi(u,v)\mathrm{P'}(u)$$

With:
$$\mathrm{P'}(u) = \alpha(\alpha+2) - 2u\alpha(\alpha-\beta-\gamma) - u^2\Lambda$$

We can follow the same method as in the preceding paragraph. P'(u) is also maximal in u_0 and is bounded by:

$$2\alpha \leq \mathrm{P'}(u) \leq \frac{2\alpha\Gamma}{\Lambda}$$

Since $\frac{\Gamma}{\Lambda} = 1 + \sinh^2 R$, by A.14 and for $(u, v) \in S$, we have:

$$\frac{2\alpha}{\Gamma} \leq G^{11}(u, v) \leq \frac{2\alpha}{\Gamma}(1 + \sinh^2 R)^2$$

However, since P'(u) is a polynomial of only one variable, the study of $G^{11}(u, v)$ is much easier and it is possible to find its critical points and extrema and thus to determine a better upper bound.

C.2.1 Critical Points of G^{11}

Computing its first partial derivatives, we find three critical point for:

$$\begin{aligned}
u_0 &= \frac{\alpha(-\alpha+\beta+\gamma)}{\Lambda} \\
v_0 &= \frac{\beta(\alpha-\beta+\gamma)}{\Lambda} \\
u_1 &= \frac{\alpha(-\alpha+\beta+\gamma) + \sqrt{\alpha^2(-\alpha+\beta+\gamma)^2 + \alpha(\alpha+2)\Lambda}}{\Lambda} \\
v_1 &= \frac{2\alpha\beta(\alpha-\beta+\gamma) + (-\alpha-\beta+\gamma) + \sqrt{\alpha^2(-\alpha+\beta+\gamma)^2 + \alpha(\alpha+2)\Lambda}}{2\,\alpha\,\Lambda} \\
u_2 &= \frac{\alpha(-\alpha+\beta+\gamma) - \sqrt{\alpha^2(-\alpha+\beta+\gamma)^2 + \alpha(\alpha+2)\Lambda}}{\Lambda} \\
v_2 &= \frac{2\alpha\beta(\alpha-\beta+\gamma) - (-\alpha-\beta+\gamma) + \sqrt{\alpha^2(-\alpha+\beta+\gamma)^2 + \alpha(\alpha+2)\Lambda}}{2\,\alpha\,\Lambda}
\end{aligned}$$

Recall that $\Lambda = -\alpha^2 - \beta^2 - \gamma^2 + 2\alpha\beta + 2\alpha\gamma + 2\beta\gamma$.
The two last critical points (u_1, v_1) and (u_2, v_2) are not interesting because they do not lie in the triangle S. u_2 is obviously smaller than 0 because $\alpha(\alpha+2)\Lambda \geq 0$ and we can show that u_1 is greater than 1:

$$\begin{array}{rrcl}
 & \sqrt{\alpha^2(-\alpha+\beta+\gamma)^2 + \alpha(\alpha+2)\Lambda} & \geq & \Lambda - \alpha(-\alpha+\beta+\gamma) \\
\Leftrightarrow & \sqrt{\alpha^2(-\alpha+\beta+\gamma)^2 + \alpha(\alpha+2)\Lambda} & \geq & -(\beta-\gamma)^2 + \alpha(\beta+\gamma) \\
\Leftarrow & \left(\sqrt{\alpha^2(-\alpha+\beta+\gamma)^2 + \alpha(\alpha+2)\Lambda}\right)^2 & \geq & \left(-(\beta-\gamma)^2 + \alpha(\beta+\gamma)\right)^2 \\
\Leftrightarrow & (2\alpha + (\beta-\gamma)^2)\Lambda & \geq & 0
\end{array}$$

The last line is true and thus we can conclude that $u_1 \geq 1$. The only critical point, which may be an extremum of G^{11} in the triangle is thus (u_0, v_0). The two first conditions for (u_0, v_0) lying in the triangle S are obviously:

$$\begin{aligned}
\alpha &\leq \beta + \gamma \\
\beta &\leq \gamma + \alpha
\end{aligned}$$

The last condition is:

$$\begin{array}{rrcl} & u_0 + v_0 & \leq & 1 \\ \Leftrightarrow & \alpha(-\alpha+\beta+\gamma)+\beta(\alpha-\beta+\gamma) & \leq & -\alpha^2-\beta^2-\gamma^2+2\alpha\beta+2\alpha\gamma+2\beta\gamma \\ \Leftrightarrow & 0 & \leq & \gamma(-\gamma+\alpha+\beta) \\ \Leftrightarrow & \gamma & \leq & \alpha+\beta \end{array}$$

Hence, (u_0, v_0) lies in the triangle S if α, β, γ satisfy the triangle inequality.

A last remark: u_1 and u_2 are the roots of P'(u) and u_0 represents its maximum. Since u_1 and u_2 lie outside S, P'(u) is always positive in S, and for a fixed $u \in [0,1]$, $G^{11}(u,v)$ is a concave parabola. Moreover, $G^{11}(u,v) = -\frac{\Lambda}{\Gamma}\Phi(u,v)(u-u_1)(u-u_2)$ and for a fixed $v \in [0,1]$, it is a polynomial of degree 4 in the variable u. $\Phi(u,v)$ is an elliptic quadratic polynomial and is maximal in (u_0,v_0) and is 1 at the vertices of S. Hence for $v \in [0,1]$, $\Phi(u,v)$ has two roots $\tilde{u}_1$ and $\tilde{u}_2$ lying on either side of S. $G^{11}(u,v) = \frac{2\beta\Lambda}{\Gamma}(u-u_1)(u-u_2)(u-\tilde{u}_1)(u-\tilde{u}_2)$ and for a fixed $v \in [0,1]$, the triangle S always has two pairs of roots on either side, and thus lies in the concave part of $G^{11}(u,v)$.

C.2.2 Extrema of G^{11}

From the preceding paragraph, we know that there are two cases to study: when α, β, γ satisfy the triangle inequality and when they do not.

If $\alpha \leq \beta+\gamma$, $\beta \leq \gamma+\alpha$ and $\gamma \leq \alpha+\beta$, it is possible to prove that (u_0, v_0) is a local maximum. We apply the Monge Theorem:

$$\frac{\partial^2 G^{11}}{\partial u^2}(u_0,v_0)\frac{\partial^2 G^{11}}{\partial v^2}(u_0,v_0) - \frac{\partial^2 G^{11}}{\partial u \partial v}(u_0,v_0)\frac{\partial^2 G^{11}}{\partial u \partial v}(u_0,v_0) = \frac{32\alpha^2}{\Lambda} \geq 0$$

And:

$$\frac{\partial^2 G^{11}}{\partial v^2}(u_0,v_0) = \frac{-8\alpha^2}{\Lambda}$$

The minimum is to be found on the boundary of the triangle. As we pointed out before, for a fixed $u \in [0,1]$, $G^{11}(u,v)$ is a concave parabola and for a fixed $v \in [0,1]$, $G^{11}(u,v)$ is a concave curve. Thus, the minimum of G^{11} is at a vertex of the triangle, that is for $(u,v) = (0,0)$ or $(u,v) = (1,0)$ or $(u,v) = (0,1)$.

If α, β, γ do not satisfy the triangle inequality, the extrema of G^{11} are to be found on the boundary of the triangle. For the same reason as before, the minimum is at a vertex of the triangle. The maximum lies, however, either at a vertex of the triangle or one of the edges of the triangle. The maximum of $G^{11}(0,v)$ is easy to find because $G^{11}(0,v)$ is a parabola, and we find:

$$\max G^{11}(0,v) = G^{11}(0,1/2) = \frac{2\alpha + \alpha^2(2+\frac{\alpha}{2})}{\Gamma}$$

The maxima of $G^{11}(u,0)$ and $G^{11}(u,1-u)$ can not be found with the symbolic mathematical software we used, but we can affirm that:

$$\max G^{11}(u,0) \leq \frac{1}{\Gamma}\Phi(1/2,0)\mathrm{P'}(u_0) = \frac{2\alpha}{\Lambda}\Big(1+\frac{\beta}{2}\Big)$$
$$\max G^{11}(u,1-u) \leq \frac{1}{\Gamma}\Phi(1/2,1/2)\mathrm{P'}(u_0) = \frac{2\alpha}{\Lambda}\Big(1+\frac{\gamma}{2}\Big)$$

C.2.3 Lower and Upper Bounds for G^{11}

We now want to find lower and upper bounds for G^{11} as well as an estimate of its variation according to h (the diameter of the triangulation). From the preceding paragraph, we know that the minimum of $G^{11}(u,v)$ is to be found among the following values:

$$G^{11}(0,0) = \frac{\alpha(\alpha+2)}{\Gamma}$$
$$G^{11}(1,0) = \frac{2\alpha+(\beta-\gamma)^2}{\Gamma}$$
$$G^{11}(0,1) = \frac{\alpha(\alpha+2)}{\Gamma}$$

It suffices to compare α and $\beta-\gamma$ to know the minimum of G^{11} (see Paragraph A.6.4 for the geometrical meaning of this comparison). However a lower bound is given by $\frac{2\alpha}{\Gamma}$.
If α, β, γ satisfy the triangle inequality, the maximum of G^{11} is:

$$G^{11}(u_0,v_0) = \frac{2\alpha\Gamma}{\Lambda^2}$$

Otherwise, an upper bound is one of the following quantities:

$$G^{11}(u,0) \leq \frac{2\alpha}{\Lambda}\Big(1+\frac{\beta}{2}\Big)$$
$$G^{11}(0,v) \leq \frac{2\alpha(1+\alpha+\frac{\alpha^2}{4})}{\Gamma}$$
$$G^{11}(u,1-u) \leq \frac{2\alpha}{\Lambda}\Big(1+\frac{\gamma}{2}\Big)$$

In any case, we can see that for $(u,v)\in S$:

$$\frac{2\alpha}{\Gamma} \leq G^{11}(u,v) \leq \frac{2\alpha}{\Gamma}(1+O(h^2))$$

where the term $O(h^2)$ is controlled.

C.3 G^{22}

$$G^{22}(u,v) = \frac{1}{\Gamma}\Big(1 + 2\beta u(1-u-v) + 2\alpha v(1-u-v) + 2\gamma uv\Big).$$
$$\Big(\beta(\beta+2) - 2v\beta(-\alpha+\beta-\gamma) - v^2\Lambda\Big)$$

Using the results for G^{11}, by symmetry, permuting α and β, u and v, we can conclude that the minimum is at a vertex of the triangle S and its value is one of the following:

$$\begin{aligned} G^{22}(0,0) &= \frac{\beta(\beta+2)}{\Gamma} \\ G^{22}(1,0) &= \frac{\beta(\beta+2)}{\Gamma} \\ G^{22}(0,1) &= \frac{2\beta + (\gamma-\alpha)^2}{\Gamma} \end{aligned}$$

If α, β, γ satisfy the triangle inequality, then the maximum of $G^{22}(u,v)$ is also in (u_0,v_0):

$$G^{22}(u_0,v_0) = \frac{2\beta\Gamma}{\Lambda^2}$$

Otherwise, an upper bound is one of the following quantities:

$$\begin{aligned} G^{22}(u,0) &\le \frac{2\beta(1+\beta+\frac{\beta^2}{4})}{\Gamma} \\ G^{22}(0,v) &\le \frac{2\beta}{\Lambda}\Big(1+\frac{\alpha}{2}\Big) \\ G^{22}(u,1-u) &\le \frac{2\beta}{\Lambda}\Big(1+\frac{\gamma}{2}\Big) \end{aligned}$$

Thus, for $(u,v) \in S$:

$$\frac{2\beta}{\Gamma} \le G^{22}(u,v) \le \frac{2\beta}{\Gamma}(1+O(h^2))$$

and again, we have a control over the term $O(h^2)$.

C.4 Γ^i_{jk}

The expressions of the Christoffel symbols are very complicated except for two components. We can not find precise lower and upper bounds as we did for the elements of G^{ij}. Instead, we provide their Taylor expansion to the order 4 in h. We recall the Heron's Formula giving the area A of an Euclidean triangle of edges of length a, b, c:

$$A = \frac{1}{4}\sqrt{(a+b+c)(-a+b+c)(a-b+c)(a+b-c)}$$

Then the Christoffel symbols are:

$$\begin{aligned}
\Gamma_{11}^1(u,v) &= \frac{2(\beta+2\beta u+(\alpha+\beta-\gamma)v)}{\Phi(u,v)}\\
&= b^2+2b^2u+(a^2+b^2-c^2)v+O(h^4)\\
\Gamma_{12}^1(u,v) &= \frac{1}{32A^2}\big(a^6-4a^4b^2-a^2b^4-2a^4c^2+a^2c^4\\
&+(-a^6+5a^4b^2+5a^2b^4-b^6+3b^4c^2-3b^2c^4+c^6-3c^4a^2+3c^2a^4-2a^2b^2c^2)u\\
&-8a^4b^2v\big)+O(h^4)\\
\Gamma_{22}^1(u,v) &= \frac{a^2}{16A^2}\big(-a^4-3a^2b^2+a^2c^2\\
&+(a^4+6a^2b^2+b^4-2b^2c^2+c^4-2c^2a^2)u+(4a^4+4a^2b^2-4a^2c^2)v\big)+O(h^4)\\
\Gamma_{11}^2(u,v) &= 0\\
\Gamma_{12}^2(u,v) &= \frac{-a^2-b^2+c^2}{8A}\big(-b^2+2b^2u+(a^2+b^2-c^2)v\big)+O(h^4)\\
\Gamma_{22}^2(u,v) &= \frac{1}{16A^2}\big(a^6+a^4b^2+2a^2b^4-2a^4c^2+a^2c^4-3a^2b^2c^2\\
&+(-a^6-3a^4b^2-3a^2b^4-b^6+3b^4c^2-3b^2c^4+c^6-3c^4a^2+3c^2a^4+6a^2b^2c^2)u\\
&+(-3a^6-2a^4b^2-3a^2b^4+6a^4c^2-3a^2c^4+6a^2b^2c^2)v\big)+O(h^4)
\end{aligned}$$

It is important to observe that their Taylor polynomial is of the order of h^2 and that there is no quadratic term in u and v in these expansions. Actually, from graphical observation on different triangles, we notice that they become flat very quickly when h becomes small.

Bibliography

[AA08] Carlos Alves and Pedro R. S. Antunes. The method of fundamental solutions applied to the calculation of eigensolutions for 2d plates. *International Journal for Numerical Method in Engineering*, pages 177–194, 2008.

[ADBS11] Aline Aigon-Dupuy, Peter Buser, and Klaus-Dieter Semmler. Hyperbolic geometry. In J. Bolte and F. Steiner, editors, *Hyperbolic Geometry and Applications in Quantum Chaos and Cosmology*, London Mathematical Society Lecture Note Series, pages 1–81. Cambridge University Press, 2011.

[AF06] Pedro R. S. Antunes and Pedro Freitas. New bounds for the principal Dirichlet eigenvalue of planar regions. *Experimental Mathematics*, 15(3):333–342, 2006.

[AF08] Pedro R. S. Antunes and Pedro Freitas. A numerical study of the spectral gap. *Journal of Physics A*, 41(5), 2008.

[AF11] Pedro R. S. Antunes and Pedro Freitas. On the inverse spectral problem for Euclidean triangles. *Proceedings of the Royal Society of London*, pages 1546–1562, 2011.

[AHTK99] Sigurd Angenent, Steven Haker, Allen Tannenbaum, and Ron Kikinis. On the Laplace–Beltrami operator and brain surface flattening. *IEEE Transactions on Medical Imaging*, 18:700–711, 1999.

[AS89] R. Aurich and F. Steiner. Periodic-orbit sum rules for the Hadamard-Gutzwiller model. *Physica D*, 39:169–193, 1989.

[AS93] R. Aurich and F. Steiner. Statistical properties of highly excited quantum eigenstates of a strongly chaotic system. *Physica D*, 64:185–214, 1993.

[Aub82] Thierry Aubin. *Nonlinear Analysis on Manifolds. Monge-Ampère Equations*. Springer, 1982.

[BC07] Annalisa Buffa and Snorre H. Christiansen. A dual finite element complex on the barycentric refinement. *Comptes Rendus Mathématique*, pages 1743–1769, 2007.

[BK11] Alexander Bobenko and Christian Klein. *Computational approach to Riemann surfaces*. Springer, 2011.

[BO91] I. Babuška and J. Osborn. Eigenvalue problems. In P. G. Ciarlet and J. L. Lions, editors, *Handbook of Numerical Analysis*, volume 2, pages 641–787. North-Holland, 1991.

[Bof10] Daniele Boffi. Finite element approximation of eigenvalue problems. *Acta Numerica*, pages 1–120, 2010.

[BS06] Andrew Booker and Andreas Strömbergsson. Effective computation of Maass cusp forms. *International Mathematics Research Notices*, pages 1–34, 2006.

[BS07a] Alexander Bobenko and Boris Springborn. A discrete Laplace-Beltrami operator for simplicial surfaces. *Discrete Computational Geometry*, 38:740–756, 2007.

[BS07b] Andrew Booker and Andreas Strömbergsson. Numerical computations with the trace formula and the Selberg eigenvalue conjecture. *Journal für die reine und angewandte Mathematik*, 607:113–161, 2007.

[Bus92] Peter Buser. *Geometry and Spectra of Compact Riemann Surfaces*. Birkhäuser, 1992.

[CR72] P. G. Ciarlet and P. A. Raviart. General Lagrange and Hermite interpolation in $\mathbb{R}^n$ with applications to finite element methods. *Archive for Rational Mechanics and Analysis*, 46:177–199, 1972.

[DD07] Alan Demlow and Gerhard Dziuk. An adaptive finite element method for the Laplace-Beltrami operator on implicitly defined surfaces. *SIAM Journal on Numerical Analysis*, 45:421–442, 2007.

[Dod76] Josez Dodziuk. Finite-difference approach to the hodge theory of harmonic forms. *American Journal of Mathematic*, 98(1):79–104, 1976.

[Fen89] Werner Fenchel. *Elementary Geometry in Hyperbolic Space*. de Gruyter, 1989.

[GT77] David Gilbarg and Neil S. Trudinger. *Elliptic Partial Differential Equations of Second Order*. Springer, 1977.

[Heb99] Emmanuel Hebey. *Nonlinear Analysis on Manifolds: Sobolev Spaces and Inequalities*. Courant Institute of Mathematical Science, 1999.

[Hej92] Denis Hejhal. Eigenvalues of the Laplacian for Hecke triangle groups. *Memoirs of the American Mathematical Society*, 97, 1992.

[Hej99] Denis Hejhal. On eigenfunctions of the Laplacian for Hecke triangle groups. In *Emerging Applications of Number Theory*, volume 109 of *The IMA Volumes in Mathematics and its Application*, pages 191–315. Springer, 1999.

[Jen81] Felix Werner Jenni. *Über das Spektrum des Laplace Operators auf einer Schar Kompakter Riemannscher Flächen*. Econom-Druck AG, Basel, 1981.

[Lar00] Mats G. Larson. A posteriori and a priori error analysis for finite element approximations of self-adjoint elliptic eigenvalue problems. *SIAM Journal on Numerical Analysis*, 38:608–625, 2000.

[Mer07] Christian Mercat. Discrete Riemann surfaces. In *Handbook of Teichmüller Theory*, volume 1. European Mathematical Society, Zürich, 2007.

[RT98] Pierre-Arnaud Raviart and Jean-Marie Thomas. *Introduction à l'Analyse Numérique des Equations aux Dérivées Partielles*. Dunod, 1998.

[SU11] Alexander Strohmaier and Ville Uski. An algorithm for the computation of eigenvalues, spectral zeta-functions and zeta-determinants on hyperbolic surfaces. Preprint, arXiv:1110.2150, 2011.

Curriculum Vitae

I was born on February 21th, 1980 and grew up in the hoods north of Bordeaux, France. From age 10 to 14, I attented the Collège du Grand Parc, Bordeaux, then the Lycée Michel Montaigne, Bordeaux, from age 14 to 17. I obtained my Baccalaureat in June 1997 with honors.

I began my higher education with the Classes Préparatoires at the Lycée Michel Montaigne, a selective French system parallel to the university which allows to enter the most reputable French engineering schools. I joined the Ecole Nationale des Ponts et Chaussée (ENPC), Paris, in September 2000.

After two years in this school studying mechanics, civil engineering and a parallel semester in the Ecole d'Architecture de Marne la Vallée, Paris, I spent a year in Switzerland for an internship at the Compagnie des Montres Longines, St-Imier.

Since my curiosity for science was not being satisfied, I negotiated an exchange between my school in Paris and the Ecole Polytechnique Federal de Lausanne (EPFL), where I finished my studies in the Physics Department and obtained my Master's in Science in April 2006. At the same time, I obtained a Master's degree from the ENPC.

After a one year break, I came back to the EPFL in September 2007 for a job as an assistant and started my collaboration with Professor Peter Buser. This collaboration developed in a Phd thesis about the eigenfunctions and eigenvalues of the Laplace operator on Riemann surfaces.